NUTRIENT AVAILABILITY MODULATES THE EFFECTS OF COREXIT 9500A ON OIL BIODEGRADATION

by

CATHRINE SHEPARD

(Under the Direction of Samantha B. Joye)

ABSTRACT

Since the 2010 Deepwater Horizon Oil Spill, numerous efforts have evaluated the impacts of the oil dispersant, Corexit 9500A, on oil biodegradation. This thesis investigates location and nutrient specific responses to Corexit 9500A, oil water accommodated fractions (WAF), and chemically enhanced WAFs (CEWAF) exposure. Trends in bacterial production and potential hydrocarbon oxidation rates indicate that site-specific geochemical differences influence Corexit's effects on microbial communities and their ability to degrade oil. Comparing bottle incubations of nutrient amended WAF, CEWAF, and Corexit treatments to unamended treatments showed distinct nutrient specific responses, most clearly evident by analysis of potential hydrocarbon oxidation rates and 16S community composition relative abundance. Demonstrating the importance of nutrient availability on Corexit's effects on oil biodegradation helps inform future oil spill remediation policy regarding dispersant application.

INDEX WORDS: Chemical Dispersant; Oil, Corexit 9500A; Gulf of Mexico; Oil Slick;
Surface Waters; Hydrocarbon Oxidation

NUTRIENT AVAILABILITY MODULATES THE EFFECTS OF COREXIT 9500A ON OIL BIODEGRADATION

by

CATHRINE SHEPARD

BS, Principia College, 2015

MAT, The University of Georgia, 2018

A Thesis Submitted to the Graduate Faculty of The University of Georgia in Partial Fulfillment of the Requirements for the Degree

MASTER OF SCIENCE

ATHENS, GEORGIA

2019

© 2019

Cathrine G. Shepard

All Rights Reserved

NUTRIENT AVAILABILITY MODULATES THE EFFECTS OF COREXIT 9500A ON OIL BIODEGRADATION

CATHRINE GRACE SHEPARD

Major Professor: Samantha B. Joye

Committee: Mary Ann Moran

Uta Passow

Electronic Version Approved

Suzanne Barbour Dean of Graduate School The University of Georgia August 2019

ACKNOWLEDGEMENTS

I would like to thank my advisor Dr. Samantha Joye for her continuous support throughout my time at the University of Georgia and express many thanks to my committee members for their continued support, and insight.

I am deeply grateful to the many current and previous members of Dr. Joye's Research Group including Hannah Choi, Tito Peña-Montenegro, Josh Parris, Lauren Carroll, Guangchao Zhuang, Andrew Montgomery, Ryan Sibert, Mary Kate Rogener, Sarah Harrison, Katie Mailloux, Norah Dorhmi, Rachael Karns, Jason Westrich, Zach Marinelli, and Kimberly Hunter. I am especially grateful to Tito Peña-Montenegro for his collaboration with DNA extraction and analysis, Josh Parris for his work with hydrocarbon extraction and analysis, Lauren Carroll for her help with water collection and geochemistry analysis, Katie Mailloux for her help with cell counts, and Kimberly Hunter for her help with water geochemistry samples.

Finally, I would like to thank my family, friends, and husband for their endless support and daily encouragement.

TABLE OF CONTENTS

Page	
DGEMENTSiv	ACKNOWLE
BLESvi	LIST OF TAI
URESviii	LIST OF FIG
	CHAPTER
INTRODUCTION AND LITERATURE REVIEW	1
1.1 Environmental Implications and Frequency of Oil Spills in U.S.	
Waters	
1.2 Oil Spill Mitigation Techniques	
1.3 Chemical Dispersants and Dispersant Policy	
1.4 Deepwater Horizon Oil Spill	
1.5 Dispersant Application During Deepwater Horizon Remediation	
Efforts in Light of Oil Spill Remediation Policy	
1.6 Corexit 9500A's Impact on Microbial Communities and Oil	
Biodegradation	
1.7 Thesis Overview and Objectives	
1.8 References	

2	INSTANTANEOUS EFFECT OF COREXIT 9500A ON COMMUNITY	7
	BACTERIAL PROTEIN PRODUCTION AND HYDROCARBON	
	OXIDATION RATES	26
	2.1 Introduction	26
	2.2 Methods	28
	2.3 Results	37
	2.4 Conclusion.	45
	2.5 References	49
3	EFFECTS OF IMPRICISE COREXIT APPLICATION ON SUBSEQUE	ENT
	CAPACITY FOR OIL BIODEGRADATION	52
	3.1 Introduction	52
	3.2 Methods	54
	3.3 Results	63
	3.4 Conclusion.	93
	3.5 References	98
4	OVERARCHING CONCLUSIONS	102
	4.1 Major Outcomes	102
	4.2 Relevance to Future Oil Spill Management	104
	4.3 References	106
APPI	ENDIX	107
	1 List of Abbreviations	107

LIST OF TABLES

	Page
Table 2.1: Geochemical characteristics of in situ samples	7
Table 2.2: Spearman's rank sum analysis of concentration and bacterial production	
correlation	41
Table 3.1: PCR mixture composition for 1 μL gDNA sample	63

LIST OF FIGURES

Page
Figure 2.1: Possible outcomes of a) dispersant application to surface oil slick b) inhibited
degradation leading to elevated oil snow, c) enhanced degradation but to incomplete,
potentially toxic byproducts (Seidel et al., 2016) or d) enhanced degradation and
complete/nonharmful degradation
Figure 2.2: a) Natural oil/gas seep area observed at GC600 on April 11, 2014, b) close view of
natural oil slick at GC600
Figure 2.3: Average bacterial production rates with increasing concentrations of Corexit and
Corexit components (DOSS, Tween 20, Tween 80, and SDS)
Figure 2.4: Average hexadecane and naphthalene oxidation potential rates (measured in nM
carbon per day) with additions increasing Corexit concentrations
Figure 3.1: a) 2L bottle incubations on roller table maintained at 24°C in the dark, b) samples
collected from control incubation bottles at Time 0, c) samples collected from all
other treatments (Corexit±nutrient, WAF±nutrient, CEWAF±nutrient) at Time 0, d)
samples collected from all treatments at Times 1-3
Figure 3.2: Average dissolved nutrient concentrations across three sampling points in Taylor
Energy incubation
Figure 3.3: Average dissolved nutrient concentrations across three sampling points in OC26
incubation
Figure 3.4: Average dissolved nutrient concentrations across four sampling points in GC600
incubation

Figure 3.5: Average dissolved ammonium (NH ₄ ', μM) after one week of treatment
incubation
Figure 3.6: Average dissolved phosphate (μ M) after one week of treatment incubation 74
Figure 3.7: Bacterial production rates in Taylor, OC26, and GC600 incubations
Figure 3.8: Potential hexadecane and naphthalene oxidation rates in OC26 incubations
Figure 3.9: Potential hexadecane and naphthalene oxidation rates in GC600 incubations 87
Figure 3.10: Microbial composition based on 16S rRNA amplicon sequences presented in
proportion of read counts in OC26 incubations across all time points
Figure 3.11: Microbial composition based on 16S rRNA amplicon sequences presented in
proportion of read counts in GC600 incubations across all time points

CHAPTER 1

INTRODUCTION

1.1 Environmental Implications and Frequency of Oil Spills in U.S. Waters

Petroleum, or crude oil, is comprised of over 17,000 different organic compounds – saturates, aromatics, resins, and asphaltenes – each having its own chemical properties (Bjorlykke et al., 2010). Petroleum discharged into U.S. waters occurs from natural seeps and anthropogenic spills (small boat, tanker and pipeline releases, and production related accidents) (National Research Council, 2003). Natural hydrocarbon seepage accounts for an estimated 47% of total petroleum inputs to the oceans (D'souza et al., 2016). Within the Gulf of Mexico (hereafter referred to as the Gulf) natural oil seepage introduces 0.38–1.0 3×10⁸ L of petroleum every year (Macdonald et al., 2015; Mitchel et al., 1999; National Research Council, 2003). The periodic exposure to elevated oil and natural gas concentrations allows specialized hydrocarbon degrading organisms to prosper (Atlas, 1981).

Unlike natural oil seeps, anthropogenic activities can introduce petroleum into the environment at high rates – on the scale of 1.6×10^7 L per day – in areas that are not specifically adapted to petroleum inputs (Reddy et al., 2012). In 2010 The U.S. Department of Energy reported that, on average, approximately 5 million liters of oil are spilled annually due to vessel and pipeline activity (Richards, 2011; Thompson, 2010). This estimate increases dramatically when a major oil spill occurs (Thompson, 2010). For example, when the *Torrey Canyon* tanker grounded on the Seven Sisters Reef in 1967, 120×10^6 L of crude oil was spilled (Kleindienst et al., 2015). In 1989, pilot error while steaming through the Valdez Narrow, Alaska, resulted in the

Exxon *Valdez* tanker running aground and spilling over 40×10^6 L of crude oil into Prince William Sound (Carson et al., 2003). In 2010 the Deepwater Horizon blowout (DWH) released of 9.94×10^8 - 1.11×10^9 L of oil into the northern Gulf of Mexico (McNutt et al. 2012; Joye, 2015). These spills had major impacts on the environment, human health, and local and global economies. The DWH oil spill alone resulted in nearly 10,000 reported cases of oil contaminated birds, along with oil contamination of sea turtles, dolphins, and whales, 140 of which were reported as dead due to oil contamination (Baron, 2012; U.S. Fish and Wildlife Service, 2011). The U.S. Bureau of Ocean Energy Management (BOEM) estimates that the DWH oil spill resulted in a 94.7 million to 1.6 billion dollar loss to the Gulf's commercial fishing industry (BOEM, 2016).

Recently BOEM published a fault tree analysis to evaluate oil spill occurrence trends (BOEM, 2018). Oil spills that discharged more than 50 barrels (bbls) (7.9×10³ L) of oil, and occurred in the U.S. Outer Continental Shelf (OCS) Gulf or Pacific Ocean (PAC) between 1972 and 2017 were considered in the analysis (BOEM, 2018). Of the 149 spills identified, 62 were classified as small (50-100 bbls; 7.9×10³-1.6×10⁴ L), 79 were classified as medium (100-1,000 bbls; 1.6×10⁴-1.6×10⁶ L), 7 were classified as large (1,000-10,000 bbls; 1.6×10⁶-1.6×10⁷ L), and 1 (the DWH oil spill) classified as huge (>10,000 bbls; >1.6×10⁷ L) (BOEM, 2018). A previous oil spill frequency analysis indicated that if the DWH oil spill volumes are ignored, volume of oil spilled annually by platforms has decreased, despite increases in total barrels of petroleum extracted (BOEM, 2016). The frequency and total volume of spilled oil from tanker spills has also decreased in general in recent years (ITOPF, 2019).

Still, in U.S. federal waters at least 6,500 oil spills occurred from 2007 to 2017 (Hoskins and Voitier, 2019). It is difficult to report with certainty the actual volume of oil spilled in these

incidences as estimate volumes of oil spills tend to be underreported (Asl et al., 2016). Asl et al. (2016) used satellite-borne Synthetic Aperture Radar (SAR) to make precise volume estimates of a portion (177 reports) of platform and tanker oil spills occurring in the Gulf that were reported to the National Response Center (NRC) between 2001 and 2012. Spills analyzed through satellite imagery showed that actual spill volume is approximately four times larger than average reported volume (Asl et al., 2016).

Since industry is drilling in increasingly deeper water, the risk of gas-driven well control problems similar to those that caused the DWH oil spill is further increased (Mason, 2019). Muchlenbachs et al. (2013) found frequency of incidents (blowouts, injuries, and oil spills) increases with well depth. Controlling for factors including age, weather, oil and gas volume extracted, and numbers of producing wells Muchlenbachs et al. (2013) estimated that the probability of company-reported incidents increases by 8.5% with every additional 100 ft increase in depth. Additionally, hurricane intensity and frequency are predicted to increase due to changing climate patterns which could further pose a threat to oil rigs operating in U.S. waters (Tin et al., 2019). With this continued (and possibly increasing) risk of oil spills, along with their negative impacts on surrounding environments, economies, and human health, it is important to address appropriate mitigation techniques to be well prepared for oil spills in the future.

1.2 Oil Spill Mitigation Techniques

Oil spill mitigation techniques include the mechanical containment and removal of oil, controlled burning, and application of chemical dispersants (Dave and Ghaly, 2011). Each of these techniques has advantages and disadvantages. Examples of mechanical containment and removal techniques include skimming, siphoning, and surface booming. Booms are intended to

prevent the spreading of oil by acting as a physical barrier in which oil cannot pass (Dave and Ghaly, 2011). Booms can be made out of rigid materials (fence booms), flexible, nonabsorbent foam (curtain booms), or fire proof material (Dave and Ghaly, 2011). They are generally long structures (>15 m in length), no more than 10 cm in height, and are not effective in high sea states (Dave and Ghaly, 2011). Booms can be combined with other remediation methods such as skimming which involves the actual collection and removal of oil from within a boomed area. Skimmers can be designed to act as a dam and collect floating oil through gravity potential (wier skimmers), soak up oil (oleophilic skimmers), or vacuum oil (suction skimmers) (Dave and Ghaly, 2011). Oil collected through skimming can be reprocessed and recycled depending on the degree of weathering and the level of debris present (Dave and Ghaly, 2011). Application (and removal) of adsorbent materials (peat moss, saw dust, clay, sand, polystyrene etc.) are also performed though typically in areas where the majority of oil has already been removed (Dave and Ghaly, 2011).

In cases of an oil discharge emanating from a damaged platform riser, a riser insertion tube tool can be utilized. The riser tool connects to the open or damaged end of the riser pipe allowing oil to flow up to a collection vessel instead of out into the environment. Ideally the riser tool would be able to completely divert the flow, but this is difficult to achieve in practice. The mitigation techniques discussed thus far result in the removal of oil from the environment. In the next section chemical dispersant application, an example of a mitigation technique that does not result in the removal of bulk crude oil but allows the oil to be partitioned into smaller droplets, is discussed.

1.3 Chemical Dispersants and Dispersant Policy

Chemical dispersants are designed to reduce the interfacial tension between oil and water allowing oil slicks to be physically separated into small oil droplets (Kujawinski et al., 2011; National Research Council, 2005). To achieve this effect dispersants contain chemicals called surfactants, which are amphiphilic molecules, having a polar head and a nonpolar tail. The polar, hydrophilic head is attracted to the water, while the nonpolar, hydrophobic tail is repelled by the water and attracted to the oil. The amphiphilic nature of surfactants reduces the interfacial tension, or the amount of energy needed to increase the oil-water interfacial area (large oil droplets to smaller droplets) (John et al., 2016). When surfactants are introduced, less wave energy is needed to break oil into small (<70 µm) droplets (John et al., 2016).

By dispersing the oil, the chemical and physical hazards that oil slicks pose to wildlife and fragile coastal ecosystems are assumed to be reduced (Powell and Chauhan, 2016).

However, this is only the case if dispersing oil also increases the biodegradability of the oil by making it more accessible to hydrocarbon degrading bacteria. Transferring oil from a slick or underwater mass to a dissolved state does not necessarily reduce the impact on wildlife or coastal systems. Though perhaps the physical concerns of oil may be reduced, toxicity of the dispersant, as well as increased oil toxicity remain problematic. It remains unclear whether dispersing oil increases or inhibits biodegradation rates of the oil (see Section 1.6).

Corexit 9500A, was developed by ExxonMobil in 1992 and is produced by Exxon Nalco Energy Products as an alternative to first generation dispersants which were discovered to be highly toxic (John et al., 2016; Zahed et al., 2011). Corexit 9500A contains an anionic surfactant, bis-(2-ethylhexyl)eulfosuccinate (DOSS) (18% w/w), and nonionic surfactants, Span 80 (4.4% w/w), Tween 80 (18% w/w), and Tween 85 (4.6% w/w) (Place, 2016). Corexit 9500A also

contains 0.28% α -/ β -ethylhexyl sulfosuccinate (α -/ β -EHSS), which may result from partial degradation of DOSS (Place, 2016). The remainder is dipropylene glycol butyl ether, an organic carrier solvent. Corexit 9527A has similar surfactant composition, but also includes a more toxic carrier solvent, 2-butoxy ethanol (National Research Council, 2005).

Corexit 9500A is effective at dispersing >50% of oil when applied at a 1:20 dispersant to oil ratio (DOR), as determined by the Environmental Protection Agency (EPA) in baffled flask tests at 20°C (NOAA, 2012). This lab derived DOR determined the target chemical dispersant quantities applied during the DWH oil spill response efforts (NOAA, 2012). Corexit 9500A's dispersing efficiency decreases as oil becomes more photo-oxidized (Ward et al., 2018). The dispersing efficiency of Corexit 9500A is also dependent on wind and wave energy present at the time of addition (Li et al., 2008; Li et al., 2009). In large tanks built to assess environmentally relevant wave energy effects on dispersant efficacy, Corexit 9500A additions under regular waves resulted in 21-36% crude oil dispersion, whereas breaking wave conditions result in 42-62% dispersion (Li et al., 2009). This underscores the important role of physics in dictating oil dispersion and indicates that wave energy dramatically influences the extent to which these chemicals disperse crude oil (Li et al., 2009). It is likely that at least some of the applied Corexit did not perform as efficiently as demonstrated in controlled laboratory testing of un-photo oxidized, well mixed oil.

Dispersants do not act upon all crude oil components uniformly or equally, even when applied to un-weathered oil with preferred wind and wave conditions (Joo et al., 2013). Some oil components remain unaffected while the dissolution of others is markedly increased upon dispersant addition. Mukherjee et al. (2011) found that oil's aromatics and combined saturates and resins concentration exerted statistically significant, positive effects on dispersion

effectiveness (p<0.05). Dispersant efficacy increased as aromatic concentration in the bulk crude oil increased, and increased efficiency when both saturates and resin concentrations were elevated (Mukherjee et al., 2011). In contrast, Fingas et al. (2003), found dispersant efficiency increased with saturates, but decreased with aromatics, resins, and asphaltene fractions. Canevari et al. (2001) observed a negative correlation between saturate fraction and dispersant efficiency and no correlation to aromatic, resins, or asphaltene fractions (Mukherjee et al., 2011). The differences in dispersant efficiency and differential component partitioning observed across studies could be due to contrasting dispersant addition techniques as well as unidentified contributing characteristics of the base oils used (Mukherjee et al., 2011).

In 1968, the first national policy related to oil spill remediation, the National Multi-Agency Oil and Hazardous Materials Pollution Contingency Plan, was passed by the Department of the Interior, Department of Transportation, Department of Defense, Department of Health, Education, and Welfare, and Office of Emergency Planning under the direction of President Lyndon B. Johnson with the intent of providing a "mechanism for coordinating the Federal response to a spill of oil or other hazardous materials" (Department of Interior, 1968). This policy was developed in part as a response to the 1967 *Torrey Canyon* tanker spill, and the ensuing remediation efforts. During the mitigation efforts following the *Torrey Canyon* tanker oil spill, chemicals originally designed to clean surfaces in ship engine rooms were applied to the 94 to 164×10⁶ L of spilled crude oil (Duda and Wawruch, 2017). 1,500 tons of napalm and 44,500 liters of kerosene were applied to disperse (or burn) oil from the spill (Duda and Wawruch, 2017). An estimated 15,000 sea birds were killed and microbial communities were severely inhibited as a result of the application of these chemicals (Duda and Wawruch, 2017). The 1968 National Multi-Agency Oil and Hazardous Materials Pollution Contingency Plan

(NCP) served as the first national contingency plan and included a section entitled *Chemicals Used to Treat Oil on Water* that detailed appropriate use of chemical oil dispersants (Department of Interior, 1968; Walker, 2018). The report did not recommend dispersant application in major shellfish or finfish nurseries, or near beaches (Department of Interior, 1968). Specific recommendations and application offsets, e.g. restrictions in distances from shoreline and definitions of what constitutes a "major" nursery, were not specified, so this document served primarily as a guideline rather than a binding agreement (Department of Interior, 1968). Soon after this initial NCP, the Water Quality Improvement Act was passed in 1970; this law required a secondary NCP be written to further specify oil spill remediation tactics (Walker, 2018). The resulting NCP called for Regional Response Teams (RRT) and detailed the first schedule of dispersants. Delegating dispersant use was left to the discretion of On Scene Coordinators (OSC) (Walker, 2018). The NCP and related acts have continued to be updated in light of 'lessons learned' after ensuing remediation efforts (Walker, 2018).

In 1990, Congress passed the Oil Pollution Act (OPA), motivated by issues that arose during the response to the Exxon *Valdez* tanker spill in 1989 (Franklin and Warner, 2011). Dispersants were not applied heavily during this oil spill in part due to the unfavorable sea state, but also because adequate volumes of dispersants and application equipment were not available for a spill of that magnitude (Franklin and Warner, 2011). The OPA outlined new responsibilities for companies and authorities at the federal, state, and local government levels, and required the development of contingency plans for worst-case scenario oil spills (Franklin and Warner, 2011). These new contingency plans were required to include guidelines regarding where and when dispersants could be used and specify how dispersant stock and application equipment would be prepared in case a major oil spill did occur (Franklin and Warner, 2011). The requirements

outlined by the OPA were later reflected in an updated version of the NCP, passed in 1994 (NCP, 59 FR 47384, 40 CFR part 300; Franklin and Warner, 2011).

Dispersant products can be added to the NCP's Dispersant Schedule after the EPA reviews the product's dispersant efficacy on different types of oils and conditions, and general toxicity (generally using shrimp, *Americamysis bahia*, or small fish, mummichog, *Fundulus heteroclitus*) (Franklin and Warner, 2011). Regional Contingency Plans (RCPs) developed by RRTs can designate which specific scheduled dispersants the federal OSCs will be allowed to use and under specific conditions, without further authorization (NCP, 40 CFR 300.910 Subpart J). Scheduled dispersants can also be utilized in ways not already specified in the RCPs, though OSCs must first consult other parties within the RRTs before doing so (NCP, 40 CFR 300.910 Subpart J).

RCPs dispersant specifications vary between regions. The Alaska RCP (ARCP) defines a singular "Preauthorization Area" in which dispersants can be utilized without further consultation with the U.S. Coast Guard, EPA, State of Alaska, and relevant local and tribal governments (ARRT 2018). Dispersant application in "Undesignated Areas" is contingent on a Case-by-Case Dispersant Use Authorization process and takes into consideration mixing energy, distance from shore, salinity, temperature, response equipment availability, weather conditions, shoreline type, extent of oil weathering, and proximity to sensitive habitats (ARRT, 2018). The ARCP continues on to describe specific dispersant application stipulations including that dispersants may only be applied where water depth exceeds 60 feet, and at "sufficient distances" from shoreline to avoid dispersant contamination of near shore benthic communities (ARRT, 2018). The ARCP also specifies that dispersants must not be applied within 500 meters of

swarming of swarming fish, rafting flocks of birds, marine mammals in the water, and/or marine mammal haul-outs (ARRT, 2018).

Dispersants have been applied in more than sixty incidences globally, twenty five of which occurred in or near U.S. waters (Franklin and Warner, 2011). Still, as is addressed in most RCPs (i.e. the ARCP, and the Central Texas Coastal Area Contingency Plan (Region 6) (ARCT, 2018; CTCACP, 2018)), dispersant application effectiveness remains unclear. Dispersant application does not remove oil but, when chemically efficient, increases the oil-water interface area so that the physical hazards of a slick to megafauna may be diminished. Increasing the oil-water interface has also been argued to make oil more available to hydrocarbon degrading organisms, and thus to increase biodegradation rates (Prince, 2015). Due to toxicity and inhibitory effects in many microorganisms, as well as lack of uniform trends found across experiments investigating dispersant influence on microbial community's ability to degrade oil/dispersed oil, the extent to which dispersants should be relied upon in remediation efforts remains unclear (Kleindienst et al. 2015a).

1.4 Deepwater Horizon Oil Spill

On April 20, 2010 the Deepwater Horizon Drilling Rig experienced a loss of well control (Dadashzadeh et al., 2013) that led to spontaneous combustion of ejected methane and a subsequent explosion that set fire to the platform. The explosion and fire led to the death of eleven workers and, ultimately, to the sinking of the drilling rig, which marked the beginning of the largest open ocean oil spill to date. When the platform collapsed, a break in a riser pipe occurred 1,520 m below the sea surface, allowing an estimated peak crude oil discharge of 1.6×10^7 L per day until the well was capped (Reddy et al., 2012). In total, an estimated 250,000

metric tonnes of natural gas and 9.94×10^8 - 1.11×10^9 L of crude oil were released over the 87 days between the start of the discharge until the well was capped on July 12, 2010 (McNutt et al. 2012, Joye, 2015).

Approximately 1.27×10⁸ L of oil were recovered at the wellhead by the riser insertion tool (LMRP cap, Top Hat no. 4) and a portion of released methane was recovered and flared. The remaining discharged oil and methane were distributed throughout the water column (Ryerson et al., 2012). About 36% of the leaked oil dissolved and all of the discharged gas remained neutrally buoyant at depth in the water column (Dubinsky et al., 2013; Ryerson et al., 2012). Subsurface plumes were found to the southwest and northeast of the wellhead at 400 and 1000-1200 m below the surface (Camilli et al., 2010; Diercks et al. 2010; Paul et al., 2013). A portion of the neutrally buoyant oil in the subsurface plume and some of the oil in surface slicks was biologically transformed, contributing to a large marine "oil snow" event (Passow et al., 2012). An estimated 14% of the total 9.94×10⁸ - 1.11×10⁹ L of oil released likely underwent sedimentation and fell to the seafloor, resulting in damage to the sensitive benthic communities below (Daly et al., 2016; Hsing et al., 2013).

Even though a third of the discharged oil remained below the surface, the large total volume of oil released meant that surface oil slicks remained a pressing threat and responding to that threat required quantification of the discharge rate. SkyTruth, a nonprofit non-governmental organization, in collaboration with scientists at Florida State University, used satellite imagery obtained during the early days of the incident to assess the oil discharge rate. While doing so they found significant fluctuations in surface slick cover from day-to-day imaging, most likely due to factors including changing wind and current patterns (Norse and Amos, 2010). The largest surface slick coverage was about 62,000 km², spreading across the northeast Gulf of Mexico

(Norse and Amos, 2010; Sammarco et al., 2013). These slicks varied in thickness and were ephemeral, so average concentrations of oil derived organics, dissolved petrocarbon, and their distribution are difficult to quantify.

Reported petroleum hydrocarbon concentrations vary between studies, likely due to the spatio-temporal variation in sampling and inconsistency between sampling techniques (Wade et al., 2016). In a review of the over 20,000 water samples available through The Gulf Science Data database found that the highest total petroleum hydrocarbon (TPH) and polycyclic aromatic hydrocarbons (PAH) concentrations were "clustered" within 25 km of the wellhead and between 1,000 and 1,500 m depth, although sporadic high concentrations (≥ 1,000 μg/L) were noted outside these areas as well (Wade et al., 2016). Water column samples collected in August of 2010 in an area east-northeast of the wellhead ranged in petroleum hydrocarbon concentrations from 24 to 298 ng/L despite oil slicks, sheens, or tar balls being absent (Paul et al., 2013).

Sediment TPH concentrations collected between September and October 2010 peaked within 5 km of well head at 19,258 μg kg⁻¹ and were lowest at the greatest distance sampled from the well head (100 to 200 km away), with the lowest TPH concentration detected at 18 μg kg⁻¹ (Mason et al., 2014). Contamination also occurred in the sands and sediments of Gulf Coast beaches and marshes, where the oil persists to some degree (Huettel et al., 2018).

1.5 <u>Dispersant Application During Deepwater Horizon Remediation Efforts in Light of Oil Spill</u> Remediation Policy

To reduce contamination of delicate coastal ecosystems from the oil discharged into the Gulf of Mexico following the DWH oil spill, approximately 8 million liters of dispersant were applied at the wellhead and to surface waters (Kujawinski et al., 2011). The majority of

dispersant application (56%) was applied to affected surface areas with aircrafts and vessels, while the remaining volume (44%) was applied directly at the discharging wellhead at 1500 m with a remotely operated vehicle (ROV) (Coastal Response Research Center, 2012). The crude oil collected from the Macondo well in June 2010 was 74% saturated hydrocarbons ($\delta^{13}C = -27.9\%$) and 16% aromatic hydrocarbons ($\delta^{13}C = -26.5\%$), and was considered relatively mature, light sweet crude oil, with little evidence of reservoir biodegradation (Reddy et al., 2011). Reddy et al. (2011) also noted that Macondo crude contained 10% polar compounds; these compounds are particularly resistant to evaporation, biodegradation, and photolysis. Bulk crude oil is less dense (820 g L⁻¹) than seawater (1024 g L⁻¹) but the nature of the explosive discharge along with the fact that some components partition into the aqueous phase, resulted in some portion of the discharged oil remaining neutrally buoyant in deep water plumes (Reddy et al., 2012). As a result of differential partitioning as bulk oil rose to the surface, the composition of sea surface mousses collected in May of 2010 was distinct from bulk crude oil (Paris et al., 2018; Liu et al., 2012; Reddy et al., 2012).

The NCP in place at the time of DWH listed eight approved oil dispersants. COREXIT 9527A and COREXIT 9500A were exclusively applied due to the limited availability and lack of capacity for production of the other approved dispersants (Coastal Response Research Center, 2012). COREXIT 9527A and 9500A were used together until the supply of the less efficient Corexit 9527A, which is more toxic because it contains 2-butoxy-ethanol, a known carcinogen, supply was exhausted. Then, Corexit 9500A became the sole dispersant utilized. During the 61 days of surface dispersant application (performed between April 22 to July 19, 2010) COREXIT 9527A comprised 22% of the total volume of surface applied dispersants (Coastal Response Research Center, 2012). Daily surface dispersant application volume ranged from 473 to 212,816

liters (averaging 60,374 liters per day) (Coastal Response Research Center, 2012). To reach the maximum efficiency of oil dispersion, Corexit was applied at 20 liters per acre to generate an optimal 1:20 dispersant to oil ratio (DOR), or the experimentally derived ideal dispersant to oil ratio for dissolution of oil.

In addition to the NCP, dispersant application was also directed by the Special Monitoring of Applied Response Technologies (SMART) guidelines, initially created by the U.S. Coast Guard (USCG) and National Oceanic and Atmospheric Administration (NOAA) in 1997, and updated in 2006 (Parscal et a., 2014). The 2006 SMART Protocol provides general guidance for operation data collection, processing, and evaluation related to oil spill (and other hazardous substance) response (Parscal et al., 2014). Although efforts were made to reduce overspraying of dispersants (such as specifying that candidate slicks must be continuous), the lack of predetermined dispersant application field protocols may have resulted in erroneous identification of candidate slicks (U.S. Coast Guard, 2011). USCG SMART teams improvised a sampling pump that contaminated following sampling efforts due to oil sticking to the walls of the hose pump (Parscal et al., 2014). The SMART protocol also did not specify data processing and quality control protocols, so early efforts to collect oil distribution data were inefficient (Parscal et al., 2014). SMART data processing was eventually standardized during the DWH remediation efforts but remain unspecified in official SMART protocol (Parscal et al., 2014). Whether these specifications are made within the main SMART protocol itself or as separate job aids or appendices, establishing these protocols prior to remediation efforts could prevent over application of dispersants in the future (Parscal et al., 2014).

Surface dispersant application during the DWH remediation efforts reflected accepted policy but it is important that such policies continue to be updated to reflect knowledge gained

during previous remediation efforts and ongoing research. Currently the Gulf's RRTs and Area Committees are working to update the pre-2010 regional policies (Walker, 2018). This work aims to further inform such regional policy amendments.

1.6 Corexit 9500A's Impact on Microbial Communities and Oil Biodegradation

Incubation experiments evaluating the effect of oil and dispersants on microbial community composition and characteristics typically expose ambient or isolated microbial communities to oil-amended water accommodated fractions (WAFs), chemically enhanced (i.e., chemically dispersed oil) WAFs (CEWAFs), where oil and dispersants are added together in a dispersant to oil ratio of 1:10 or 1:20, and dispersant accommodated fractions, where dispersant is added to sterile seawater and allowed to solubilize. WAF, CEWAF, and dispersant addition procedures – all of which are prepared as water accommodated fractions – are prepared by adding bulk crude oil to sterilized or artificial sea water and gently mixing for up to 48 hours in the dark (Singer et al., 2000).

Results from previous microcosm experiments indicated that deep water plume dispersant application negatively impacted the microbial community's ability to degrade oil, citing observed inhibition of hydrocarbon oxidation, microbial activity, and significant shifts in microbial community composition (Kleindienst et al., 2015b). After one week, incubations performed with water collected from 1178 m depth at a natural seep site in the Gulf (GC600) and incubated at 5 °C led to an increase in *Colwellia* abundance from 1% to 26-43% in CEWAF (with and without nutrients) and in Corexit-only treatments (Kleindienst et al., 2015b). WAF amendment showed an increased abundance of *Marinobacter*, from 2% to 42% and in *Cycloclasticus*, from 12% to 23%. An increase in *Cycloclasticus* was apparent to a lesser extent

in the CEWAF+nutrient treatment, but not the CEWAF or Corexit-only treatments (Kleindienst et al., 2015). Oceaniserpentilla (DWH Oceanospirillum) abundance decreased in all treatments (Kleindienst et al., 2015b) because the oil utilized in the experiments did not contain cycloalkanes (the oil used in these experiments was a Macondo surrogate provided by BP). Similar shifts in the microbial community composition occurred in microcosm incubations performed at 25°C with enrichment cultures generated from samples collected close to site of the DWH spill, though incubations performed at 5°C did not show such shifts (Techtmann et al., 2017). Bacterial strains isolated from beached oil were also found to have a strain specific response to oil, dispersed oil, and dispersant treatments (Overholt et al., 2016). Hamdan and Fulmer (2011) also saw strain specific response to Corexit additions, with *Marinobacter* being almost entirely inhibited when cultures isolated from freshly beached oil from the DWH oil spill was exposed to environmentally relevant dispersant concentrations (1 to 10 mg/L). Whether shifts in the microbial community composition and resulting community function are due to toxicity of the dispersant and/or dispersed oil, or if the shift is instead result from competition between heterotrophs exposed to different carbon sources remains unclear (Kleindienst et al., 2015b).

The microbial composition of water collected at the time of the DWH indicates significant shifts compared to conditions pre-DHW, although the impact of Corexit application is difficult to separate from oil infusion since Corexit application began soon after the oil discharge began. Samples collected in a plume at a 1000 to 1300 m depth located to the southwest of the wellhead at the time of the DWH oil spill were enriched in *Oceanosprillum*, *Cycloclasticus*, and *Colwellia*, while the typically abundant hydrocarbon degraders found in natural seep samples in the Gulf were in low abundance or absent (Kleindienst et al., 2015b). Hazen et al. also saw

enriched populations of *Oceanospirillales* in subsurface samples close to the wellhead, and Valentine et al. found that *Cycloclasticus* and *Colwellia* dominated populations (Hazen et al., 2010; Valentine et al., 2010). Plume affected sites exhibited significantly reduced diversity compared to surrounding, unaffected sites (Kleindienst et al., 2015a). This result was also observed in other works comparing plume affected and surrounding, unaffected areas (Hazen et al., 2010; Valentine et al., 2012).

Shifts in the microbial community in response to Corexit application could have significant impacts on the community's ability to degrade oil as microorganisms generally have a specific range of chain length and chemical structures they are able to degrade (Kleindienst et al., 2016). *Cycloclasticus*, for example, can utilize PAHs such as naphthalene, phenanthrene, anthracene, and toluene as sole carbon sources (Dyksterhouse et al., 1995). *Cycloclasticus* strains isolated from the Gulf and Puget Sound can degrade substituted naphthalenes, phenanthrene, and fluorene (Geiselbrecht et al., 1998). Ace-naphthenequinone was partially degraded by both strains tested (Geiselbrecht et al., 1998). Biphenyl removal was dependent on a specific *Cycloclasticus* strain tested with removal ranging from complete to $43\% \pm 10\%$ (Geiselbrecht et al., 1998). Fluoranthene, chrysene, and pyrene, were partially removed when added in the presence of phenanthrene, but could not serve as sole carbon sources when applied individually (Geiselbrecht et al., 1998).

A single amplified genome (SAG) of *Colwellia* isolated from a DWH plume indicated genes for denitrification and a capability to degrade gaseous and aromatic hydrocarbons (Mason et al., 2014). *Colwellia* species isolated from deepwater plumes were able to assimilate ethane, propane, and benzene, as evidenced by ¹³C label incorporation experiments (Redmond and Valentine, 2012). A SAG of *Oceanospirillales* isolated from a DWH plume indicated genes for

cyclohexane and non-gaseous n-alkanes degradation (Mason et al., 2014). Redmond and Valentine saw slight trends in stimulated growth in *Oceanospirillales* with the addition of ethane and propane (Redmond and Valentine, 2012).

Marinobacter can degrade linear and branched aliphatic compounds, as well as polycyclic aromatics (Dombrowski et al., 2016; Golyshin et al., 2003). Alcanivorax also degrades straight chain alkanes, and reduce nitrate (Dombrowski et al., 2016; Yakimov et al., 1998). Other PAH degrading genera include Aeromonas, Flavobacterium, Beijerinckia, Alcaligenes, Micrococcus, Vibrio, Flavobacterium, and Mycobacterium (Dyksterhouse et al., 1995).

1.7 Thesis Overview and Objectives

The aim of this thesis is to evaluate how surface dispersant application affects microbial communities and their collective ability to degrade oil. To address the question of Corexit 9500A's influence on the oil biodegradation capacity of surrounding microbial communities, the first chapter addresses how Corexit and its major components impact bacterial community protein production and hydrocarbon oxidation rates. The second chapter addresses whether surface application of Corexit leads to shifts in the microbial community that could impact the community's ability to degrade oil subsequently.

1.9 References

- ARRT. Alaska Regional Response Team. Alaska Regional Contingency Plan Appendix III Dispersant Use Plan for Alaska. **2018**. https://alaskarrt.org/PublicFiles/AK_Dispersant_Use_Guidelines.pdf. Accessed July 2019.
- Asl, S. D.; Amos, J.; Woods, P.; Garcia-Pineda, O.; & MacDonald, I. R. Chronic, anthropogenic hydrocarbon discharges in the Gulf of Mexico. *Deep Sea Res. Part II Top. Stud. Oceanogr.* **2016**, *129*, 187-195; DOI: 10.1016/j.dsr2.2014 .12.006.
- Atlas, R. M. Microbial degradation of petroleum hydrocarbons: an environmental perspective. *Microbiological Rev.* **1981**, *45* (1), 180-209.
- Bjorlykke, K. *Petroleum geoscience: From sedimentary environments to rock physics*. Springer, New York, US. 2010.
- BOEM, Bureau of Ocean Energy Management. Carroll, M., Gentner, B., Quigley, K., Dehner, L., & Perlot, N. An Analysis of the Impacts of the Deepwater Horizon Oil Spill on the Gulf of Mexico Seafood Industry. **2016**. https://www.boem.gov/ESPIS/5/5518.pdf. Accessed June 2019.
- BOEM, Bureau of Ocean Energy Management. 2016 Update of Occurrence Rates for Offshore Oil Spills. **2016**. https://www.bsee.gov/sites/bsee.gov/files/osrr-oil-spill-response-research/1086aa.pdf. Accessed June 2019.
- BOEM, Bureau of Ocean Energy Management. Roberts, B., Myers, J. US Outer Continental Shelf Oil Spill Statistics. **2018**. https://www.boem.gov/BOEM-2018-006/. Accessed June 2019.
- Camilli R.; Reddy C.M.; Yoerger D.R.; Van Mooy B.A.; Jakuba M.V.; Kinsey, J.C.; McIntyre, C.P.; Sylva, S.P.; Maloney, J.V. Tracking hydrocarbon plume transport and biodegradation at Deepwater Horizon. *Science*. **2010**, *330* (6001): 201-204; DOI: 10.1126/science.1195223.
- Canevari, G.P., Calcavecchio, P., Lessard, R.R., Becker, K.W.; Fiocco, R.J. Key Parameters Affecting the Dispersion of Viscous Oil. *Int. Oil Spill Conf. Proc.* **2001**, *2001* (1), 479-483; DOI: 10.7901/2169-3358-2001-1-479.
- Carson, R. T., Mitchell, R. C., Hanemann, M., Kopp, R. J., Presser, S.; Ruud, P. A. Contingent Valuation and Lost Passive Use: Damages from the Exxon Valdez Oil Spill. *Environ. Resour. Econ.* **2003**, *25* (3), 257-286; DOI: 10.1023/A:1024486702104
- CTCACP. Central Texas Coastal Area Contingency Plan. **2018**. http://www.glo.texas.gov/ost/acp/houston/sectorhoustongalveston_acp.pdf. Accessed June 2019.

- Coastal Response Research Center, Research Planning Incorporated, National Oceanic and Atmospheric Administration. **2012**. The Future of Dispersant Use in Oil Spill Response Initiative. https://crrc.unh.edu/sites/crrc.unh.edu/files/media/docs/Workshops/dispersant future 11/Dispersant Initiative FINALREPORT.pdf. Accessed June 2019.
- D'souza, N. A.; Subramaniam, A.; Juhl, A. R.; Hafez, M.; Chekalyuk, A.; Phan, S.; Yan, B.; MacDonald, I. R.; Weber, S. C.; Montoya, J. P. Elevated surface chlorophyll associated with natural oil seeps in the Gulf of Mexico. *Nat. Geosci.* **2016**, *9* (3), 215-2018; DOI: 10.1002/2015JC011062.
- Dadashzadeh, M.; Abbassi, R.; Khan F.; Hawboldt, K. Explosion modeling and analysis of BP Deepwater Horizon accident. *Safety Sci.* **2013**, *57*, 150-160; DOI: 10.1016/j.ssci.2013.01.024.
- Daly, K.L.; Passow, U.; Chanton, J.; Hollander D. Assessing the impacts of oil-associated marine snow formation and sedimentation during and after the Deepwater Horizon oil spill. *Anthropocene*. **2016**, *13*, 18-33; DOI: 10.1016/j.ancene.2016.01.006.
- Dave, D.; Ghaly, A. E. Remediation technologies for marine oil spills: A critical review and comparative analysis. *Am. J. Environ. Sci.* **2011**, *7* (5), 423-440.
- Department of Interior. Department of Transportation. Department of Defense, Department of Health, Education and Welfare. Office of Emergency Planning. National Multi-Agency Oil and Hazardous Materials Pollution Contingency Plan. 1968. https://ntrl.ntis.gov/NTRL/dashboard/searchResults/titleDetail/PB216561.xhtml. Accessed June 2019.
- Dubinsky, E. A.; Conrad, M. E.; Chakraborty, R.; Bill, M.; Borglin, S. E.; Hollibaugh, J. T.; Mason, O.U.; Piceno, Y. M.; Reid, F. C.; Singfellow, W. T.; Tom, L. M.; Hazen, T. C.; Anderson. Succession of hydrocarbon-degrading bacteria in the aftermath of the Deepwater Horizon oil spill in the Gulf of Mexico. *Environ. Sci. Technol.* **2013**, *47* (19), 10860-10867; DOI: 10.1021/es401676y
- Duda, D.; Wawruch, R. The impact of major maritime accidents on the development of international regulations concerning safety of navigation and protection of the environment. Sci. J. Polish Nav. Acad. 2017, 211 (4), 23-44; DOI: 10.5604/01.3001.0010.6741.
- Dyksterhouse, S.E.; Gray, J.P.; Herwig, R.P.; Lara, J.C.; Staley, J.T. Cycloclasticus pugetii gen. nov., sp. nov., an aromatic hydrocarbon-degrading bacterium from marine sediments. *Int. J. Syst. and Evol.* **1995**, *45* (1), 116-123. DOI: 10.1099/00207713-45-1-116.
- Fingas, M.; Fieldhouse, B. Studies of the formation process of water-in-oil emulsions. *Mar. Pollut. Bull.* **2003**, *47* (9-12), 369-396; DOI: 10.1016/S0025-326X(03)00212-1
- Franklin C. L.; Warner L. Fighting chemicals with chemicals: the role and regulation of dispersants in oil spill response. *Nat. Resources & Env't.* **2011**, *26* (2), 7-11.

- Geiselbrecht, A. D.; Hedlund, B. P.; Tichi, M. A.; Staley, J. T. Isolation of marine polycyclic aromatic hydrocarbon (PAH)-degrading Cycloclasticus strains from the Gulf of Mexico and comparison of their PAH degradation ability with that of Puget Sound Cycloclasticus strains. *Appl. Environ. Microbiol.* **1998**, *64* (12), 4703-4710.
- Hamdan, L. J.; Fulmer, P. A. Effects of COREXIT® EC9500A on bacteria from a beach oiled by the Deepwater Horizon spill. *Aquat. Microb. Ecol.* **2011**, *63* (2), 101-109; DOI: 10.3354/ame01482.
- Hazen, T. C.; Dubinsky, E. A.; DeSantis. T. Z.; Andersen, G. L.; Piceno, Y. M. Deep-sea oil plume enriches indigenous oil-degrading bacteria. *Science*. **2010**, *330* (6001): 204-208; DOI: 10.1126/science.1195979.
- Hoskins, D.; Voitier, M. Dirty Drilling: Trump Administration Proposals Weaken Key Safety Protections and Radically Expand Offshore Drilling. *Oceana.* **2019**, 1-30. DOI: 10.31230/osf.io/fbgnc.
- Hsing, P. Y.; Fu, B.; Larcom, E. A.; Berlet, S. P.; Shank T. M. Evidence of lasting impact of the Deepwater Horizon oil spill on a deep Gulf of Mexico coral community. *Anthropocene.* **2013**, *57*, 1-15; DOI: 10.12952/journal.elementa.000012.
- Huettel, M.; Overholt, W.A.; Kostka, J. E.; Hagan C.; Kaba, J.; Wells, W. B.; Dudley, S. Degradation of Deepwater Horizon oil buried in a Florida beach influenced by tidal pumping. *Mar. Pollut. Bull.* **2018**, *126*, 488-500; DOI: 10.1016/j.marpolbul.2017.10.061
- ITOPF. 2018 Tanker Oil Spill Statistics: Number of Oil Spills Remains Low. **2019**. https://www.itopf.org/news-events/news/article/2018-tanker-oil-spill-statistics-number-of-spills-remains-low/. Accessed June 2019.
- John, V.; Arnosti, C.; Field, J.; Kujawinski, E.; McCormick, A. The role of dispersants in oil spill remediation: fundamental concepts, rationale for use, fate, and transport issues. *Oceanography*. **2016**, *29* (3), 108-117; DOI: 10.5670/oceanog.2016.75.
- Joo, C.; Shim, W. J.; Kim, G. B.; Ha, S. Y.; Kim, M.; An, J. G.; Kim, E.; Kim, B.; Jung, S. W.; Kim, Y. O.; Yim, U. H. Mesocosm study on weathering characteristics of Iranian Heavy crude oil with and without dispersants. *J. Hazard. Mater.* **2013**, *248-249*, 37-46; DOI: 10.1016/j.jhazmat.2012.12.050.
- Joye, S. B. Deepwater Horizon, 5 years on. *Science*. **2015**, *349* (6248), 592-593. DOI: 10.1126/science.aab4133.
- Kleindienst, S.; Paul, J. H.; Joye, S. B. Using dispersants after oil spills: impacts on the composition and activity of microbial communities. *Nat. Rev. Microbiol.* **2015**, *13* (6), 388-396; DOI: 10.1038/nrmicro3452.

- Kleindienst, S.; Grim, S.; Sogin, M; Bracco, A; Crespo-Medina, M.; Joye, S. B. Diverse, rare microbial taxa responded to the Deepwater Horizon deep-sea hydrocarbon plume. *ISME*. **2016**, *10* (2): 400-415; DOI: 10.1038/ismej.2015.121.
- Kujawinski, E. B.; Kido M. C.; Valentine D. L.; Boysen, A. K.; Longnecker, K.; Redmond, M. C. Fate of dispersants associated with the Deepwater Horizon oil spill. *Environ. Sci. Technol.* **2011**, *45* (4): 1298-1306; DOI: 10.1021/es103838p.
- Leahy, J. G., Colwell, R. R. Microbial degradation of hydrocarbons in the environment. *Microbiol. Mol. Biol. Rev.* **1990**, *54* (3), 305-315.
- Li, Z.; Lee, K.; King, T.; Boufadel, M. C.; Venosa A. D. Assessment of chemical dispersant effectiveness in a wave tank under regular non-breaking and breaking wave conditions. *Mar. Pollut. Bull.* **2008**, *56* (5): 903-912; DOI: 10.1016/j.marpolbul.2008.01.031
- Li, Z.; Lee, K.; King, T.; Kepkay, P.; Boufadel, M. C., Venosa, A. D. Evaluating chemical dispersant efficacy in an experimental wave tank: 1, dispersant effectiveness as a function of energy dissipation rate. *Environ. Eng. Sci.* **2009**, *26* (6), 1139-1148; DOI: 10.1089/ees.2008.0377
- Liu, Z.; Liu, J.; Zhu, Q.; Wu W. The weathering of oil after the Deepwater Horizon oil spill: insights from the chemical composition of the oil from the sea surface, salt marshes and sediments. *Environ. Res. Lett.* **2012**, *7* (3) 035302; DOI: 10.1088/1748-9326/7/3/035302.
- Mason, O.U.; Scott, N.M.; Gonzalez, A.; Robbins-Pianka, A.; Baelum, J.; Jansson,...J. K. Metagenomics reveals sediment microbial community response to Deepwater Horizon oil spill. *ISME*. **2014**, *8* (7): 1464-1475; DOI: 10.1038/ismej.2013.254.
- Mason, C. F. Policy Brief—Regulating Offshore Oil and Gas Exploration: Insights from the Deepwater Horizon Experience in the Gulf of Mexico. *Rev. of Environ. Econ. and Pol.* **2019**, *13* (1), 149-154; DOI: 10.1093/reep/rey018
- McNutt, M. K., Camilli, R., Crone, T. J., Guthrie, G. D., Hsieh, P. A., Ryerson, T. B.,... Shaffer, F. Review of flow rate estimates of the Deepwater Horizon oil spill. *Proc. Natl. Acad. Sci.*, **2012**, *109* (50), 20260-20267; DOI: 10.1073/pnas.1112139108.
- Mukherjee, B.; Turner, J.; Wrenn, B. A. Effect of oil composition on chemical dispersion of crude oil. *Environ. Eng. Sci.* **2011**, *28* (7), 497-506; DOI: 10.1089/ees.2010.0226.
- Muehlenbachs, L.; Cohen, M. A.; Gerarden, T. The impact of water depth on safety and environmental performance in offshore oil and gas production. *Energy Policy*. **2013**, *55*, 699-705. DOI: 10.1016/j.enpol.2012.12.074.

- National Research Council. *Oil in the sea III: Inputs, Fates, and Effects*. National Academies Press, US, 2003.
- National Research Council (U.S.). Committee on Understanding Oil Spill Dispersants: Efficacy and Effects. *Oil Spill Dispersants: Efficacy and Effects*. The National Academies Press, Washington, DC: The National Academic Press, 2005. DOI: 10.17226/11283.
- NOAA (National Oceanic and Atmospheric Administration), Coastal Response Research Center, Research Planning Incorporated. The Future of Dispersant Use in Oil Spill Response Initiative. 2012.
- Norse, E. A.; Amos, J. Impacts, perception, and policy implications of the Deepwater Horizon oil and gas disaster. Environmental Law Reporter. **2010**, *40*, 11058-11073.
- Overholt, W. A.; Marks, K. P.; Romero, I. C.; Hollander, D. J.; Snell, T. W.; Kostka, J. E. Hydrocarbon-degrading bacteria exhibit a species-specific response to dispersed oil while moderating ecotoxicity. *Appl. Environ. Microbiol.* **2016**, *82* (2), 518-527. DOI: 10.1128/AEM.02379-15.
- Parscal, B.; Young, R.; Barone R. Modernization of Special Monitoring of Applied Response Technologies (SMART) Technology and Methods-2014. Coast Guard New London CT Research and Development Center. **2014**. https://apps.dtic.mil/dtic/tr/fulltext/u2/a613265.pdf. Accessed June 2019.
- Passow, U.; Ziervogel, K.; Asper,V; Diercks, A. Marine snow formation in the aftermath of the Deepwater Horizon oil spill in the Gulf of Mexico. *Environ. Res. Lett.* **2012**, *7* (3): 035301; DOI: 10.1088/1748-9326/7/3/035301.
- Paul, J. H.; Hollander D.; Coble, P.; Daly, K. L.; Murasko S.; English, D.; Basso, J.; Delaney, J.; McDaniel, L.; Kovach, C. W. Toxicity and mutagenicity of Gulf of Mexico waters during and after the Deepwater Horizon oil spill. *Environ. Sci. Technol.* **2013**. *47* (17), 9651-9659; DOI: 10.1021/es401761h.
- Place, B. J.; Perkins, M. J.; Sinclair, E.; Barsamian, A. L.; Blakemore, P. R.; Field, J. A. Trace analysis of surfactants in Corexit oil dispersant formulations and seawater. *Deep Sea Res. Part II Top. Stud. Oceanogr.* **2016**, *129*, 273-281; DOI: 10.1016/j.dsr2.2014.01.015.
- Powell, K. C.; Chauhan, A, J, C; Physicochemical, S. A.; Aspects, E. Dynamic interfacial tension and dilational rheology of dispersant Corexit 9500. *Colloids Surf A: Physicochem Eng Asp.* **2016**, *497*, 352-361; DOI: 10.1016/j.colsurfa.2016.03.009.
- Prince, R. C. Oil Spill Dispersants: Boon or Bane? *Environ. Sci. Technol.* **2015**, *49* (11), 6376–6384; DOI: 10.1021/acs.est.5b00961.

- Reddy, C. M.; Arey, J. S.; Seewald, J. S.; Sylva, S. P.; Lemkau, K. L.; Nelson, R. K.; Carmichael, C. A.; McIntyre, C. P.; Fenwick J.; Ventura, T., Van Mooy, B. A. S.; Camilli, R. Composition and fate of gas and oil released to the water column during the Deepwater Horizon oil spill. *Proc. Natl. Acad. Sci.* **2012**, *109* (50), 20229-20234; DOI: 10.1073/pnas.1101242108.
- Redmond, M. C.; Valentine, D. L. Natural gas and temperature structured a microbial community response to the Deepwater Horizon oil spill. *Proc. Natl. Acad. Sci.* **2012**, *109* (50), 20292-20297; DOI: 10.1073/pnas.1108756108.
- Richards, R. K. Deepwater Mobile Oil Rigs in the Exclusive Economic Zone and the Uncertainty of Coastal State Jurisdiction. *J. Int'l Bus. & L.*. 2011, *10* (2), 387-412.
- Ryerson, T. B.; Camilli, R.; Kessler, J. D.; Kujawinski, E. B.; Reddy, C. M.; Valentine, D. L.; Atlas, E.; Blake, D. R.; de Gouw, J.; Meinardi, S.; Parrish, D. D.; Peischl, J.; Seewald, J. S.; Warneke, C. Chemical data quantify Deepwater Horizon hydrocarbon flow rate and environmental distribution. *Proc. Natl. Acad. Sci.* **2012**, *109* (50), 20246-20253; DOI: 10.1073/pnas.1110564109.
- Sammarco, P. W.; Kolian, S. R.; Warby, R. A.; Bouldin, J. L.; Subra, W. A.; Porter, S. A. Distribution and concentrations of petroleum hydrocarbons associated with the BP/Deepwater Horizon Oil Spill, Gulf of Mexico. *Mar. Pollut. Bull.* **2013**, *73* (1), 129-143; DOI: 10.1016/j.marpolbul.2013.05.029.
- Singer, M. M.; Aurand, D.; Bragin, G. E.; Clark, J. R.; Coelho, G. M.; Sowby, M. L.; Tjeerdema, R. S. Standardization of the preparation and quantitation of water-accommodated fractions of petroleum for toxicity testing. *Mar. Pollut. Bull.* **2000**, *40* (11), 1007-1016; DOI: 10.1016/S0025-326X(00)00045-X.
- Techtmann, S. M.; Zhuang, M.; Campo, P.; Holder, E.; Elk, M.; Hazen T. C., ... Santo Domingo, J. W. Corexit 9500 enhances oil biodegradation and changes active bacterial community structure of oil-enriched microcosms. *Appl. Environ. Microbiol.* **2017**, *83* (10), e03462-16; DOI: 10.1128/AEM.03462-16.
- Thompson, A. FAQ: The Science and History of Oil Spills. Live Science. **2010**. https://www.livescience.com/9885-faq-science-history-oil-spills.html. Accessed June 2019.
- Ting, M.; Kossin, J. P.; Camargo, S. J.; Li, C. Past and future hurricane intensity change along the US East Coast. *Scientific Reports*. **2019**. *9* (1), 7795; DOI: 10.1038/s41598-019-44252-w.
- US Coast Guard. On Scene Coordinator Report Deepwater Horizon Oil Spill. Submitted to the National Response Team. **2011**.

- US Fish and Wildlife Service. Deepwater Horizon Response Consolidated Fish and Wildlife Collection Report. **2011**. https://www.fws.gov/home/dhoilspill/pdfs/Consolidated% 20Wildlife%20Table%2001252011.pdf. Accessed June 2019.
- Valentine, D. L.; Kessler, J. D.; Redmond, M. C.; Mendes, S. D.; Heintz, M. B...Villanueva, C. J. Propane respiration jump-starts microbial response to a deep oil spill. *Science*. **2010**, *330* (6001), 208-211; DOI: 10.1126/science.1196830.
- Wade TL, Sweet ST, Sericano JL, Guinasso NL, Diercks A-R, Highsmith, R. C.; Asper, V. L.; ...Joye, S. B. Analyses of water samples from the Deepwater Horizon oil spill: Documentation of the subsurface plume. *Monitoring and Modeling the Deepwater Horizon Oil Spill: A Record-Breaking Enterprise*. **2011**, *195*, 77-82; DOI; 10.1029/2011GM001103.
- Wade, T. L.; Sericano, J. L.; Sweet, S. T.; Knap, A. H.; Guinasso Jr, N. L. Spatial and temporal distribution of water column total polycyclic aromatic hydrocarbons (PAH) and total petroleum hydrocarbons (TPH) from the Deepwater Horizon (Macondo) incident. *Mar. Pollut. Bull.* **2016**, *103* (1-2): 286-293; DOI: 10.1016/j.marpolbul.2015.12.002.
- Walker, A. H.; Scholz, D.; McPeek, M.; French-McCay, D.; Rowe, J.; Bock, M.; Robinson, H.; Wenning, R. Comparative risk assessment of spill response options for a deepwater oil well blowout: part III. Stakeholder engagement. *Mar. Pollut. Bull.* **2018**, *133*, 970-983; DOI: 10.1016/j.marpolbul.2018.05.009.
- Ward, C. P.; Armstrong, C. J.; Conmy, R. N.; French-McCay, D. P.; Reddy, C. M.. Photochemical oxidation of oil reduced the effectiveness of aerial dispersants applied in response to the Deepwater Horizon spill. *Environ. Sci. Technol. Lett.* **2018**, *5* (5), 226-231; DOI: 10.1021/acs.estlett.8b00084.
- Zahed, M. A.; Aziz, H. A.; Isa, M. H.; Mohajeri, L.; Mohajeri, S.; Kutty, S. R. M. Kinetic modeling and half life study on bioremediation of crude oil dispersed by Corexit 9500. *J. Hazard. Mater.* **2011**, *185* (2-3), 1027-1031; DOI: 10.1016/j.jhazmat.2010.10.009

CHAPTER 2

INSTANTANEOUS EFFECT OF COREXIT 9500A ON COMMUNITY BACTERIAL PROTEIN PRODUCTION AND HYDROCARBON OXIDATION RATES

2.1 Introduction

Oil slicks represent a danger to living organisms and coastal environments. Moving oil from a concentrated slick and dispersing it throughout a water column can reduce the slick's physical threats to megafauna due to oiling, and reduces the number of oil slicks reaching coastal environments. However, dispersing oil also increases the toxicity of oil to many members of the biological community (Rico-Martinez et al., 2013) and dispersed oil can still reach coastlines, fouling shorelines and marshes. Acute toxicity tests with the marine rotifer, *Brachionus plicatilis*, revealed that CEWAF was 52-fold more inhibitory than WAF or Corexit alone (Rico-Martinez et al., 2013). Similar synergistic effects of dispersant and oil toxicity have been observed in a variety of other organisms, including herring and rainbow trout embryos (Greer et al., 2012; Wu et al., 2012). Phytoplankton and bacterial toxicity were assessed using QwikLite and Microtox assays, respectively, in August of 2010 at various water column depths surrounding the DWH wellhead (Paul et al., 2013). The results showed phytoplankton toxicity in several subsurface stations (from 35 to 275 m), and bacterial toxicity in surface waters (Paul et al., 2013).

The rate of and extent to which Corexit components are degraded in the environment is debated. Campo et al. (2013) studied the degradation of Corexit and found that incubations with Corexit, oil, and bacteria performed at 25°C exhibited 99% removal of the DOSS after 14 days.

Abiotic degradation also occurred: after 28 days, killed controls at 25°C had only 10% of original DOSS remaining in the dispersed oil incubation, while 33% of DOSS remained within the same time frame in Corexit 9500 alone treatments (Campo et al., 2013). In contrast, laboratory incubation experiments performed by Kleindienst et al. (2015) and Seidel et al. (2016) analyzed DOM and found that DOSS and DOSS derived metabolites (with and without S) were detectable after six weeks of incubation.

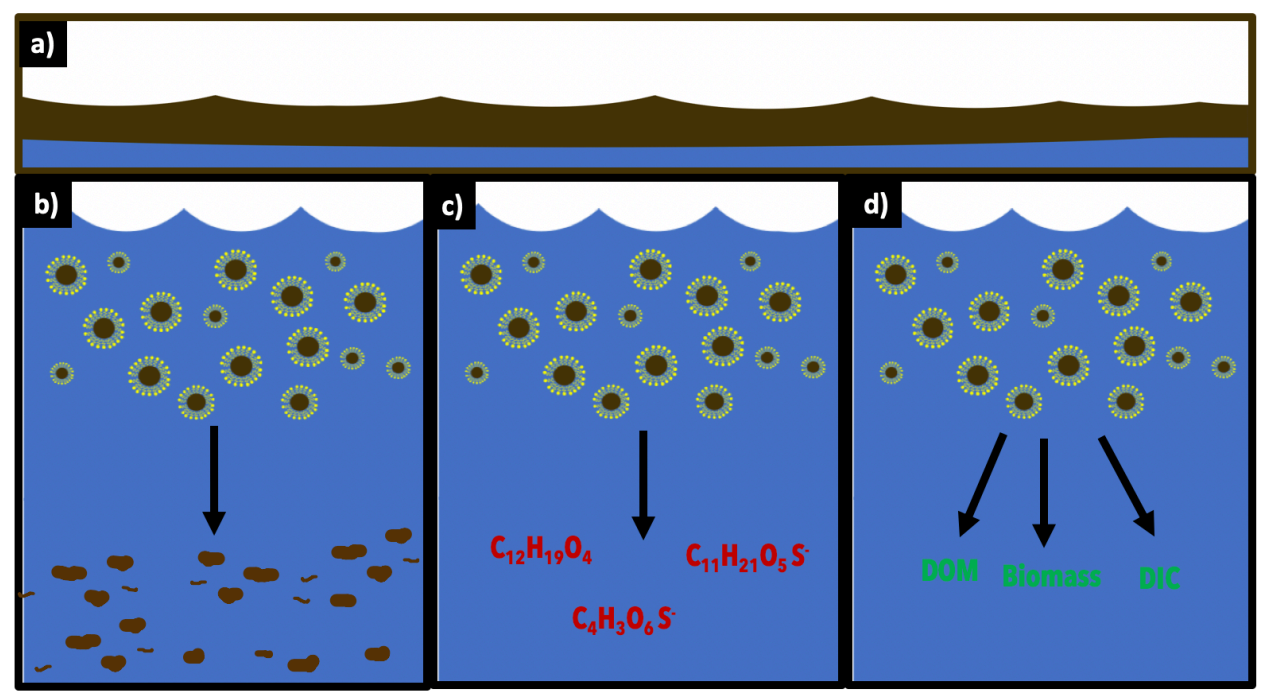


Figure 2.1: Possible outcomes of a) dispersant application to surface oil slick b) inhibited degradation leading to elevated oil snow, c) enhanced degradation but to incomplete, potentially toxic byproducts (Seidel et al., 2016) or d) enhanced degradation and complete/nonharmful degradation.

The impact of dispersants on microbial communities – whether it be stimulation, inhibition or toxicity – is unclear. Dispersants may alter the composition of microbial communities or the activity of particular organisms. Either effect could reduce the microbial community's ability to degrade dispersed oil, even though the oil may have a higher surface area and therefore presumably be more bioavailable when it is dispersed. In the wake of the DWH oil

spill, an intensive effort to assess whether applying chemical dispersants, such as Corexit 9500A, resulted in increased or inhibited oil biodegradation was undertaken. To this day, however, whether dispersing oil results in more rapid and efficient turnover of hydrocarbons, or ultimately a quicker rate of *complete* oil degradation, remains unclear due to confounding results observed in these studies. The conflicting results could be attributed to variations in experimental designs, differences in oil composition, or differences in initial microbial communities and/or the physicochemical conditions between the water samples examined. Nutrient limitation could constrain the oil degradation capability of microbial communities during spills like the DWH (Edwards et al., 2011).

At present, it is not possible to say what effect Corexit 9500 has on oil biodegradation. Variability in the experimental protocols that aimed to assess the efficacy of Corexit 9500 and differences in samples (nutrient or redox regime, temperature, oil properties, etc.) has led to conflicting reports and the specific reasons driving these differences remain unclear. This chapter assesses Corexit 9500's immediate effects on microbial community activity, as assessed through bacterial production, and attempts to identify the primary component of the surfactant that triggers the observed response. In parallel samples at one site (GC600 August sampling), I assessed the immediate effect of Corexit 9500 (concentrations at 10⁻⁴, 10⁻³, and 10⁻² g/L) on naphthalene and hexadecane potential oxidation rates.

2.2 Methods:

Description of Study Sites

Surface water was collected from four sites with contrasting water depth, distance from shoreline, and proximity to natural or anthropogenic hydrocarbon inputs. Movement of

tectonically active salt bodies beneath shallow sediments across the northern Gulf results in the formation of faults and fractures that facilitate hydrocarbon migration through sediments and into the water column (Conti et al., 2016). Site GC600 is a natural hydrocarbon seep site found at a water depth of 1250 m. Sediment carbonate content ranged between 2 and 6%. Sediment carbonate at GC600 occurs in large slabs (10's of cm to m across) and often these slabs contain biodegraded crude oil (Roberts et al., 2010). Due to persistent oil seepage, surface slicks of rainbow sheen, generally 1 µm thick, are often observed floating at GC600 (see Figure 2.2). For these experiments, water samples were collected within and outside of these slicks, allowing us to contrast the effects of dispersant in waters impacted by oiling. By comparing the response of within slick and outside of slick samples, we evaluated the potential for communities to be primed for oil degradation over even short time periods.

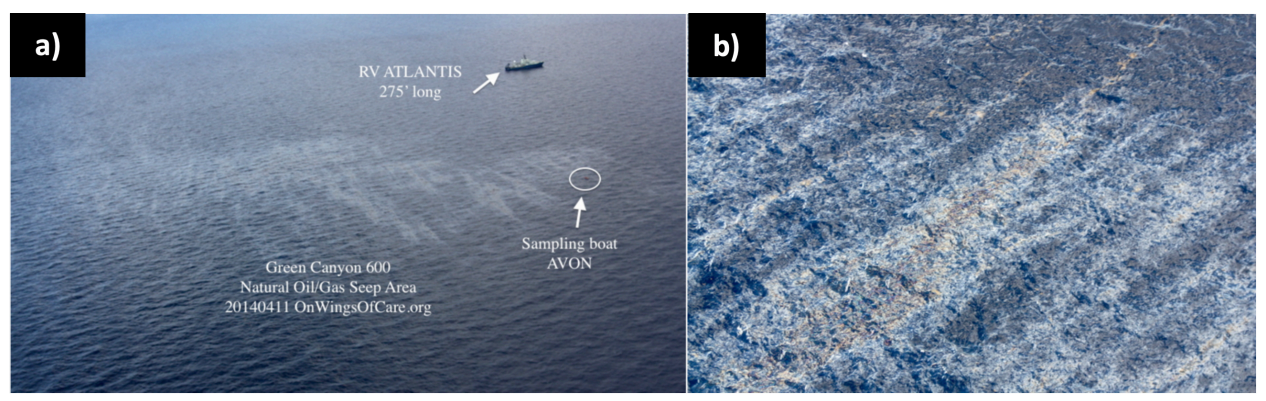


Figure 2.2: a) Natural oil/gas seep area observed at GC600 on April 11, 2014, b) close view of natural oil slick at GC600.

The DWH oil spill occurred in the east Mississippi Canyon area (lease block MC252, 28° 44.2' N, 88° 23.2' W), 77 km from the shoreline, where the seafloor and shallow subsurface sediment lie within the methane hydrate stability zone (Conti et al., 2016). The OC26 sampling site is approximately 5 km from the DWH spill site, on the western slope of the Gloria Dome at a water depth of 1,600 m, approximately 100 km southeast of the Birdsfoot delta of the Mississippi

River (Conti et al., 2016). Gas plumes near this site originate from long tension faults running along the edge of the dome (Conti et al., 2016).

The Taylor Energy sampling site is impacted by an on-going oil spill and is closer to shore, resulting in higher nutrient concentrations than the other two sites (Harrison, 2017). In 2004, the storm surge caused by Hurricane Ivan resulted in a regional slope failure, leading to the sinking of the Taylor Energy Company platform (23051) (Harrison, 2017). Despite the \$435 million dollar effort made by the Taylor Energy Company to decommission the platform and wells, an estimated 9 to 47 barrels (1,430-7,472 L) of oil (based on acoustic survey) or 19 to 108 barrels (3,021-17,170 L) of oil (based on bubblometer survey) continued to leak each day and create surface slicks until April 2019 (Mason et al., 2019). The site lies in an area with a water depth of about 150 m and has elevated nutrient levels due to its proximity to the Mississippi and Atchafalaya rivers.

GB480 served as a non-hydrocarbon influenced control site; the site is also well offshore so is oligotrophic.

Water Collection

Surface water was collected by bucket casts during three cruises, EN600 in June 2017, PE-18-06 in August 2017, and PE-18-08 in September 2017. Bucket casts were carried out by rinsing a clean 5 L HDPE plastic bucket three times with site water. All sample collection bottles were rinsed three times with site water from the clean bucket. Samples for total petroleum hydrocarbons (TPH) were collected in 1 L glass amber bottles and frozen immediately at -20 °C. DNA was collected in 5 L PETG bottles and filtered immediately. Water samples for rate measurements and nutrient processing were collected in 1 L glass amber bottles and stored at 4°C

until processing. On the EN600 cruise, water was collected from three lease blocks: GB480 at 27° 29.90'N, 91° 59.06'W, OC26 at 28° 42.234' N, 88° 21.629' W, GC600 at 27° 21.5387' N, 90° 33.682' W for outside the slick and 27° 22.245' N, 90° 33.566' W for inside the slick. At each site, samples were processed, amended, and treated – as described below – within 24 hours of collection. During the PE-18-06 cruise, water was collected from GC600 at 27° 22.2'N and 90° 34.14' W for out of slick and 27° 22.2' and 90° 34.14' for in slick sample. The Taylor Energy site (28° 59.509' N 88° 53.412' W for out of slick sample, 28° 56.401' N, 88° 57.864 W for in slick sample) was sampled on the PE-18-08 cruise. For the R/V Pelican expeditions, aside from TPH samples, which were frozen immediately, water was stored at 4°C, transported in coolers on blue ice, and processed, amended, and injected back in the UGA lab within three days of collection.

Initial Parameters

Water samples were collected for initial assessment of DNA, cell counts, DOC/nutrients, and TPH. For DNA, 5 L of water was filtered through a 0.2 µM Sterivex filter. The tubing was cleaned before and after sample processing using 10% bleach; the bleach rinse was followed by a copious milliQ water rinse and then a sterile-filtered seawater rinse. After filtration, filters were flash frozen in liquid nitrogen and stored at -80°C. Samples for cell counts were collected by transferring 9 mL of sample water (unfiltered) into a scintillation vial containing 1 mL of sterile-filtered 37% formaldehyde and freezing at -20°C. Samples for DOC and nutrients were collected by filtering approximately fifty mL of sample through a 0.2 µm target filter into 60 mL acid washed Nalgene bottles. Samples were frozen at -20°C upright and transported on dry ice (for EN600 samples).

Component Dilution Preparations

Component treatments were prepared for four Corexit 9500 components and whole Corexit 9500 to achieve final incubation concentrations of 10⁻⁹ g/L, 10⁻⁶ g/L, 10⁻³ g/L, 0.1 g/L. All components were dissolved in Milli-Q water at 10 g/L and then serially diluted. Due to the insolubility of bulk crude oil, a 10 g/L stock was mixed in the dark on a shaker table for 24 hours. The resulting WAF was subsampled and diluted serially to achieve the final amendment concentrations. 100 µL of each dilution was added to combusted 20 mL scint vials and covered with foil-lined caps until the experiment. An environmental control (no COREXIT added) and MQ control (100 µL MQ added) were also prepared. Next, 9.9 mL of sample seawater was added to each of the prepared vials and swirled gently to ensure thorough mixing. At sites where in slick and out of slick samples were collected (GC600 June and August sampling, and Taylor), concentration effects on bacterial production was only tested with in slick water.

Rates of Bacterial Production

Bacterial production rates in *in situ* samples and in the Corexit 9500/component amended samples were determined using the ³H-leucine incorporation method (Smith et al., 1992). Exactly 1.5 mL of *in situ* water or sample was added to a 2 mL plastic microcentrifuge tube. Three replicates and one killed control were included for each sample/treatment. Killed controls were achieved by adding 100 μL of trichloroacetic acid (100% TCA) prior to addition of 10⁶ DPM ³H-leucine. Samples were incubated in the dark at room temperature for three hours and then killed by adding 100 μL of TCA. Killed samples were stored at room temperature for up to two months before processing.

Samples were centrifuged at 10,300 RPM for 15 minutes to isolate the biomass pellet and the remaining liquid was aspirated. Then, 1.5 mL of 5% TCA was added to each sample before centrifuging again at 10,300 RPM for 5 minutes. The remaining liquid was again aspirated and 1.5 mL of eighty percent ethanol was added to each sample before centrifuging a final time at 10,300 RPM for 5 minutes. Ethanol was aspirated taking care to avoid the solid pellet and the sample was left uncapped to dry in the fume hood overnight. Once dry, 1.75 mL of scintillation fluid (BioSafe II Scintillation Cocktail; Fisher) was added to each sample; the sample was closed and vortexed, and placed into a plastic 20 mL scintillation vial. Samples were counted at for 5 minutes on a Beckman 6500 liquid scintillation counter. Bacterial production rates were calculated using the equation of Kirchman et al. (2001).

Hydrocarbon Oxidation

Samples for determining hydrocarbon oxidation rates were assessed in the presence of Corexit (final concentrations of 10⁻⁴, 10⁻³, and 10⁻² g/L) using water collected during the GC600 August sampling. Rates of hydrocarbon oxidation were determined using the methods described by Kleindienst et al. (2015) and Sibert et al. (2016) for ¹⁴C-hexadecane and ¹⁴C-napthalane oxidation. A 8.125 mL sample of COREXIT-amended or *in situ* water was added to a 7 mL glass scintillation vials. Each vial was sealed with PTFE Teflon lined septa and a screw cap. Care was taken to ensure that no bubbles were present in the sealed vials. Samples were injected with 10⁶ DPM of ¹⁴C hexadecane or naphthalene (10⁶ DPM per 20 μL, dissolved in molecular grade ethanol) using a glass syringe. Each sample was run in triplicate with a killed control. Killed controls were amended with radiotracer and immediately transferred to 50 mL plastic centrifuge tubes containing 2 mL 2 M NaOH. Killed vials were rinsed with basified tap water twice and

rinses were also added to the sample's plastic centrifuge tube. Live samples were incubated for two days in the dark at room temperature (21°C) and after incubation, each sample was terminated as per the killed controls.

To recover the product (¹⁴CO₂), samples were transferred to 250 mL Erlenmeyer flasks containing 1 gram of activated charcoal, and in the case of hexadecane samples, 250 mg of C₁₈ reverse phase silica gel, to trap the hydrocarbon tracer. Falcon tubes were rinsed with basified tap water and rinsate was added to the same glass flask. The flasks were then capped with rubber stoppers and clamps and shaken for at least 18 hours to allow unmetabolized tracer to bind to the charcoal/charcoal-silica mixture. Samples were removed from the shaker table and a carbon dioxide trap (7 mL glass scintillation vials containing a glass fiber filter soaked with 1.5 mL of CarboSorb (Perkin Elmer)) was secured within each flask, above the liquid sample. Samples were acidified with 5 mL of concentrated phosphoric acid, taking care to avoid the CO₂ traps, and quickly stoppered. Samples were allowed to shake overnight after which 4.5 mL of scintillation fluid was added to each trap. The sample was then counted on a Beckmann 9500 liquid scintillation counter for 5 minutes.

Dissolved Organic Carbon and Nutrient Collection and Analysis

In situ water was filtered using a 0.2 μm target filters and frozen and stored upright at -20°C. Target filters were rinsed with 20 mL of MQ and dried, and then rinsed with 5 mL of sample prior to sample filtration. Prior to freezing 2.5 mL of filtered sample was subsampled into 15 mL falcon tubes and preserved with 100 μL phenol at 4°C and ammonium was analyzed according to the colorimetric protocol described by Solorzano (1969). Samples were thawed to

analyze dissolved organic carbon (DOC), total dissolved nitrogen (TDN), ammonium (NH₄⁺), NO_x⁻, nitrite (NO₂⁻), and phosphate (HPO₄³⁻).

DOC was analyzed on a total organic carbon analyzer (Shimadzu TOC-Vcph). Samples were run in tandem with potassium hydrogen phthalate standards to determine concentrations. TDN was also measured using the Shimadzu analyzer (utilizing a TNM-1 module). Samples were run in tandem with glycine standards.

NO_x⁻ concentrations were determined using a vanadium reduction assembly, Antek 745, and chemiluminescent nitric acid detector, Antek 7050, as described by Braman and Hendrix (1989) and Garsie et al. (1982). Concentrations were determined by comparing sample peak area to peak areas of potassium nitrate standards. NO₂⁻ was determined by calorimetry (Bendschneider and Robinson, 1952). Finally, phosphate concentrations (PO₄³⁻) were determined using a molybdate blue calorimetric method (Solorzano and Sharp, 1980).

Statistical Analysis

Data was analyzed for possible outliers by comparing three times the standard deviation of replicate points with the possible outlier removed to the mean of the comparable points (with the possible outlier also omitted). If this mean minus the possible outlier was greater than three times the standard deviation (possible outlier omitted) the point was considered an outlier and removed from statistical analysis. JMP® Pro 14.1.0 Software was utilized to evaluate normal distribution, Spearman's rank sum correlation, and Wilcoxon/Kruskal-Wallis Test significance. All graphs were made using KaleidaGraph Version 4.5.4.

DNA Filtering, Extraction, and Sequencing

Five liters of *in situ* water was filtered using a peristaltic pump. The pump tubing was cleaned prior to each sample with 10% percent bleach, rinsed with milliQ, and finally sterile-filtered seawater before attaching 0.2 µm Sterivex filters to tubing. Four samples were filtered in parallel. After filtration, each filter was plugged with sterile putty at the bottom and a sealing cap at the top and flash frozen in liquid nitrogen before storing at -80°C.

To recover DNA for sequencing, samples were thawed on ice and extracted according to the DNAeasy kit instructions with minor modifications to enhance DNA recovery. Extraction yields were evaluated using a Nanodrop and gel imagining. No samples required amplification prior to sequencing. Extracted samples were sequenced at University of Illinois at Chicago's Sequencing Core (IUSQC).

2.3 Results and Discussions

In Situ Geochemical Characteristics

The in and out of slick samples at Taylor Energy had higher concentrations of DOC, TDN, NH₄, and PO₄ than the other sites (Table 2.1). DOC concentrations were higher in the slick conditions, compared to the out of slick site in the June GC600 and Taylor sampling. The average DOC difference between in slick and out of slick conditions was 27 µM across the Taylor Energy and GC600 June samplings. Nitrite was below detection limit in all samples.

All sites were nutrient limited (DOC:TDN > 6.6 and DOC:PO₄ > 106 based on the Redfield C: N: P (molar) ratio of 106: 16: 1) with the exception of Taylor Energy in slick water, which had an excess of PO₄. GB480, and GC600 June sampling (in and out of slick) were limited by nitrogen while OC26, GC600 August, and Taylor out of slick sites were phosphorus limited.

Table 2.1: Geochemical characteristics of in situ samples. BDL indicates below detection limit. NT indicates samples were not tested.

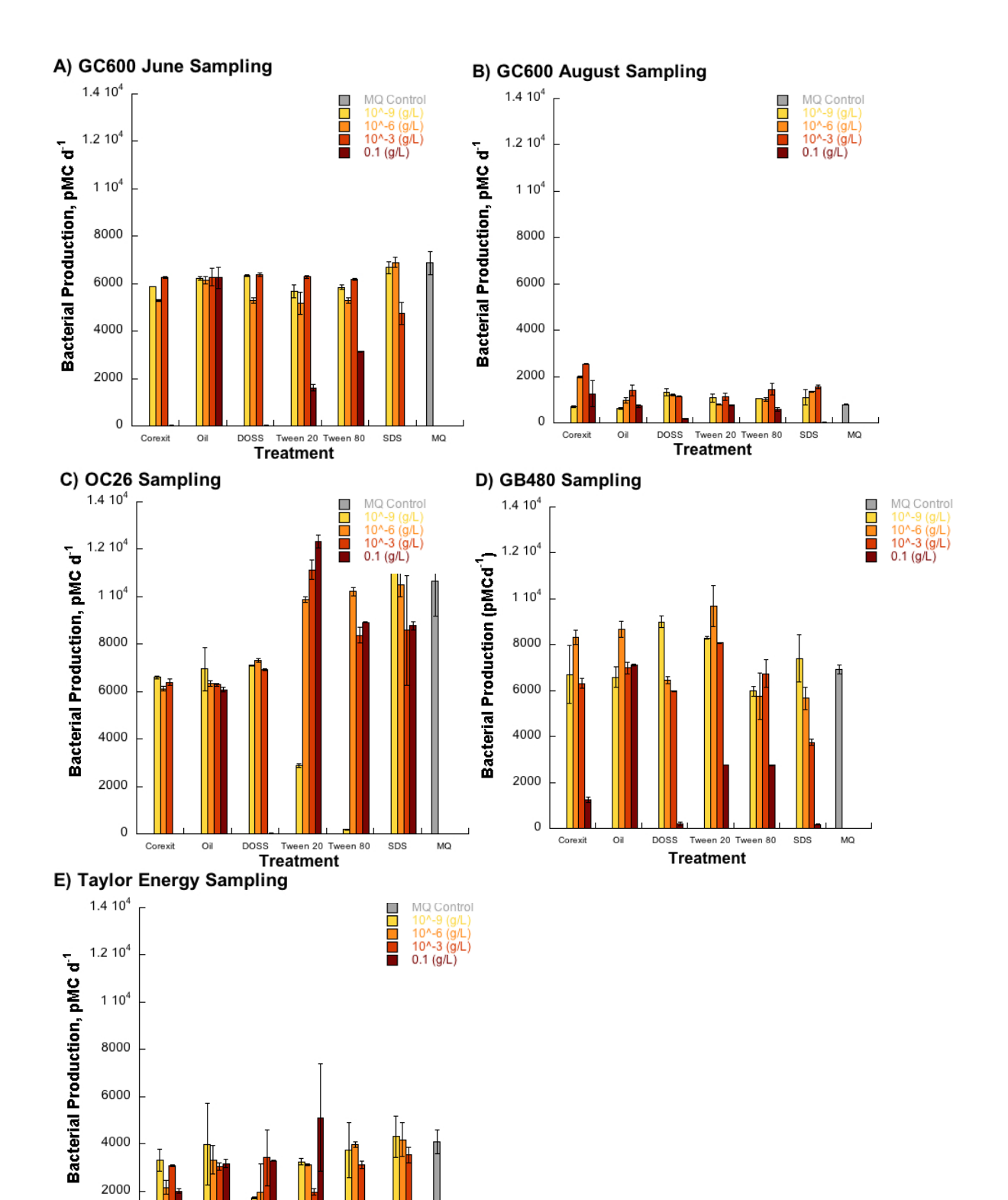
Site	Slick Present	DOC μM	TDN µM	NH4 μM	NOx μM	Nitrite µM	PO ₄ μM
GB480	NO	105	8	0.19	0.46	BDL	BDL
GC600 June	YES	121	6	0.12	1.24	BDL	BDL
GC600 June	NO	96	8	0.25	0.65	BDL	0.01
OC26	NO	116	6	0.32	0.59	BDL	0.18
GC600 August	YES	124	7	0	ND	BDL	0.76
GC600 August	NO	132	7	0.34	ND	BDL	0.58
Taylor	YES	179	15	1.73	ND	BDL	3.3
Taylor	NO	150	10	1.40	ND	BDL	1.25

Notes: BDL indicates below detection limit. ND = no data.

Instantaneous Bacterial Production Response

A Wilcoxon / Kruskal-Wallis Test indicated significantly different bacterial production responses across all sites when rates in each treatment and concentration were assessed by site (chi-square = 128.8195, df = 4, p = <0.0001). A following Wilcoxon Each Pair nonparametric test further indicated each site's unique response (p-values ranged from <0.0001-0.0098 in nonparametric comparisons for each pair using Wilcoxon method). This difference was even observed between the two sampling points at GC600 (June and August sampling) (p-value = <0.0001). Bacterial production rates were much lower during the GC600 August sampling with average unamended bacterial production rates measured as $1,186 \pm 615$ pMC/day in August versus the $8,628 \pm 591$ pMC/day measured in June. The bacterial production at the GC600 August sampling was similar to the Taylor sampling ($3,499 \pm 337$ pMC/day), which was also performed in the fall (September). This pattern could be due to a seasonal difference.

Figure 2.3: Average bacterial production rates with increasing concentrations of Corexit and Corexit components (DOSS, Tween 20, Tween 80, and SDS). Bars represent standard deviation. Grey indicates MQ control condition, yellow indicates 10^{-9} g/L addition, orange 10^{-6} g/L, red 10^{-3} g/L, and maroon 0.1 g/L.



0

Corexit

Oil

DOSS Tween 20Tween 80

Treatment

SDS

Table 2.2: Spearman's rank sum analysis of concentration and bacterial production correlation. Asterisks (*) indicate significant negative relationship.

Site	Treatment	Rho	Prob> p
GB480	Corexit	-0.5047	0.1133
	Oil	0.4431	0.1996
	DOSS	-0.8736	0.0002*
	Tween 20	-0.2954	0.4073
	Tween 80	-0.4630	0.1515
	SDS	-0.9093	<0.0001*
GC600 June	Corexit	-0.7629	0.0063*
	Oil	-0.3816	0.1983
	DOSS	-0.7617	0.0025*
	Tween 20	-0.7154	0.0040*
	Tween 80	-0.7611	0.0065*
	SDS	-0.8454	0.0005*
GC600 August	Corexit	0.5834	0.0595
	Oil	0.1969	0.5855
	DOSS	-0.3751	0.2557
	Tween 20	-0.1204	0.7244
	Tween 80	0.0278	0.9354
_	SDS	-0.2478	0.4375
Taylor	Corexit	-0.7733	0.0052*
	Oil	-0.5295	0.0627
	DOSS	-0.1426	0.6583
	Tween 20	-0.1605	0.6184
	Tween 80	-0.7025	0.0109
_	SDS	-0.6458	0.0126
OC26	Corexit	-0.8890	0.0006*
	Oil	-0.1607	0.6177
	DOSS	-0.9159	<0.0001*
	Tween 20	0.6401	0.0462
	Tween 80	-0.0648	0.8498
,	SDS	-0.6775	0.0155

Notes: * indicates negative significant correlation according to Spearman's rank correlation.

Despite the unique responses observed at each site, certain trends were apparent across sites. A Spearman's Rank Correlation test was performed for each treatment, at each site (Table 2.2). A negative correlation between Corexit concentration and bacterial production was observed in the Taylor, OC26, and GC600 June incubations (Table 2.2). Average bacterial

production rate with the addition of Corexit 9500 at 0.1 g/L during the Taylor, OC26, and GC600 June sampling were $2,000 \pm 83$ pM C/day, 0 ± 19 pM C/day, and 0 ± 52 pM C/day respectively, in comparison to the average bacterial production rates in the control condition of these site's incubations, $4,081 \pm 492$ pM C/day, $10,642 \pm 1474$ pM C/day, and $6,883 \pm 486$ pM C/day respectively.

Similarly, a negative correlation between DOSS concentration and bacterial production was observed during the GC600 June, GB480, and OC26 incubations (Table 2.2). DOSS concentrations at 0.1~g/L resulted in almost total inhibition of communities at these sites. Average bacterial production rate with the addition of DOSS at 0.1~g/L during the GC600 June, GB480, and OC26 samplings were $0\pm30.58~pM$ C/day, $197\pm60~pM$ C/day, $0\pm34~pM$ C/day respectively, in comparison to the average bacterial production rates in the control condition of these site's incubations, $6,883\pm486~pM$ C/day, $6,926\pm206~pM$ C/day, $10,642\pm1,474~pM$ C/day. The GC600 August sampling did not illustrate a significant correlation between DOSS concentration and bacterial production, even though bacterial production with the addition of 0.1~g/L DOSS resulted in bacterial production rate of $180\pm12~pM$ C/day in comparison to the average control rate of $798\pm15~pM$ C/day. This is because slight promotion of bacterial production occurred at the lower concentration additions (Figure 2.3). A similar increase in bacterial production occurred with the addition of low concentrations of DOSS at GB480 (Figure 2.3).

DOSS concentrations present during the BP oil spill cleanup efforts are unclear. DOSS concentrations in water taken near the wellhead at the surface ranged from below detection limit to 2.29×10^{-4} g/L (229 µg/L) when quantified between May 27 and June 2, 2010 (Gray et al., 2014). These DOSS measurements were not reported in conjunction with surface dispersant

application records however so it is challenging to conclude whether this patchiness captured the full range of DOSS concentrations. The concentration of DOSS immediately after a dispersant application event is not known. Regardless of DOSS' (and other components of Corexit) degradability and diffusion through the water column, this analysis of bacterial production response to various component concentrations indicates that even if Corexit can be quickly degraded or concentrations diminished by water column mixing, immediate effects on the bacterial community activity occur. Overall a Kruskal-Wallis rank sum test detected a significant difference in bacterial production response to amendment concentration when rates from all sites were collated by concentration (Kruskal-Wallis chi-squared = 38.5917, df = 5, p-value = <0.0001).

It is also possible that high concentrations of Corexit or its components interfere with the recovery of incorporated leucine. This is extremely unlikely as even at the highest concentrations of Corexit or its components, at least one site showed no difference in bacterial production rates in the highest Corexit dose when compared to the control; this possibility will be evaluated directly in the future.

Potential Hydrocarbon Oxidation Rates

A Wilcoxon / Kruskal-Wallis Test indicated a significant difference in potential naphthalene oxidation rates between in slick and out of slick samples (chi-square = 9.7287, DF = 1, p = 0.0018). A Spearman's Rank sum test indicated no correlation between Corexit concentration and resulting naphthalene oxidation potential rate in out of slick samples (rho=-0.2515, p=0.5139). There was also no correlation observed between Corexit concentration and the naphthalene oxidation potential rate in the in slick samples (rho=-0.4670, p=0.2050).

However significant inhibition of potential naphthalene oxidation rates occurred in the highest Corexit addition (0.01 g/L) to in slick samples. While the MQ control potential naphthalene oxidation rate was 0.008 ± 0.0003 pM C/day, the 0.01 g/L Corexit amended sample had a rate of 0.001 ± 0.0001 pM C/day. This inhibition was not observed in the out of slick sampling where the MQ control had a rate of 0.012 ± 0.0002 pM C/day in comparison to the 0.01 g/L rate of 0.011 ± 0.0001 pM C/day.

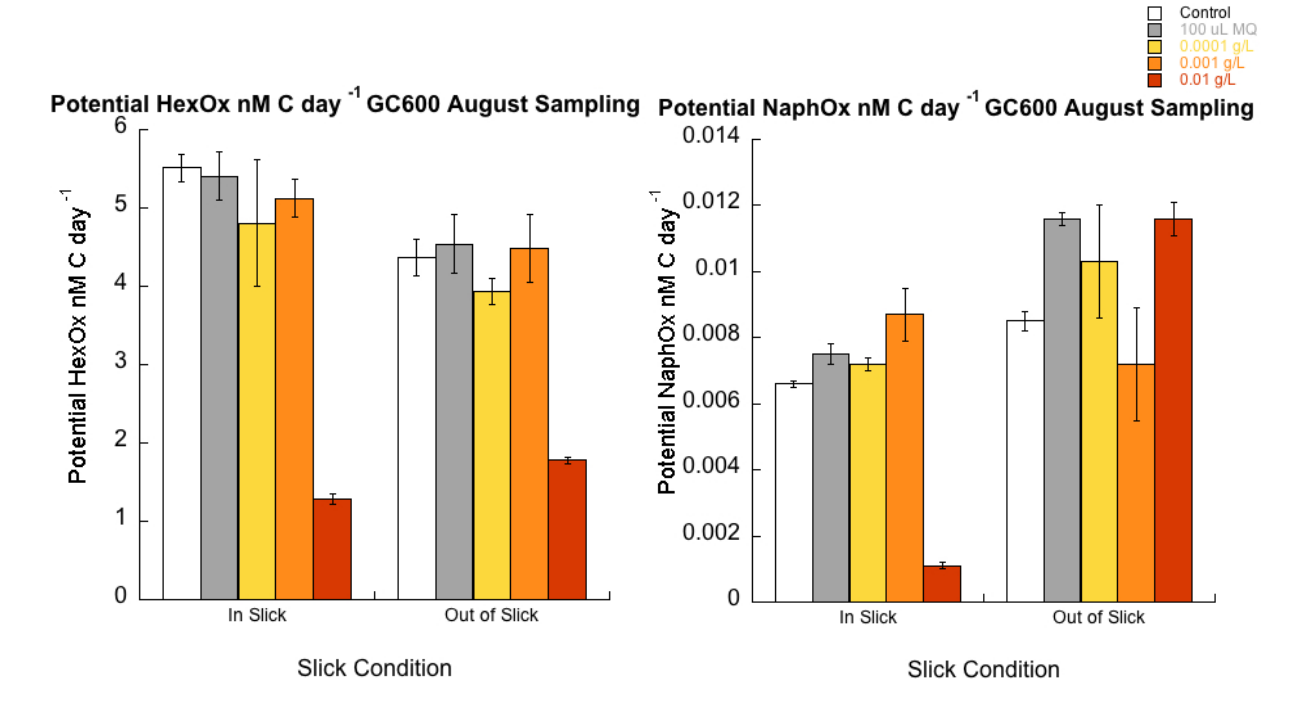


Figure 2.4: Average hexadecane and naphthalene oxidation potential rates (measured in nM carbon per day) with additions increasing Corexit concentrations. Bars represent standard deviation. White bars indicate no amendment, grey indicates MQ control condition, yellow indicates 10^{-4} g/L addition, orange 10^{-3} g/L, and red 10^{-2} g/L.

No significant difference in hexadecane oxidation rates was observed between in slick and out of slick samples when comparing all Corexit concentrations (chi-square = 3.4021, df = 1, p = 0.0644). A negative relationship between Corexit concentration and potential hexadecane oxidation rate was observed with in slick incubations (rho=-0.7504, p=0.0124). A negative relationship between Corexit concentration and potential hexadecane oxidation rate was

observed when both in slick and out of slick rates where combined (rho=-0.5883, p=0.0064). No correlation was found in the out of slick samples between Corexit concentration and potential hexadecane oxidation rate (rho=-.5065, p=0.1352). Despite this, out of slick samples still showed inhibition of potential hexadecane oxidation rates at the 0.01 g/L concentration with average out of slick MQ control rates equaling 4.54 ± 0.38 pM C/day, and 0.01 g/L addition equaling 1.78 ± 0.04 pM C/day.

2.4 Conclusions

Trends in Bacterial Production

A negative correlation between DOSS concentration and bacterial production was observed in GB480, OC26, and the June GC600 incubations. The Taylor and August GC600 incubations did not show this same pattern. Taylor incubation water was characterized by elevated ammonium concentrations and both Taylor and August GC600 incubation water had elevated phosphate concentrations. The Taylor and August GC600 incubations showed no correlation of any component concentration (Corexit, SDS, oil, Tweens etc.) with bacterial production, except Corexit additions to the Taylor incubation. This could perhaps be in part due to these sites' elevated nutrient concentrations allowing for more efficient degradation of Corexit and its components, as has been observed with oil degradation (Edwards et al., 2011) and in other surface water dispersant addition experiments from the Gulf of Mexico (Malkin et al., In Review).

Oil additions did not inhibit or stimulate bacterial production immediately in any of the incubations (Figure 2.3). This is similar to findings by Kleindienst et al. (2015a) who saw no significant difference in bacterial production between control, WAF, Corexit, and CEWAF (with

and without nutrients) at the initial sampling time point, though elevated bacterial production was observed after two and a half weeks had passed in the WAF treatment.

Trends in hydrocarbon oxidation

Overall potential naphthalene oxidation rates were significantly lower than potential hexadecane oxidation rates. Initial hydrocarbon concentrations may dictate naphthalene oxidation rates. Since the bacterial communities in slick vs. out of slick samples had limited differences in community composition, the difference in behavior between in slick and out of slick response could result from differential carbon (oil) exposure.

The introduction of Corexit did not equally inhibit/promote naphthalene and hexadecane oxidation rates. This may indicate differential effects on individual members of the microbial community. Since Corexit additions did not reduce bacterial production in the August GC600 sampling (the same site in which the hydrocarbon oxidation experiments were run) it is likely that reduction of oxidation rates was due to inhibition rather than toxicity. To evaluate why differences in in slick and out of slick responses to Corexit additions, initial bacterial community composition and characteristics should be considered. Introduction of crude oil has repeatedly been shown to result in blooms of hydrocarbon metabolizing bacteria, most typically:

Alcanivorax, Marinobacter*, Thallassolituus*, Cycloclasticus*, Oleispira* (Yakimov et al., 2007).

Since these samples were collected from a seep site, it is likely these bacteria were more common. The range of hydrocarbons metabolized by each microorganism is typically restricted to a narrow range of chain lengths and structures. Cycloclasticus* spp. metabolize naphthalene, phenanthrene, anthracene, and toluene (Dyksterhouse et al., 1995). Alcanivorax borkumenis oxidizes an "exceptionally broad range" of hydrocarbons, such as linear (C5–C16 alkanes),

isoprenoids, alkylarenes, and alkylcycloalkanes (Kleindienst et al., 2015b; Yakimov et al., 1998). These species are not equally affected by dispersants or dispersed oil. *Cyclocasticus spp.* have been shown to be elevated in dispersant treated bottle experiments in comparison to *Marinobacter* (Kleindienst et al., 2015a). This genus specific response to Corexit or dispersed oil may help explain the differences between in slick and out of slick samples to increasing Corexit concentrations.

Oil Spill Response Implications

Immediate effects of Corexit and Corexit components were observed even within a relatively short incubation period of three hours. Though it is not possible to conclude whether the reductions in bacterial production with certain component concentrations at certain sites were due to inhibition or mortality, it does demonstrate clearly that community behavior changes immediately after Corexit application. Similar findings have been previously observed by Doyle et al. (2018) who observed significant shifts in microbial community composition occur within a few hours of dispersant introduction to surface water communities. Dispersant application could thus quickly generate microbial communities better or less equipped to react to new inputs of carbon, such as oil, which could impact the ultimate fate of spilled oil.

Additionally, the observed site specific trends in bacterial production response to Corexit and component additions indicate the importance of nutrient dynamics and initial bacterial community structure in evaluating the impacts of Corexit on oil biodegradation potential. The site specific response supports the idea that differences in findings across studies working to evaluate how Corexit impacts oil biodegradation are in part due to differences in nutrient availability and community structure. Contingency plan development and delineation of "Preauthorization Areas" thus may benefit from site specific dispersant toxicity/response evaluations.

2.5 References

- Bendschneider K.; Robinson R.J. A new spectrophotometric method for the determination of nitrite in sea water. *University of Washington Oceanographic Laboratories*. **1952**.
- Braman, R.S.; Hendrix, S.A. Nanogram nitrite and nitrate determination in environmental and biological materials by vanadium (III) reduction with chemiluminescence detection. *Am. J. Analyt. Chem.* **1989**, *61* (24), 2715-8.
- Campo, P.; Venosa, A. D.; Suidan, M. T. Biodegradability of Corexit 9500 and dispersed South Louisiana crude oil at 5 and 25 °C. *Environ. Sci. Technol.* **2013**, **47** (4), 1960-1967; DOI: 10.1021/es303881h.
- Conti, A.; D'Emidio, M.; Macelloni, L.; Lutken, C.; Asper, V.; Woosley, R. J.; Diercks, A.; Highsmith, R. C. Morpho-acoustic characterization of natural seepage features near the Macondo Wellhead (ECOGIG site OC26, Gulf of Mexico). *Deep Sea Res. Part II Top. Stud. Oceanogr.* **2016**, *129*, 53-65; DOI: 10.1016/j.dsr2.2015.11.011.
- Doyle, S. M.; Whitaker, E. A.; De Pascuale V.; Wade, T. L.; Knap, A.H.; Santschi, P. H.; Quigg, A.; Sylvan, J. B. Rapid formation of microbe-oil aggregates and changes in community composition in coastal surface water following exposure to oil and the dispersant Corexit. *Frontiers in microbiology.* **2018**, *9*: 689; DOI: 10.3389/fmicb.2018.00689.
- Dyksterhouse, S.E.; Gray, J.P.; Herwig, R.P.; Lara, J.C.; Staley, J.T. Cycloclasticus pugetii gen. nov., sp. nov., an aromatic hydrocarbon-degrading bacterium from marine sediments. *Int. J. Syst. and Evol.* **1995**, *45* (1), 116-123. DOI: 10.1099/00207713-45-1-116.
- Edwards, B. R.; Reddy, C. M; Camilli, R.; Carmichael, C.A.; Longnecker, K.; Van Mooy, B. A. S. Rapid microbial respiration of oil from the Deepwater Horizon spill in offshore surface waters of the Gulf of Mexico. *Environ. Res. Lett.* **2011**, *6* (3): 035301; DOI: 10.1088/1748-9326/6/3/035301
- Gray, J. L.; Kanagy, L. K.; Furlong, E. T.; Kanagy, C. J.; McCoy, J. W.; Mason, A.; Lauenstein, G. Presence of the Corexit component dioctyl sodium sulfosuccinate in Gulf of Mexico waters after the 2010 Deepwater Horizon oil spill. *Chemosphere*. **2014**, *95*, 124-130. DOI: 10.1016/j.chemosphere.2013.08.049.
- Greer CD, Hodson PV, Li Z, King T, Lee KJEt, et al. 2012. Toxicity of crude oil chemically dispersed in a wave tank to embryos of Atlantic herring (Clupea harengus). *Environ. Toxicol. Chem.* **2012**, 31 (6), 1324-1333. DOI: 10.1002/etc.1828.
- Harrison, S. J. Lessons from the Taylor energy oil spill: history, seasonality, and nutrient limitation. M. S. Thesis. University of Georgia, Athens, GA, 2017.

- Hu L.; Yvon-Lewis, S. A.; Kessler, J. D.; MacDonald, I. R. Methane fluxes to the atmosphere from deepwater hydrocarbon seeps in the northern Gulf of Mexico. *Journal of Geophysical Research: Oceans.* **2012**; *117* (C1); DOI: 10.1029/2011JC007208.
- Kirchman, D. Measuring Bacterial Biomass Production and Growth Rates from Leucine Incorporation in Natural Aquatic Environments. *Methods Microbiol.* **2001**, 30, 227–237.
- Kleindienst, S.; Seidel, M.; Ziervogel, K.; Grim, S.; Loftis, K.; K.; Harrison, S.; Malkin, S. Y.; Perkins, M. J.; Field, J.; Sogin, M. L.; Dittmar, T.; Passow, U.; Medeiros, P. M.; Joye, S. B. Chemical dispersants can suppress the activity of natural oil-degrading microorganisms. *Proc. Natl. Acad. Sci.* **2015a**, *112* (48), 14900-14905; DOI: 10.1073/pnas.1507380112.
- Kleindienst, S.; Paul, J. H.; Joye, S. B. Using dispersants after oil spills: impacts on the composition and activity of microbial communities. *Nat. Rev. Microbiol.* **2015b**, *13* (6), 388-396; DOI: 10.1038/nrmicro3452.
- Malkin, S.; Saxton, M.; Harrison, S.; Sweet, J.; Passow, U.; Joye, S. Remarkable variability in microbial hydrocarbon oxidation rates in offshore surface waters in Gulf of Mexico. *Anthropocene*. In Review.
- Mason, C. F. Policy Brief—Regulating Offshore Oil and Gas Exploration: Insights from the Deepwater Horizon Experience in the Gulf of Mexico. *Rev. of Environ. Econ. and Pol.* **2019**, *13* (1), 149-154; DOI: 10.1093/reep/rey018
- Paul, J. H.; Hollander D.; Coble, P.; Daly, K. L.; Murasko S.; English, D.; Basso, J.; Delaney, J.; McDaniel, L.; Kovach, C. W. Toxicity and mutagenicity of Gulf of Mexico waters during and after the Deepwater Horizon oil spill. *Environ. Sci. Technol.* **2013**. *47* (17), 9651-9659; DOI: 10.1021/es401761h.
- Rico-Martínez, R.; Snell, T. W.; Shearer, T. L. Synergistic toxicity of Macondo crude oil and dispersant Corexit 9500A® to the Brachionus plicatilis species complex (Rotifera). *Environ. Pollut.* **2013**, 173, 5-10; DOI: 10.1016/j.envpol.2012.09.024
- Roberts, H. H.; Feng, D.; Joye, S. B. Cold-seep carbonates of the middle and lower continental slope, northern Gulf of Mexico. *Deep Sea Res. Part II Top. Stud. Oceanogr.* **2010**, *57* (21-23), 2040-2054; DOI: 10.1016/j.dsr2.2010.09.003.
- Seidel, M; Kleindienst, S.; Dittmar, T; Joye, S. B; Medeiros, P. M. 2016. Biodegradation of crude oil and dispersants in deep seawater from the Gulf of Mexico: Insights from ultra-high resolution mass spectrometry. *Deep Sea Res. Part II Top. Stud. Oceanogr.* **2016**, *129*, 108-118; DOI: 10.1016/j.dsr2.2015.05.012.
- Sibert, R.; Harrison, S.; Joye, S. B. Protocols for Radiotracer Estimation of Primary Hydrocarbon Oxidation in Oxygenated Seawater. *Hydrocarbon and Lipid Microbiology Protocols*. **2016**, 263-276.

- Smith, D. C.; Azam, F. J. A simple, economical method for measuring bacterial protein synthesis rates in seawater using 3H-leucine. *Mar. Microb. Food Webs.* **1992**, *6*(2), 107-114.
- Solorzano, L. Determination of ammonia in natural waters by phenolhypochlorite method. *Limnol. Ocean.* **1969**, *9*, 799-801.
- Solorzano, L.; Sharp, J. H. Determination of Total Dissolved Phosphorous and Particulate Phosphorous in Natural Waters. *Limnol. Ocean.* **1980**, *25* (4), 754–758.
- Wu ,D.; Wang, Z.; Hollebone, B.; McIntosh, S.; King, T.; Hodson, P. T. Comparative toxicity of four chemically dispersed and undispersed crude oils to rainbow trout embryos. *Environ. Toxicol. and Chem.* **2012**, *31* (4), 754-765; DOI: 10.1002/etc.1739.
- Yakimov, M. M.; Timmis, K. N.; Golyshin, P. N. Obligate oil-degrading marine bacteria. *Curr. Opin. Biotechnol.* **2007**, *18* (3), 257-266; DOI: 10.1016/j.copbio.2007.04.006.

CHAPTER 3

EFFECTS OF IMPRICISE COREXIT APPLICATION ON SUBSEQUENT CAPACITY FOR OIL BIODEGRADATION

3.1 Introduction

Application of chemical dispersants was a prominent response measure during the Deepwater Horizon (DWH) oil spill. To evaluate and maximize dispersant application efficiency during the DWH response, a portion of the dispersant application efforts were directed with the Special Monitoring of Applied Response Technologies (SMART) dispersant monitoring model. SMART was first established in 1997 as an interagency effort – U.S. Coast Guard (USCG), the National Oceanic and Atmospheric Administration (NOAA), Environmental Protection Agency (EPA), and Center for Disease Control (CDC) – to establish guidelines for monitoring and implementing response technologies (Parscal et al., 2014). Following this first iteration of SMART, several refinements were made in response to various issues that came to light during oil spill response efforts, with the most recent iteration implemented in 2006 (Parscal et al., 2014).

The 2006 SMART dispersant monitoring module outlines three tiers of monitoring (U.S. Coast Guard et al., 2006). Tier One involves visual observations by a SMART trained observer. The observer takes pictures and videos, using recommended guides such as the NOAA Dispersant Application Observer Job Aid for consistency (USCG et al., 2006). Tier Two supplements the visual observations of Tier One with onsite water sampling. Tier Three further adds to the analysis of Tier I and II by evaluating dispersed oil movement within the water

column by collecting water samples along transects or at different depths (USCG et al., 2006). Of the 412 dispersant sortic efforts made in response to DWH, 118 were SMART missions. Of this 118, 77 were Tier I, 30 were Tier II/III, and 11 were Tier III+ (USCG et al., 2006).

Since SMART had never before been utilized during a spill of national significance, several issues quickly arose (Parscal et al., 2014). SMART protocols were intentionally left vague to allow rapid inclusion of developing response technology (Parscal et al., 2014). However, this resulted in a lack of well-defined field protocols and the need for SMART response teams to improvise and develop solutions quickly in response. Some of the solutions that were developed quickly – but not fully vetted before implementation – may have resulted in inaccurate identification of candidate slicks. For example, during early SMART missions, USCG SMART teams developed a sampling pump that was easily contaminated as residual oil adhered within the hose (Parscal et al., 2014). Data analysis and data quality constraints were not specified within SMART and this resulted in non-uniform data analysis. By the end of surface dispersant application, this issue was resolved so that collected data could be evaluated in a consistent manner. However, the initial problems resulted in inconsistent or inappropriate dispersant application (Parscal et al., 2014). About one fourth of total dispersant missions were associated with SMART analysis, and the extent to which dispersant application at the surface resulted in efficient (>50%) dispersal of oil was deemed inconclusive (Lehr et al., 2010). Moreover, it is likely that "some sprayed dispersant missed oil slicks entirely" (Lehr et al., 2010).

Although numerous research efforts have been made to investigate dispersant efficiency and dispersant application effects on surrounding microbial community's ability to degrade spilled oil, studies have not investigated the implications of imprecise dispersant application. We

anticipated that when waters are "preconditioned" with Corexit 9500 prior to oil introduction, as would occur in the case of imprecise surface dispersant application, the resulting bacterial communities may not be able to degrade bulk crude oil as efficiently as native water samples, i.e. lacking previous exposure to Corexit 9500.

To evaluate whether pre-exposure to chemical dispersant resulted in community shifts that altered the hydrocarbon degradation capacity, we conducted preconditioning experiments at three sites with different microbial communities and nutrient characteristics within the Gulf of Mexico (Taylor Energy, OC26, and GC600). Nutrient amendments were performed for all treatments to further evaluate the controlling factors and to determine whether nutrient limitation influenced dispersant effectiveness or preconditioning response.

3.2 Methods

Description of Sampling Sites

Incubations were conducted with surface water from three contrasting Gulf of Mexico sites: Taylor Energy, OC26, and GC600. Site GC600 is a vigorous natural oil seep that occurs offshore in blue water. Site OC26 was chosen because of its proximity to the DWH oil spill site. Like GC600, OC26 is oligotrophic but OC26 is not near a vigorous seep. Taylor Energy is an anthropogenic discharge site with a water depth of 150 m. Due to its proximity to the shore and the Mississippi River, nutrient concentrations are elevated at this site. Microorganisms in offshore waters, especially in the Gulf, have been shown to be limited phosphorus limited (Pomeroy et al., 1995; Edwards et al., 2011).

Water Collection and Storage

Water was for the Taylor Energy and OC26 trials of the experiment on PE-18-08 during September 2017. Taylor incubation water at 28° 55.295'N, 88° 56.698'W and OC26 incubation water at 28° 40.706'N, 88° 21.403'W. The details of water sampling are presented in Section 2.2.

WAF, CEWAF, and Corexit Preparation

WAFs, CEWAFs, and Corexit amendments were prepared following Kleindienst et al. (2015) methods. Seawater was sterile-filtered with Millipore Express PLUS 0.22 µm filters and then pasteurized at 65°C for 2 hours. Once the water cooled to room temperature, oil, Corexit 9500, or oil + Corexit 9500 were added to prepare water accommodated fractions of oil, Corexit oil, and oil plus Corexit solutions. The oil WAF (WAF) treatment was prepared by adding 0.15 L Macondo surrogate oil to 0.85 L of prepared sterile filtered and pasteurized seawater. The Corexit WAF (Corexit) was made by adding 0.015 L of Corexit to 0.85 L of sterile seawater. The oil+Corexit WAF (CEWAF) treatment was prepared by adding 0.015 L of Corexit 9500 and 0.15 L of Macondo surrogate oil to 0.85 L of sterile seawater. All treatments were wrapped in aluminum foil and mixed for 48 hours in the dark at room temperature.

After 48 hours, solutions were transferred to combusted separatory funnels and allowed to settle for one hour. The water-soluble fraction was then separated into combusted glass bottles and stored at 20°C. Within two days total organic carbon (TOC) was analyzed (using a Shimadzu TOC-Vcph) to allow for standardized TOC addition to all microcosms at environmentally relevant concentrations (~400 µM TOC) (Kleindienst et al., 2015). TOC concentrations were analyzed on unfiltered samples because the solutions contained both small droplets of oil and aqueous phase oil, i.e. truly dissolved oil, and we aimed to add both components to the experimental treatments.

Microcosm Preparation and Sampling

Microcosms were prepared in combusted and autoclaved 2 L glass Schott bottles with Teflon lined caps. All treatments received an amendment of either dispersant-derived, oilderived, or dispersant and dispersed oil-derived organic carbon to result in equal TOC concentrations in all carbon amended treatments. The total sample volume was 1.8 L. CEWAF and Corexit solution additions varied slightly between experiments due to small variations in prepared Corexit, WAF, and CEWAF TOC concentration. Corexit, WAF, and CEWAF treatments were thus diluted with ambient surface sea water and/or sterile filtered and pasteurized surface sea water. Nutrient amended samples were prepared to achieve a $10~\mu M$ ammonium chloride and $1~\mu M$ and potassium phosphate concentration increase. Three replicate bottles were prepared for each treatment with the exception of the Control condition (no carbon or nutrient amendment) which had four treatment bottles prepared, allowing for the extra bottle to be used for the Time 0 DNA (See Figure 3.1).

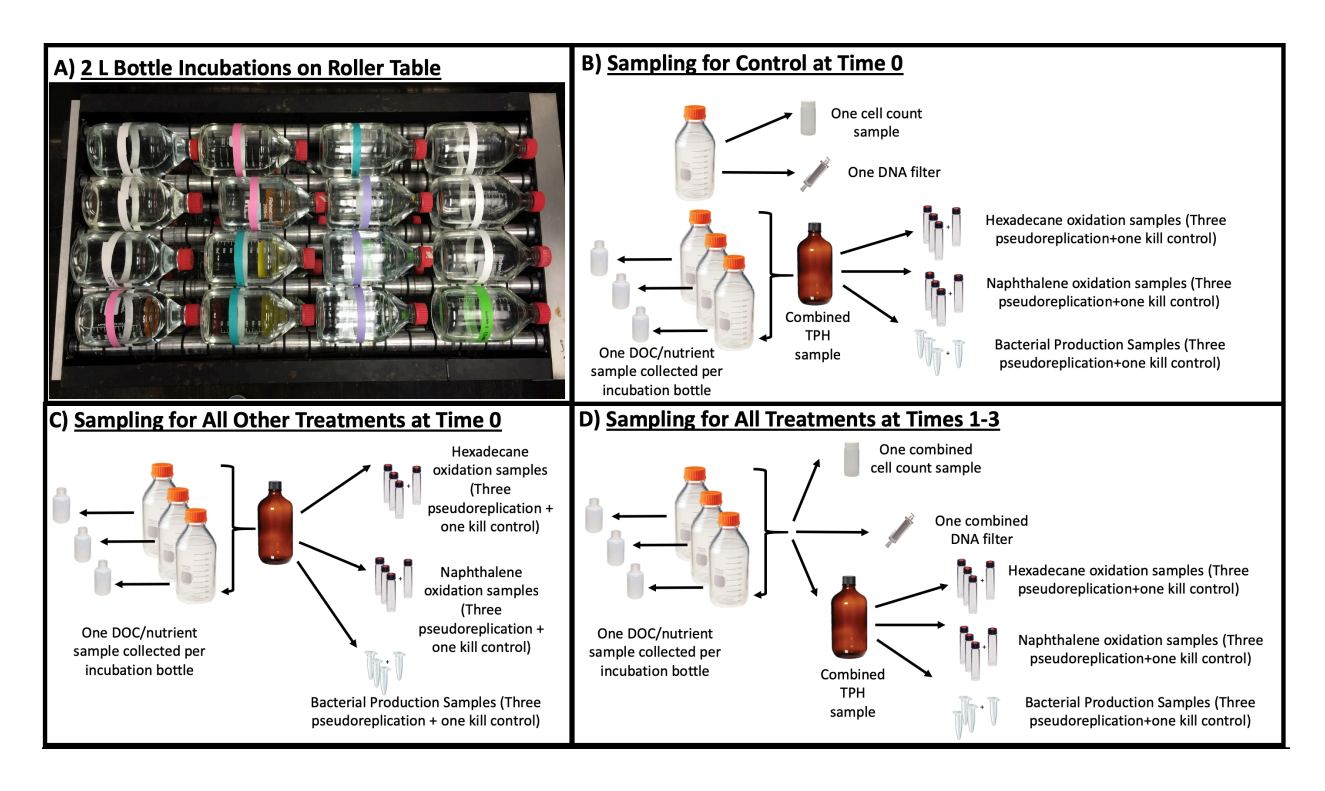


Figure 3.1: a) 2L bottle incubations on roller table maintained at 24°C in the dark, b) samples collected from control incubation bottles at Time 0, c) samples collected from all other treatments (Corexit±nutrients, WAF±nutrients, CEWAF±nutrients) at Time 0, d) samples collected from all treatments at Times 1-3. Time 3 sampling was only conducted on GC600 samples. Hexadecane and naphthalene oxidation rates were not collected in Taylor incubations.

Each treatment was prepared in triplicate and maintained at 24°C on a roller table in the dark. Microcosms were sampled on three separate instances during Taylor Energy, and OC26 incubations. Time 0 refers to samples collected directly after the bottles were exposed to the treatment amendments. Time 1 refers to samples collected after a one-week incubation period (24°C on a roller table in the dark). After Time 1 sampling, 2 mL of bulk crude oil was added to each bottle. Bottles were returned to roller table and maintained at 24°C in the dark for thirty two hours and which point Time 2 samples were collected. A fourth sampling time (Time 3, one week after the crude oil addition) was added to the final GC600 incubation to evaluate long-term community effects.

Sampling Scheme

At Time 0 DOC/nutrient samples were collected from each incubation bottle (resulting in three true replicates per treatment). One TPH sample was collected per amendment condition by combining equal volumes of each sample treatment replicate into one 1 L amber bottle. Prior to freezing and storing at -20 C, a 50 mL sub-sample from the combined TPH samples was subsampled into combusted glass Schott bottles to be further aliquotted for bacterial production and hydrocarbon oxidation rate measurements (see Figure 3.1). One DNA filter and AODC sample was collected from the extra Control treatment bottle prepared for this purpose. This extra Control treatment bottle was then removed from the incubation. Sampling at Time 1, and 2 (and Time 3 in the case of GC600 incubations) was very similar to Time 0 except that one DNA filter and AODC sample was collected for each treatment condition by combining equal parts of each treatment replicate. Samples were pooled to conserve volume over the course of the experiment. Samples after bulk crude oil addition (Time 2 and Time 3) were collected by stoppering the bottle with a rubber stopper with a glass tube positioned through it. Water samples were collected carefully by inverting the stoppered bottle and measuring the desired volume into the appropriate containers, avoiding the added bulk crude oil.

It should be noted that Time 0 nutrient samples of the GC600 incubation were lost due to a storage issue. Time 0 nutrient samples were recovered from the TPH samples by thawing TPH samples, and filtering them with 0.2 µm target filters. Neither hexadecane nor naphthalene oxidation samples were not collected for Taylor incubations. Potential hydrocarbon oxidation rates and bacterial production rates in this experiment reflect pseudoreplicates, since replicates were pulled from the combined TPH sampling; this may mask some of the within treatment variability.

Dissolved Organic Carbon and Nutrient Collection and Analysis

A DOC/nutrient sample was collect for each bottle at each time, resulting in three true replicates per treatment. DOC and nutrient *in situ* water was filtered using a 0.2 μm target filters and frozen and stored upright at -20°C. Target filters were rinsed with 20 mL of MQ and dried, and then rinsed with 5 mL of sample prior to filtration to avoid contamination. Prior to freezing, 2.5 mL of filtered sample was subsampled into 15 mL falcon tubes and preserved with 100 μL phenol at 4°C and analyzed for ammonium according to the colorimetric protocol described by Solorzano (1969). Samples were thawed to analyze dissolved organic carbon (DOC), total dissolved nitrogen (TDN), ammonium (NH₄⁺), NO_x⁻, nitrite (NO₂⁻), and phosphate (HPO₄³⁻).

DOC was analyzed on a total organic carbon analyzer (Shimadzu TOC-Vcph). Samples were run in tandem with potassium hydrogen phthalate standards to determine concentrations. TDN was also measured using the Shimadzu analyzer (utilizing a TNM-1 module). Samples were run in tandem with glycine standards.

NO_x⁻ concentrations were determined using a vanadium reduction assembly, Antek 745, and chemiluminescent nitric acid detector, Antek 7050 as is described by Braman and Hendrix, and Garsie et al. (Braman and Hendrix, 1989, and Garsie et al., 1982). Concentrations were determined by comparing sample peak area to peak areas of potassium nitrate standards. NO₂⁻ was determined by calorimetry (Bendschneider and Robinson, 1952). Finally, dissolved phosphate concentrations were determined using a molybdate blue calorimetric method (Solorzano and Sharp, 1980).

Rates of Bacterial Production

Bacterial production rates in *in situ* samples and in the amended samples were determined using the ³H-luccine incorporation method (Smith et al., 1992). Exactly 1.5 mL of in situ water or amended sample was added to a 2 mL plastic microcentrifuge tube. Three replicates and one killed control were included for each sample/treatment. Kill controls were achieved by adding 100 μL of trichloroacetic acid (100% TCA) to select samples prior to addition of 10⁶ dpm ³H-leucine. Samples were incubated in the dark at room temperature for three hours and then killed by adding 100 μL of TCA. Killed samples were stored at room temperature for up to two months before processing.

Samples were centrifuged at 10,300 RPM for 15 minutes to isolate the biomass pellet and the remaining liquid was aspirated. Then, 1.5 mL of 5% TCA was added to each sample before centrifuging again at 10,300 RPM for 5 minutes. The remaining liquid was again aspirated and 1.5 mL of eighty percent ethanol was added to each sample before centrifuging a final time at 10,300 RPM for 5 minutes. Ethanol was aspirated taking care to avoid the solid pellet and the sample was left uncapped to dry in the fume hood overnight. Once dry, 1.75 mL of scintillation fluid (BioSafe II Scintillation Cocktail; Fisher) was added to each sample; the sample was closed and vortexed, and placed into a plastic 20 mL scintillation vial. Samples were counted at for 5 minutes on a Beckman 6500 liquid scintillation counter. Bacterial production rates were calculated using the equation of Kirchman et al. (2001).

Hydrocarbon Oxidation

Rates of hydrocarbon oxidation were determined using the methods described by Kleindienst et al. (2015) and Sibert et al. (2016) for ¹⁴C-hexadecane and ¹⁴C-napthalane

oxidation. A 8.125 mL sample of *in situ* water or experimental sample was added to a 7 mL glass scintillation vials. Each vial was sealed with PTFE Teflon lined septa and a screw cap. Care was taken to ensure that no bubbles were present in the sealed vials. Samples were injected with 10⁶ dpm of ¹⁴C hexadecane or naphthalene (10⁶ dpm per 20 μL, dissolved in molecular grade ethanol) using a glass syringe. Each sample was run in triplicate with a killed control. Killed controls were inoculated at the same time as the samples and were immediately transferred to 50 mL plastic centrifuge tubes containing 2 mL 2 M NaOH. Killed vials were rinsed with basified tap water twice and rinses were also added to the sample's plastic centrifuge tube. Live samples were incubated for two days in the dark at room temperature and after incubation, each sample was terminated as per the killed controls.

After the experiment, samples were stored at room temperature for no more than two months. To recover the product (14CO₂), samples were transferred to 250 mL Erlenmeyer flasks containing 1 gram of activated charcoal, and in the case of hexadecane samples, 250 mg of C₁₈ reverse phase silica gel, to trap the hydrocarbon tracer. Falcon tubes were rinsed with basified tap water and rinsate was added to the same glass flask. The flasks were then capped with rubber stoppers and clamps and shaken for at least 18 hours to allow parent tracer to bind to the charcoal/charcoal-silica mixture. Samples were removed from the shaker table and a carbon dioxide trap (7 mL glass scintillation vials containing a glass fiber filter soaked with 1.5 mL of CarboSorb (Perkin Elmer)) was secured within each flask, above the liquid sample. Samples were acidified with 5 mL of concentrated phosphoric acid, taking care to avoid the CO₂ traps, and quickly stoppered. Samples were allowed to shake overnight after which 4.5 mL of scintillation fluid was added to each trap. The sample was then counted on a Beckmann 9500 liquid scintillation counter for 5 minutes.

Statistical Analysis

Data was analyzed for possible outliers by comparing three times the standard deviation of replicate points with the possible outlier removed to the mean of the comparable points (with the possible outlier also omitted). If this mean minus the possible outlier was greater than three times the standard deviation (possible outlier omitted) the point was considered an outlier and removed from statistical analysis. JMP® Pro 14.1.0 Software was utilized to evaluate normal distribution, and Wilcoxon/Kruskal-Wallis Test significance. All graphs were made using KaleidaGraph Version 4.5.4.

DNA Filtering, Extraction, and Sequencing

One L (made up of three equal parts from each replicate bottle) was filtered for each treatment. Peristaltic pump tubing was cleaned prior to each sample with 10% percent bleach, rinsed with milliQ, and sterile-filtered seawater before attaching 0.2 µm Sterivex filters to tubing. After filtration, each filter was plugged with sterile putty at the bottom and a sealing cap at the top and flash frozen in liquid nitrogen before storing at -80°C.

To recover DNA for sequencing, samples were thawed on ice and extracted according to the DNAeasy kit instructions with minor modifications to enhance DNA recovery. Extraction yields were evaluated using a Nanodrop and gel imagining. Based on these quality tests some samples were required PCR amplification prior to sequencing. To amplify samples a PCR was run using genomic DNA and the component volumes identified in Table 3.1. Primers 515F-Y CS1 / 926R CS2 were utilized (Walters et al., 2016).

Table 3.1: PCR mixture composition for $1 \mu L gDNA$ sample.

PCR Mixture per one 1 μL gDNA sample
Component Volume (μL)
PCR grade water 18.9

 Component
 Volume (μL)

 PCR grade water
 18.9

 10x HIFI Buffer
 2.5

 50 mM MgSO₄
 1

 dNTPS Mix
 0.5

 515F-Y_CS1(10uM)
 0.5

 926R_CS2 (10 uM)
 0.5

 TAQ
 0.1

The prepared PCR mixture was aliquoted into sterilized microcentrifuge tubes and 1 μL of sample was added to each microcentrifuge tube. Samples were centrifuged briefly (<15 seconds) and loaded randomly into the Bio-Rad C10000 Touch Thermal Cycler (looped/repeated 32 times – 3:00 min at 94°C, 0:45 min at 94°C, 1:00 min at 50°C, 1:30 min at 72°C –, 10:00 min at 72°C, infinite hold at 4°C). Triplicate replicates were combined and then cleaned using the Wizard SV Gel and PCR Clean-Up System. Extracted samples were sequenced at University of Illinois at Chicago's Sequencing Core (IUSQC).

3.3 Results and Discussions

Geochemistry Trends Across Incubations

Figures 3.2-3.4 present DOC and dissolved nutrient concentrations across sampling time points for the three incubations. DOC concentrations generally increased in samples collected thirty two hours after the bulk crude oil addition, reflecting oil partitioning into the aqueous phase. In the Taylor incubation, all Time 2 DOC concentrations increased, though there was high variability between replicate samples. In the OC26 incubation, all but one bottle (one of the three WAF+nutrient samples) showed increased DOC concentrations at Time 2. GC600 DOC concentrations at Time 2 decreased compared to those measured at Time 1 with the exception of

three of the four nutrient amendment treatments (Control, Corexit, and CEWAF nutrient amended treatments) (Figure 3.3). A week after the bulk crude oil addition, DOC increased in all treatments, reflecting movement of oil into the aqueous phase.

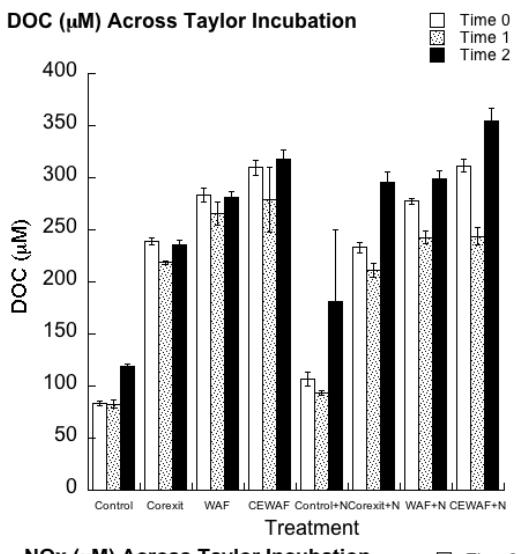
NOx⁻ concentrations did not change drastically during the preconditioning period at OC26 or GC600. In the Taylor incubations, the Corexit, WAF (±nutrients), and CEWAF treatments showed decreased NOx⁻ concentrations after pre-conditioning. Thirty-two hours after the bulk crude oil addition, all treatments showed a dramatic decrease in NOx (except the WAF±nutrients which were already <1 µM). The Control treatment had significantly elevated NOx^{-} concentrations at this time point (chi-square = 15.6487, df = 7, p = 0.0285). If this Control treatment was removed, no statistical difference was detected between the remaining treatments (chi-square = 11.4536, df = 6, p = 0.0753). The dramatic decreases in NOx⁻ concentrations observed after bulk crude oil addition to Taylor incubations were not observed in the OC26 and GC600 incubations. During these incubations almost all treatments showed an increase in NOxconcentrations thirty two hours after crude oil addition. Since NO₂- remained below detection limit throughout all experiments this increase in NOx was due to an increase in NO₃. The increase in NOx was also associated with a complete drawdown of ammonium indicating the NO₃ increase is likely due to nitrification. NOx⁻ concentrations in the Corexit amendments were elevated in both OC26 and GC600 incubations at Time 2. This trend was not observed in Corext+nutrient treatments at either OC26 or GC600 incubations. Samples collected a week after crude oil addition in the GC600 incubation all had NOx- levels below the detection limit.

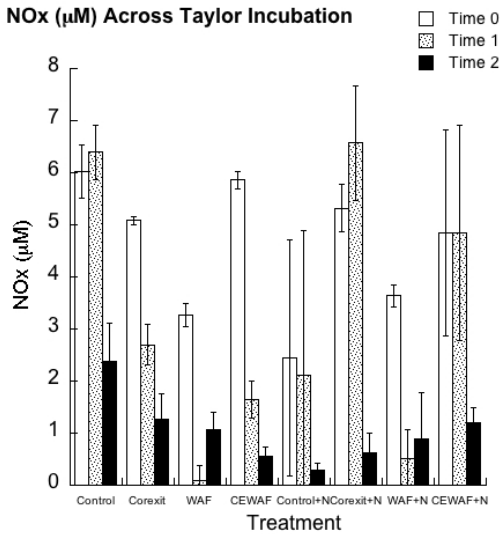
The *in situ* (Control) concentrations for Taylor were $2.38 \pm 0.74 \,\mu\text{M NOx}^-$, while OC26 and GC600 concentrations were much lower, at 0.3 ± 0.1 and $0.57 \,\mu\text{M NOx}^-$, respectively. In all incubation sites NOx⁻ concentrations only increased between sampling time points if previous

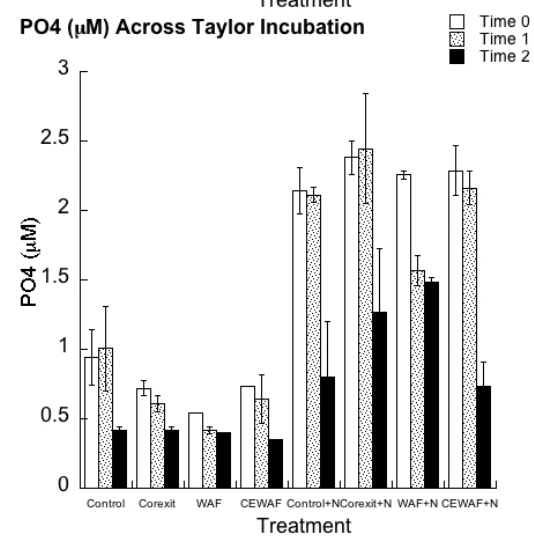
concentration was <1 μ M. Changes in nitrite concentrations are not presented because nitrite was below detection limit in all samples. Increases in NOx⁻ concentrations likely came from metabolization of oil.

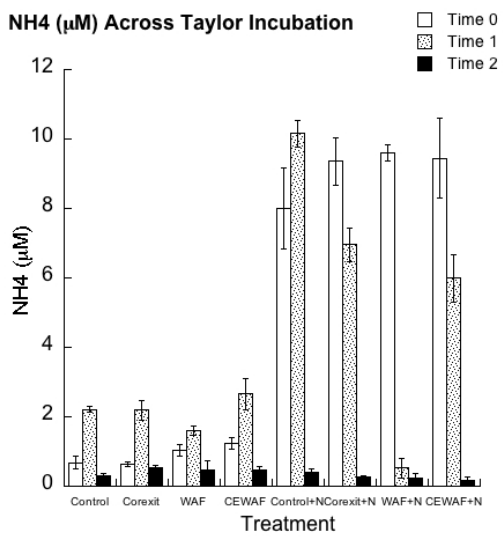
TDN concentrations after the preconditioning period (Time 1) did not differ significantly between control treatments during any of the incubations (Taylor Wicoxon/Kruskal-Wallis Test chi-square = 7.7554, DF=3, p=0.0513; OC26 incubation chi-square = 6.5593, DF=3, p=0.0874; GC600 incubation chi-square = 5.2038, DF=3, p=0.1575). All sites showed dramatic TDN drawdown in the WAF+nutrient treatment after the preconditioning period. These differences in TDN concentrations were significant at OC26 (chi-square = 9.4917, DF=3, p=0.0234) but not Taylor and GC600 incubations (Taylor Wicoxon/Kruskal-Wallis Test chi-square = 6.1550, DF=3, p=0.1043; GC600 incubation chi-square = 7.5019, DF=3, p=0.0575). During Taylor, OC26, and GC600 incubations, TDN concentrations decreased in all treatments after bulk crude oil addition, resulting in no significant difference among final TDN concentrations.

Figure 3.2: Average dissolved nutrient concentrations across three sampling points in Taylor Energy Incubation. Time 0 indicates samples collected directly after amendment set up, Time 1 indicates samples collected after seven days of roller table incubations, and Time 2 indicates samples collected 32 hours after oil additions. Bars represent standard deviation.









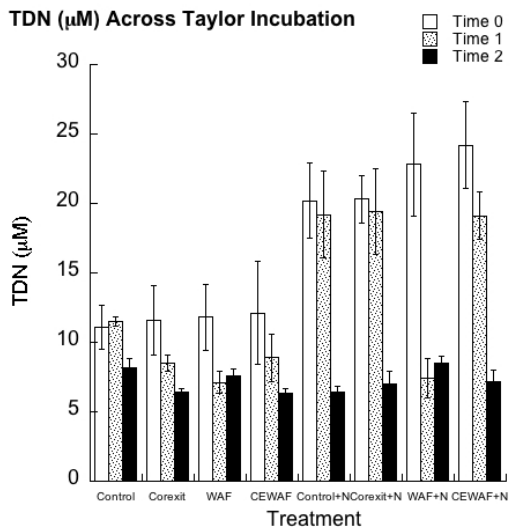
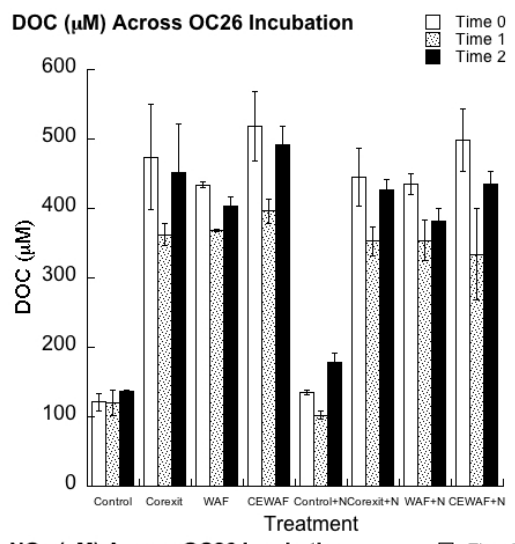
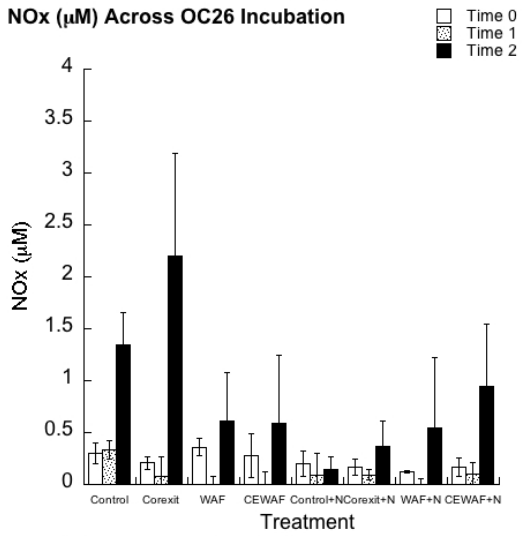
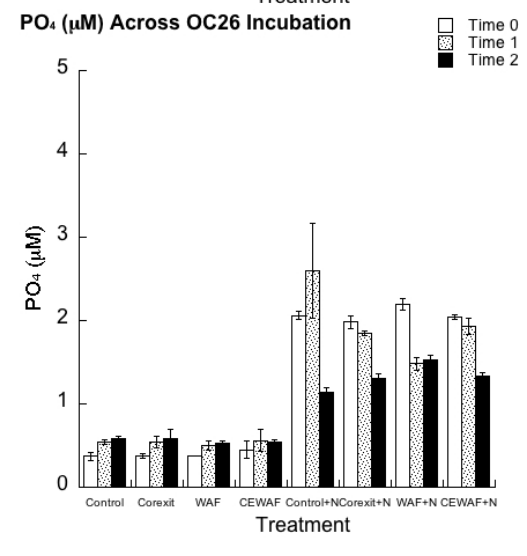
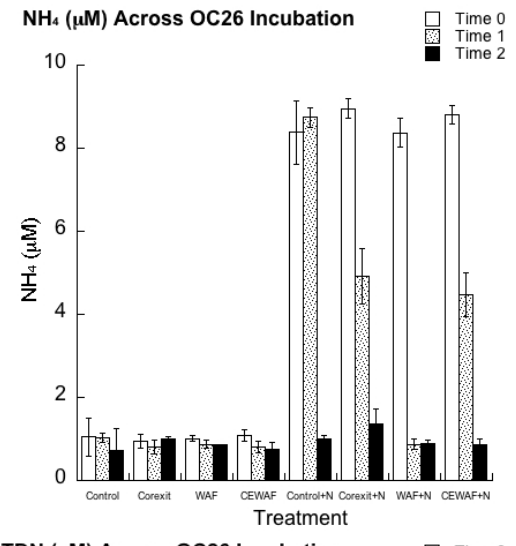


Figure 3.3: Average dissolved nutrient concentrations across three sampling points in OC26 incubation. Time 0 indicates samples collected directly after amendment set up, Time 1 indicates samples collected after seven days of roller table incubations, and Time 2 indicates samples collected 32 hours after oil additions. Bars represent standard deviation.









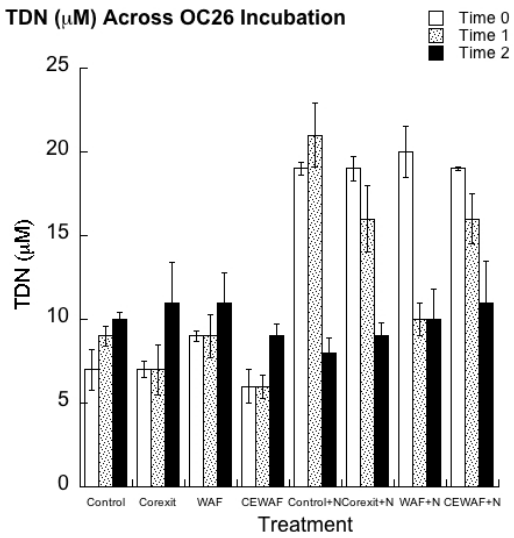
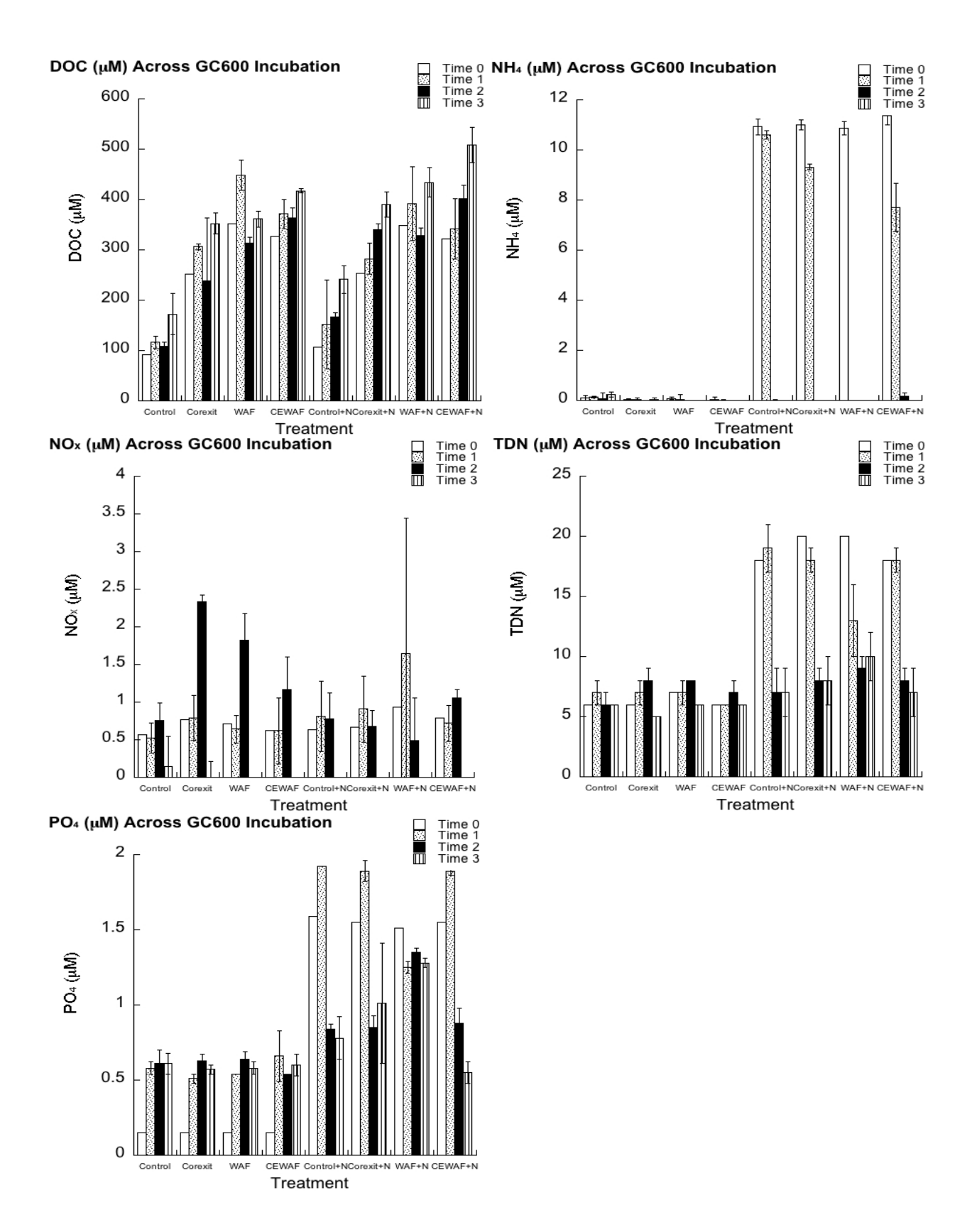


Figure 3.4: Average dissolved nutrient concentrations across four sampling points in GC600 incubation. Time 0 indicates samples collected directly after amendment set up, Time 1 indicates samples collected after seven days of roller table incubations, and Time 2 indicates samples collected 32 hours after oil additions. Time 3 indicates samples collected one week after oil additions. Bars represent standard deviation.



NH₄ (µM) After Pre-Incubation Across all Incubations 12 10 8 4 2 Control Corexit WAF CEWAF Control+NCorexit+N WAF+N CEWAF+N

Figure 3.5: Average dissolved ammonium $(NH_4^+, \mu M)$ after one week of treatment incubation. This figure shows that ammonium was completely depleted after the one week preconditioning period in WAF+nutrient amendment of all incubations. Bars represent standard deviation

Treatment

In all three incubations, the WAF+nutrient treatment showed complete ammonium depletion after the preconditioning period (Figure 3.5). Ammonium concentrations were significantly different in nutrient amended treatments after one week of preconditioning in each incubation (Taylor Wicoxon/Kruskal-Wallis Test chi-square = 9.4954, DF=3, p=0.0234; OC26 incubation chi-square = 9.6667, DF=3, p=0.0216; GC600 incubation chi-square = 10.4211, DF=3, p=0.0153). This drawdown was accompanied by TDN depletion but not uniform NOxdepletion, as discussed above. Since these changes were not accompanied with increases in NOxdepletions in OC26 and GC600 incubations, calculated DON (DON=[TDN]-[NOx-]-[NH4+]) concentrations also decreased.

Significant differences in ammonium concentrations after the one week preconditioning between the samples without nutrient amendments were not observed (Wicoxon/Kruskal-Wallis

Test Taylor incubation chi-square = 7.4377, DF=3, p=0.0592; OC26 incubation chi-square = 4.3491, DF=3, p=0.2261; GC600 incubation chi-square = 4.4108, DF=3, p=0.2204). Thirty two hours after the bulk crude oil addition, there was no longer a significant difference in ammonium depletion among nutrient amended treatments in the Taylor and OC26 incubations (Wicoxon/Kruskal-Wallis Test Taylor incubation chi-square = 5.8014, DF=3, p=.1217; OC26 incubation chi-square = 6.6723, DF=3, p=0.0831). All of the GC600 ammonium concentrations at this sampling time point were below detection limit except in the CEWAF+nutrient condition. The replicates of this treatment had ammonium concentrations of 0.33, 0.10, and $0.10 \mu M$, so were very low as well.

Addition of the oil and dissolved oil (in the absence of Corexit) appears to be a trigger for significant ammonium drawdown, presumably reflecting N assimilation by the microbial community. A similar trend of nitrogen depletion in WAF amended treatments was observed by Seidal et al. (2016), where relative abundance of N- and S-containing hydrocarbons decreased during WAF incubations. Malkin et al. (2019) also observed drastic ammonium drawdown in WAF+nutrient amended surface water incubations, in comparison to CEWAF+nutrient treatments (no other nutrient amendment conditions were tested). Ammonium drawdown in the WAF+nutrient treatment was observed after only two days of incubation. Malkin et al. also performed an extended incubation experiment lasting a total of twenty-six days. Ammonium drawdown in WAF+nutrient treatment was observed at the first time point (after seven days of incubation) but ammonium levels then increased after 14 and 26 days of incubation (0.01 \pm 0.02 μ M increased to 0.13 \pm 0.20 μ M), illustrating recycling of N in the treatments.

The major drawdown in ammonium was accompanied with a large increase in the proportion of *Marinobacter* read counts in OC26 incubations, more so than any other treatment at Time 1 (See Figure 3.9). In GC600, the major draw down in ammonium was accompanied by an increased proportion of read counts in *Flavobacteriales* (see Figure 3.10). Whether or not these strains were the cause of the ammonium drawdown remains unclear.

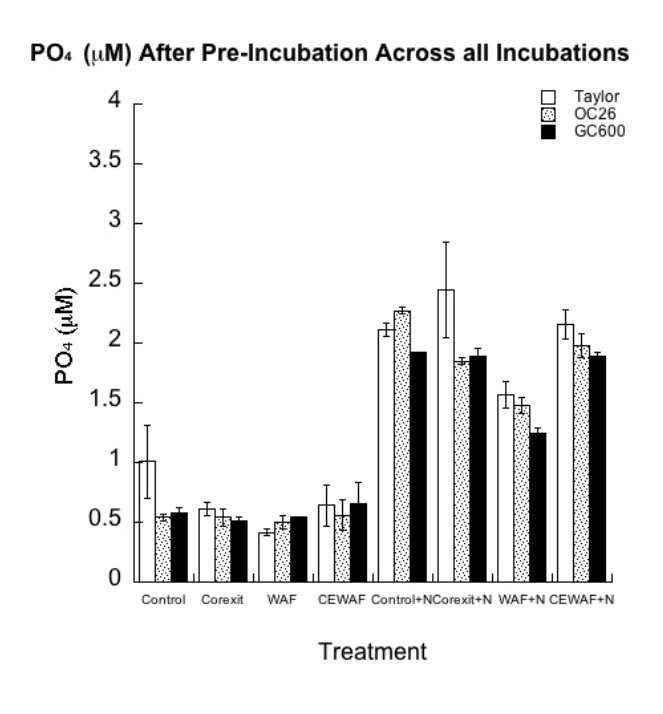


Figure 3.6: Average dissolved phosphate (μ M) after one week of treatment incubation. This figure shows that phosphate was completely depleted after the one week preconditioning period in at all sites in the WAF+Nutrient amendment. Bars represent standard deviation.

Similar depletion trends were observed in phosphate concentrations in the WAF+nutrient treatments after the first week of incubation, while phosphate concentrations increased in Control+nutrient, Corexit+nutrient, and CEWAF+nutrient conditions after the preconditioning period of the GC600 incubation (Figure 3.6). However, unlike what was observed in the other tested nutrient samples, the WAF+nutrient treatment did not show any further change in

phosphate concentrations in the following sampling timepoints. WAF+nutrient phosphate concentrations remained around $1.32 \pm 0.05~\mu M$ for the remainder of the GC600 experiment. Phosphate concentrations at Time 3 (one week after crude oil addition) in the other nutrient amended treatments either remained at Sampling Time 2 levels (Control+nutrient and Corexit+nutrient) or continued to decrease (CEWAF+nutrient). In unamended treatments, average initial phosphate concentrations were $0.15~\mu M$. Concentrations increased in all nutrient unamended treatments during the preconditioning period and remained stable for the remainder of the GC600 incubation experiment.

A similar trend of increasing phosphate concentrations in nutrient unamended incubations over time was observed by Kleindeinst et al. (2015) and Malkin et al. (In Review), though not in all treatments. Increasing phosphate concentrations could indicate organic P mineralization during the experiment (Paytan and McLaughlin, 2007; Filippelli, 2008). Trends in phosphate concentrations in Taylor and OC26 incubations were similar to those observed at GC600. At both sites the WAF+nutrient treatment saw the lowest phosphate concentrations after the preconditioning period (1.57 \pm 0.11 μ M and 1.48 \pm 0.07 μ M in Taylor and OC26 incubations respectively) as opposed to concentrations measured prior to preconditioning (2.26 \pm 0.03 μ M and 2.20 \pm 0.07 μ M in Taylor and OC26 incubations respectively). The fact that phosphate concentrations in the WAF+nutrient were lower than those in the other treatments indicates more rapid phosphate drawdown in this treatment.

The unamended treatments at Taylor did not show an increase in phosphate concentrations, as was observed in the GC600 and OC26 incubations. Instead phosphate concentrations decreased or remained the same throughout the experiment. This site-specific response could again be due to differences in the initial phosphate concentrations. The average phosphate concentration at Time 0 in the unamended treatments was $0.74 \pm 0.16~\mu M$ in the Taylor incubations in comparison to $0.39 \pm 0.038~\mu M$ and $0.15 \pm 0.00~\mu M$ in the OC26 and GC600 incubations, respectively.

Bacterial Production Trends Across Incubations

Hydrocarbon and nutrient additions resulted in significant instantaneous differences in bacterial production rates in each set of incubations (Wicoxon/Kruskal-Wallis Test Taylor incubation chi-square = 17.5211, DF=7, p=0.0143; OC26 incubation chi-square = 15.4526, DF=7, p=0.0306; GC600 incubation chi-square = 16.3203, DF=7, p=0.0223). At time 0, immediately after treatments were employed for Taylor incubations, the WAF±nutrient treatments showed the highest bacterial production rates compared to other treatments. This increase in activity corresponded to elevated nutrient depletion in the WAF+nutrient treatment at Time 1 (most notably in ammonium drawdown but also in TDN, NOx and phosphate as described above). Bacterial production in the WAF+nutrient treatment was also elevated in the OC26 incubations at Time 0. However elevated bacterial production rates were also observed in Corexit±nutrient treatments at OC26. Greatest bacterial production rates at Time 0 in GC600 incubations were observed in all carbon+nutrient amended treatments (Corexit+nutrient, WAF+nutrient, and CEWAF+nutrient but not the Control+nutrient). Thus, although nutrient depletion in WAF+nutrient treatments was observed in all incubations, this was not accompanied

by elevated bacterial production rates at Time 0 at all sites. A contributing factor to this observation could be the "luxury uptake" of nutrients in the presence of excess carbon and nutrients, previously observed in oligotrophic communities in which communities incorporate nutrients but instead of subsequently growing, "hoard" these nutrients (Ammerman, 2003). This phenomenon could explain assimilation of nutrients without growth at oligotrophic OC26 and GC600 sites. In contrast Taylor incubations, relatively nutrient rich site, the uptake of nutrients is associated with greater community growth.

After the preconditioning period, Taylor incubations exhibited an increase in bacterial production rates across treatments, except in the WAF±nutrient treatments, possibly due to the near-complete depletion of nutrients that had occurred by this time. As a result, the Corexit+nutrient treatment exhibited the highest bacterial production rate after the preconditioning period. The addition of crude oil increased bacterial production across all treatments during the Taylor incubation at Time 2 but little difference was observed across treatments at Time 2, except in the case of the Corexit+nutrient treatment, which exhibited the highest bacterial production (719.1 \pm 71.1 nM C/day). Bacterial production rates increased in the WAF±nutrient treatment (from 321.7 \pm 6.5 nM C/day at Time 1 to 466.5 \pm 40.7 nM C/day at Time 2) even though rates had decreased after the preconditioning period and nutrients remained depleted (Figure 3.7).

As was observed in the Taylor incubations, there was a general trend of increased bacterial production at Time 1 in OC26 incubations in comparison to initial bacterial production rates measured at Time 0. This trend was consistent across treatments with the exception of bacterial production rates in the Corexit treatment which remained relatively constant (309.4 \pm 19.2 nM C/day at Time 0 vs. 262.9 \pm 53.6 nM C/day at Time 1). Similar to what was observed in

Taylor incubations, Control+nutrient, Corexit+nutrient, and CEWAF+nutrient showed large increases in bacterial production and WAF+nutrient bacterial production remained similar between Time 1 and Time 2.

In contrast, GC600 incubations did not show a trend of increased bacterial production rates after the preconditioning period (Time 1). Bacterial production responses varied with each treatment, though not significantly (chi-square = 12.9150, DF=7, p=0.0742). Notably in GC600 incubations, bacterial production increased to 543.6 ± 28.4 nM C/day and 978.0 ± 22.4 nM C/day for WAF and WAF+nutrient treatments respectively, in comparison to rates of 441 ± 16.2 nM C/day and 570.9 ± 10.1 nM C/day, respectively, at Time 0.

Unlike trends observed in the Taylor incubation, at Time 2 in the OC26 incubation most treatments showed a decrease in bacterial production when compared to Time 1 rates (except in the Control+nutrient treatment). However even with increased bacterial production in the Control+nutrient treatment, the activity did not exceed that observed in the other treatments. This could indicate that bulk crude oil did not result in increased toxicity and could infer that the Control+nutrient treatment had been carbon limited, and that oil addition relieved this limitation.

In the GC600 incubations, bulk crude oil addition led to either an increase or no change in bacterial production. This could reflect the fact that GC600 communities are accustomed to oil exposure and thus more able to respond to the oil addition in comparison to OC26, which does not experience periodic hydrocarbon exposure. On the other hand, at Time 3 the majority of treatments showed a decrease in bacterial production, so community progression may have simply been delayed in the GC600 incubation in comparison to the OC26 incubation.

Alternatively decreased bacterial production at Time 3 of the GC600 incubation could be due to nutrient limitation in contrast to the abundance of carbon.

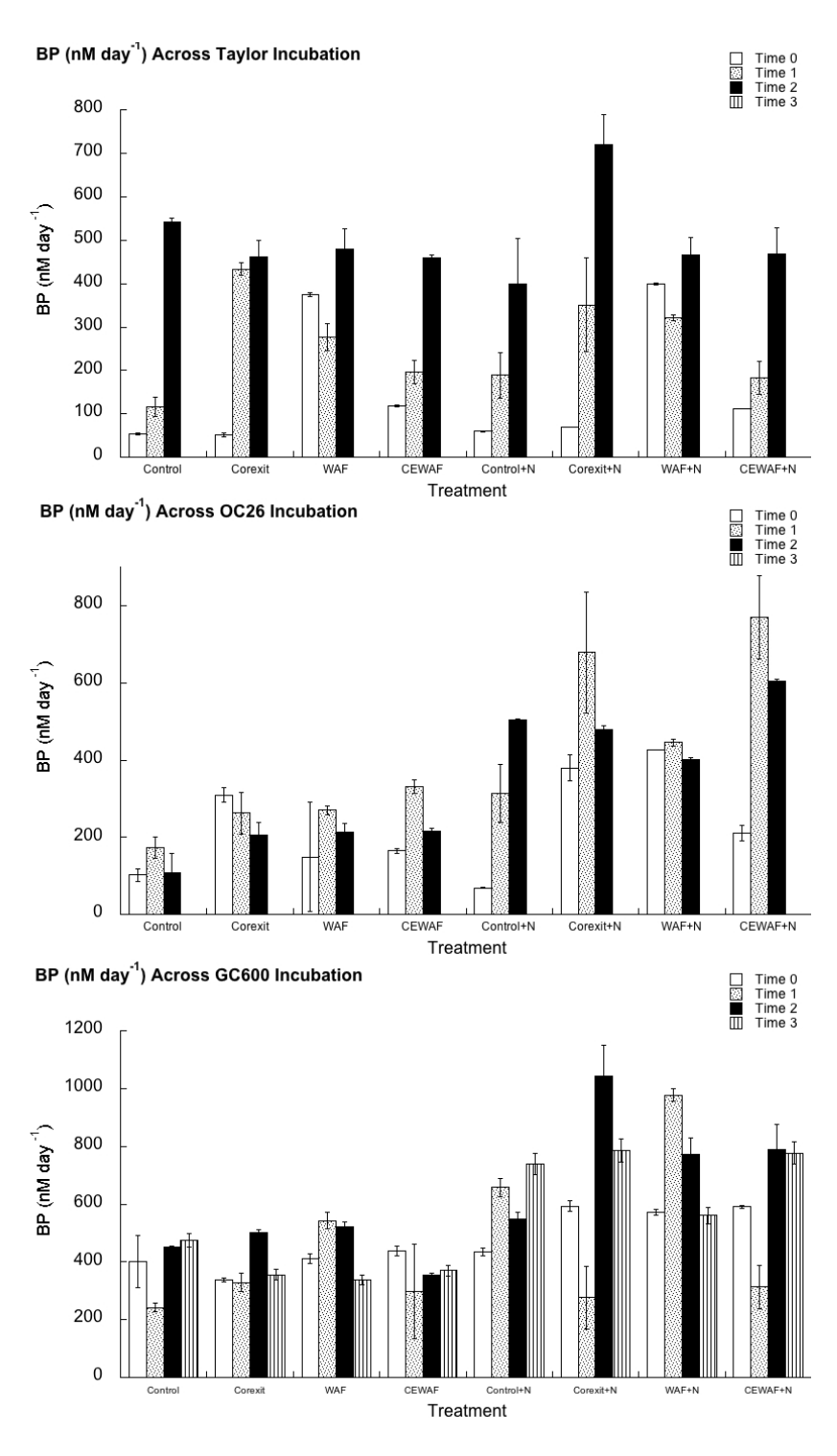


Figure 3.7: Bacterial production rates in Taylor, OC26, and GC600 incubations. Time 0 indicates samples collected directly after amendment set up, Time 1 indicates samples collected after seven days of roller table incubations, and Time 2 indicates samples collected 32 hours after oil additions. Bars represent standard deviation. Time 3 indicates samples collected one week after oil additions. Samples were only collected at Time 3 for the GC600 incubation.

Trends in Potential Hydrocarbon Oxidation Rates Across Incubations

Potential hexadecane and naphthalene oxidation rates for each time point in the OC26 incubation were not normally distributed so a Wilcoxon / Kruskal-Wallis Test was used (p values ranged between <0.0001-0.0004). Initial rates resulted in significantly elevated hexadecane oxidation potential rates in the Corexit+nutrient treatment when all rates were compared to one other (chi-square = 14.5817, df = 7, p = 0.0418). Average hexadecane oxidation rate potentials in the Corexit+nutrient treatment were 179 ± 2.61 pMC/day, over five times greater than the next highest hexadecane potential rate, observed in the CEWAF+nutrient of 34.54 ± 4.72 nM C/day.

The increased potential hexadecane oxidation rate observed at the initial sampling time point in the Corexit+nutrient condition was not maintained to the end of the preconditioning period. Instead, after the preconditioning period the rates in the Control+nutrient treatment were highest (59.03 \pm 23.15 nM C/day), followed by rates in the CEWAF+nutrient and Corexit potential hexadecane rates (31.61 \pm 1.56 nM C/day and 27.02 \pm 22.54 nM C/day respectively). Rates compared across all treatments at this time point were not significantly different (chi-square = 14.0368, df = 7, p = 0.0505) (Figure 3.8).

Potential hexadecane oxidation rates measured at Time 2 showed that Control+nutrient and Corexit+nutrient treatments had the highest potential hexadecane oxidation rates and were very similar to one another (35.36 ± 0 nM/day and 31.00 ± 5.06 nM/day, respectively). Rates compared across all treatments varied significantly at this time point (chi-square = 14.1374, df = 7, p = 0.0488) (Figure 3.8).

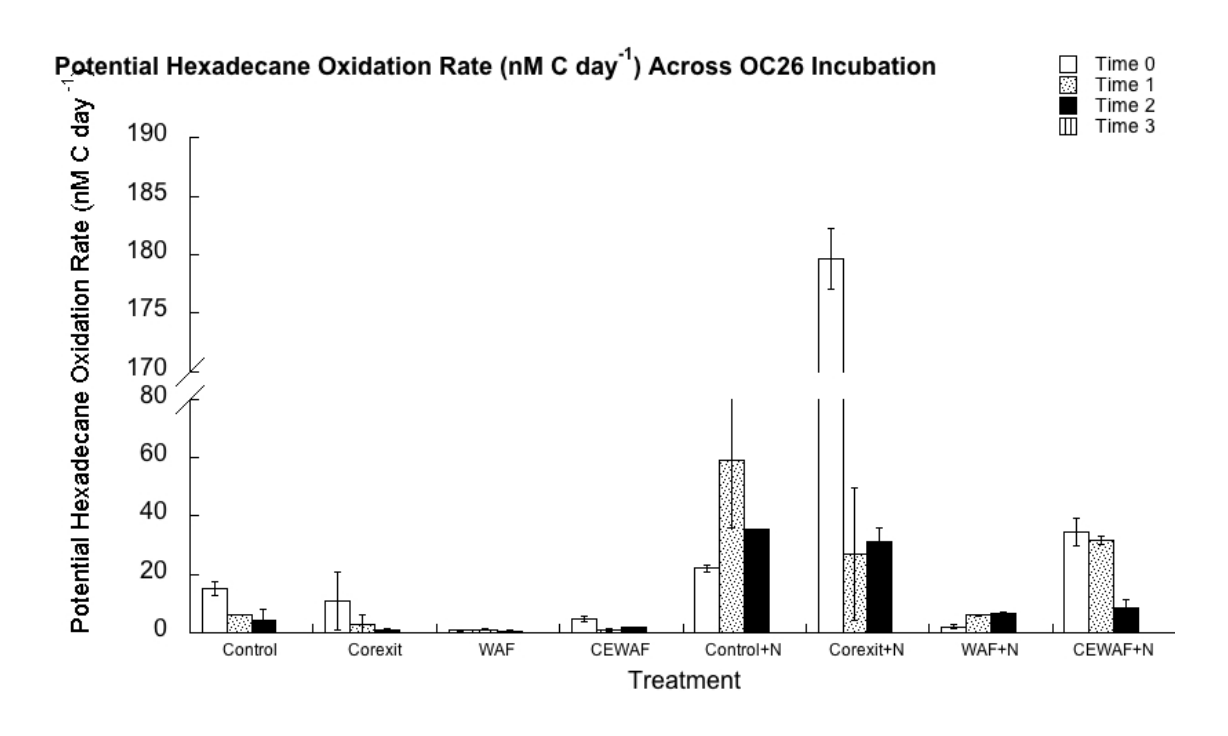
No significant difference among the initial potential naphthalene oxidation rates was observed at Time 0 OC26 incubation treatments (chi-square = 15.3464, df = 9, p = 0.0818). The Control+nutrient (0.119 ± 0.15 nM C/day) had the most elevated potential naphthalene oxidation

rates at Time 0. Potential naphthalene oxidation rates decreased in the Control+nutrient treatment by Time 1 to below detection limit. Instead WAF+nutrient treatment was elevated but with high variability between replicates (0.5522 ± 0.2371 nM C/day). Significant variability was found among potential naphthalene oxidation rates in all treatments after the one-week preconditioning period (chi-square = 14.9357, df = 7, p = 0.0368). The final incubation time point (Time 2) again showed the greatest potential naphthalene oxidation rates again in the WAF+nutrient treatment (0.2371 nM C/day 0.0279). Significant variability among treatments was not observed at this final time point (chi-square = 13.6405, df = 7, p = 0.0580) (Figure 3.8).

As was the case with the OC26 incubations for potential hexadecane oxidation rates, the treatment with the highest potential naphthalene oxidation rates at the initial time point remained the treatment with the highest rate throughout the remainder of the experiment. Naphthalene oxidation rates were elevated in the WAF+nutrient treatment at Time 1 and remained elevated after the addition of bulk crude oil. Rates did not increase in response to oil additions which could be due to preferential degradation of oil derived dissolved n-alkanes over the less labile radiolabeled hexadecane and naphthalene tracers (Harrison, 2017).

The trends of elevated potential hexadecane oxidation in the Corexit+nutrient and the Control+nutrient conditions, and elevated potential naphthalene oxidation rates in the WAF+nutrient treatment, were not mirrored in their corresponding nutrient unamended treatments. This indicates that a community's response to Corexit and/or oil exposure is highly dependent upon nutrient availability, though not exclusively so. Previous work has identified significant correlation to nutrient concentrations and naphthalene oxidation rates (Harrison, 2017). This observation calls into question the unilateral applicability of previous works that have solely reported dispersant dynamics with nutrient amended water (Campo et al., 2013;

Techtmann et al., 2017; Zahed et al., 2011; McFarlin et al., 2014). At the same time however it is important to note that potential hydrocarbon oxidation rates were not solely dependent on nutrient concentrations, or in other words not all of the nutrient amended treatments had elevated/inhibited rates. This could possibly have been due to unequal nutrient depletion throughout the incubations.



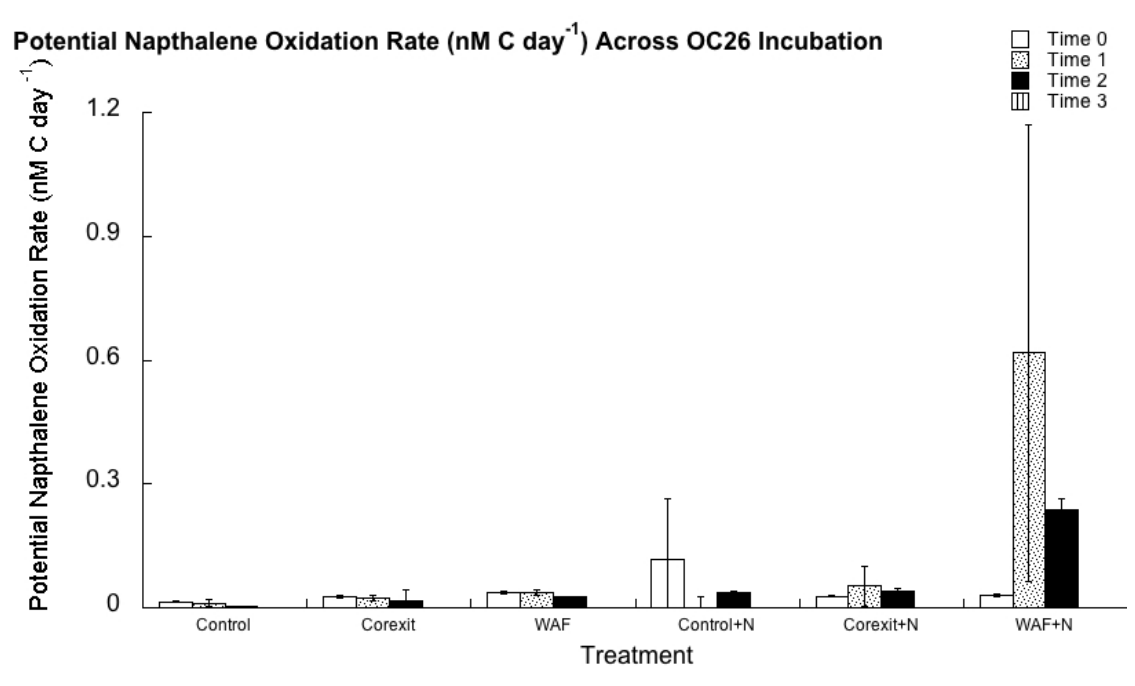


Figure 3.8: Potential hexadecane and naphthalene oxidation rates in OC26 incubations. Time 0 indicates samples collected directly after amendment set up, Time 1 indicates samples collected after seven days of roller table incubations, and Time 2 indicates samples collected 32 hours after oil additions. Bars represent standard deviation. Time 3 indicates samples collected one week after oil additions. Samples were only collected at Time 3 for the GC600 incubation. CEWAF±nutrient samples were excluded from the OC26 naphthalene oxidation graph and following analysis due to a labeling issue.

Wilcoxon/Kruskal-Wallis Tests were used to evaluate potential hexadecane and naphthalene oxidation rates measured for each time point in the GC600 incubation, as they were not normally distributed. Time 0 potential hexadecane oxidation rates in the GC600 CEWAF+nutrient treatment (53.4 \pm 14.40 nM C/day) was most elevated among all Time 0 rates, followed by rates measured in the WAF+nutrient incubations (39.6 \pm 6.6 nM C/day). This is in contrast to OC26 where Corexit+nutrient potential hexadecane oxidation rates were most elevated at this time point. Significant difference between treatments at Time 1 was detected (chi-square=15.3860, df=7, p=0.0314). The CEWAF and Control+nutrient were most elevated after the preconditioning period with rates of 31.9 ± 5.46 nM C/day and 32.6 ± 17.3 nM C/day respectively. Thirty two hours after the crude oil addition, potential hexadecane oxidation rates in the Control+nutrient were still the most elevated (38.9 \pm 16.7 nM C/day), with Corexit+nutrient following (18.5 \pm 6.2 nM C/day) and the formally elevated CEWAF treatment decreasing to 14.7 ± 1.9 nM C/day (Figure 3.9). Differences in treatment rates were significantly different at this time point and likely reflect differential nutrient limitation (chi-square=16.0994, df=7, p=0.0242). The Control+nutrient potential hexadecane oxidation rates may have been the highest because these samples were not as nutrient stressed at the time of the bulk crude oil addition. In contrast incubations with added carbon sources made the communities more nutrient stressed and less able to responds to additional oil.

Rates of potential hexadecane oxidation in Control+nutrient remained most elevated at Time 3 and differences in treatment rates remained significantly different at Time 3 (chi-square=16.0632, df=7, p=0.0245). However it is important to note that after additional time had elapsed, the Control+nutrient treatment, although remaining the highest rate, decreased to 14.1 ± 2.2 nM C/day. Similar decreasing hexadecane oxidation trends over time were observed in

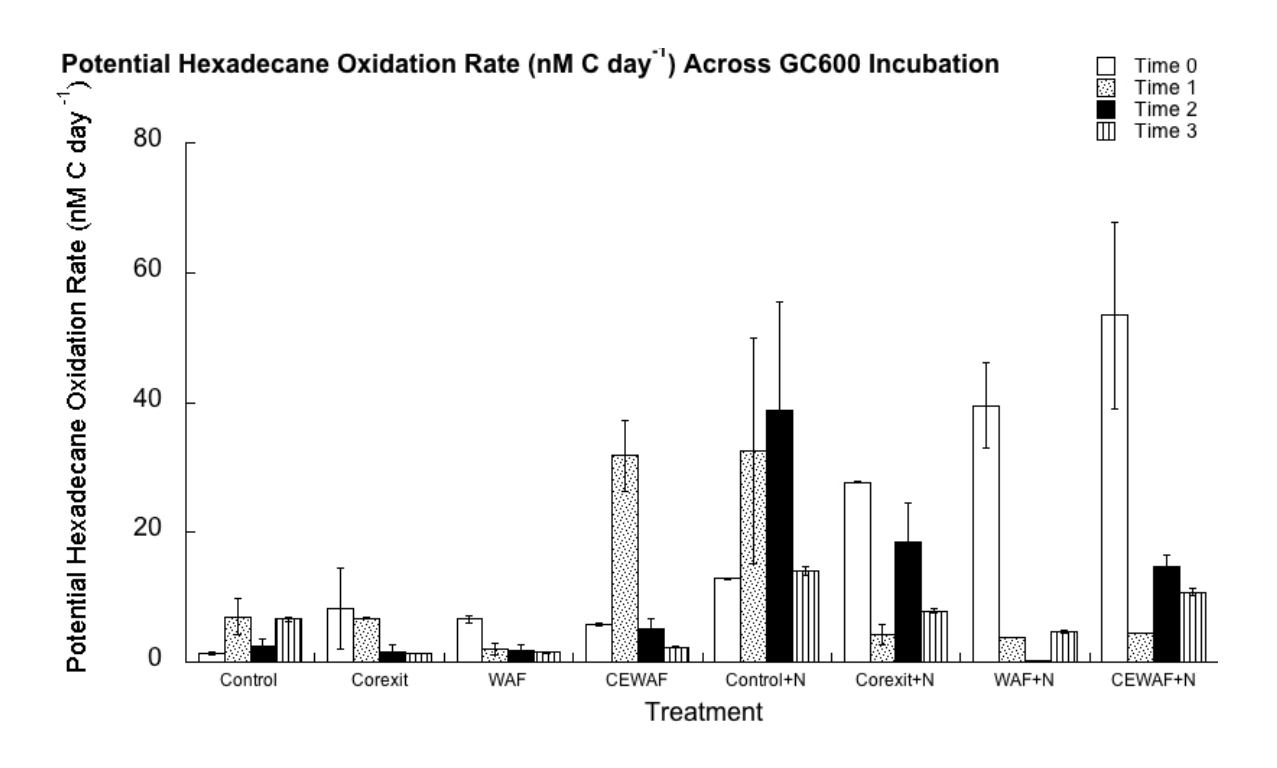
previous incubation experiments performed with bottom water (Kliendienst et al., 2015). In Kliendienst et al.'s (2015) work this trend was due to the removal of hexadecane over time.

As was the case with OC26 incubation the trends, GC600 potential hexadecane oxidation rates differed from potential naphthalene oxidation rates. All time points showed significantly unique responses in potential naphthalene oxidation rates across all incubation treatments. Rates measured following the initial treatment addition (Time 0) were most elevated in the Control+nutrient amendment (74.80 ± 3.93 pM C/day). At Time 0 nutrient amended treatments had higher potential naphthalene oxidation rates than the unamended treatments. Nutrient dependent potential naphthalene oxidation rates were also observed in OC26 incubations and identified among in situ samples by Harrison (2017). Unlike the potential hexadecane oxidation rates trends in the OC26 and potential hexadecane oxidation rates trends GC600, at this initial time point elevated potential naphthalene oxidation rates in Control+nutrient coincided with elevated trends in the Control without nutrients.

After the preconditioning period (Time 1), rates of potential naphthalene oxidation across treatments remained statistically different (chi-square = 16.7381, df=8, p=0.0030). Potential naphthalene oxidation rates in the Control+nutrient treatment remained the highest at Time 1 while rates in the Control without nutrients no longer showed elevated potential naphthalene oxidation activity. The Control+nutrient potential naphthalene oxidation rate after the preconditioning period was 3.18 ± 0.24 nM C/day. All other treatments had much lower potential naphthalene oxidation rates (ranging from 0.02-0.1870 nM C/day).

Control+nutrient potential naphthalene oxidation rates continued to increase over time, with the highest rates observed at Time 3 (43.19 \pm 20.06 nM C/day), likely due to a substrate concentration affect. Potential naphthalene oxidation rates increased in most other treatments

thirty two hours after the oil addition but decreased by Time 3 sampling taken one week after the oil addition. CEWAF+nutrient treatment increased thirty two hours after bulk crude oil addition and one week after the oil addition with potential naphthalene oxidation rates of 2.36 1.941 nM C/day and 20.48 4.32 nM C/day respectively. At sampling Time 3 naphthalene oxidation rates significant difference remained across treatments (chi-square = 18.6714, df=8, 0.0167) due to the elevated Control+nutrient and CEWAF+nutrient potential naphthalene oxidation rates at Time 3 (43.18 ± 20.06 nM C/day and 20.48 ± 4.32 nM C/day respectively).



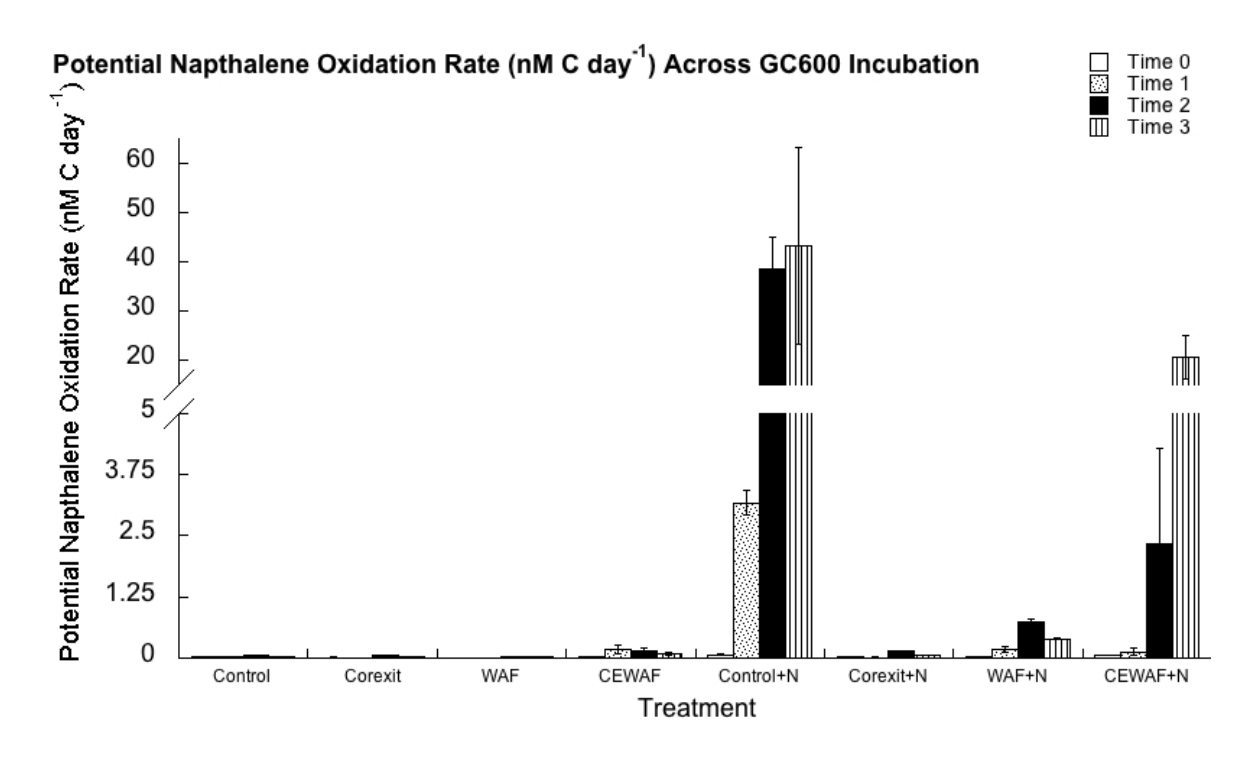


Figure 3.9: Potential hexadecane and naphthalene oxidation rates in GC600 incubations. Time 0 indicates samples collected directly after amendment set up, Time 1 indicates samples collected after seven days of roller table incubations, and Time 2 indicates samples collected 32 hours after oil additions. Bars represent standard deviation. Time 3 indicates samples collected one week after oil additions. Time 3 samples were only collected in the GC600 incubation.

Community Composition

Dispersant application frequently results in microbial community compositional changes. A decrease in *Marinobacter* relative abundance following addition of Corexit 9500 was observed in Keindienst et al.'s (2015) deepwater incubations. In that work while WAF treatments resulted in *Marinobacter*-dominated communities after two weeks incubations of plume depth water, CEWAF, Dispersant-only, and CEWAF+nutrient treatments resulted in increases in *Colwellia*. Relative abundance of *Colwellia* increased from 1% to 26-43% in dispersant-only, and CEWAF (± nutrients) treatments while *Colwellia* remained at 1-4% in WAF treatments (Kleindienst et al., 2015). Corexit 9500A additions to culture enrichments of surface water close to the DWH spill resulted in decreased *Marinobacter* relative abundance, though bottom water experiments did not see a significant community structure changes (Techtmann et al., 2017). In contrast, in surface community incubations, Doyle et al. (2018) found WAF treatments resulted in about 3-5% relative abundance of *Marinobacter*-related OTUs, while CEWAF treatments resulted in much higher *Marinobacter*-related OTUs. *Marinobacter* was not dominant in either incubation treatment.

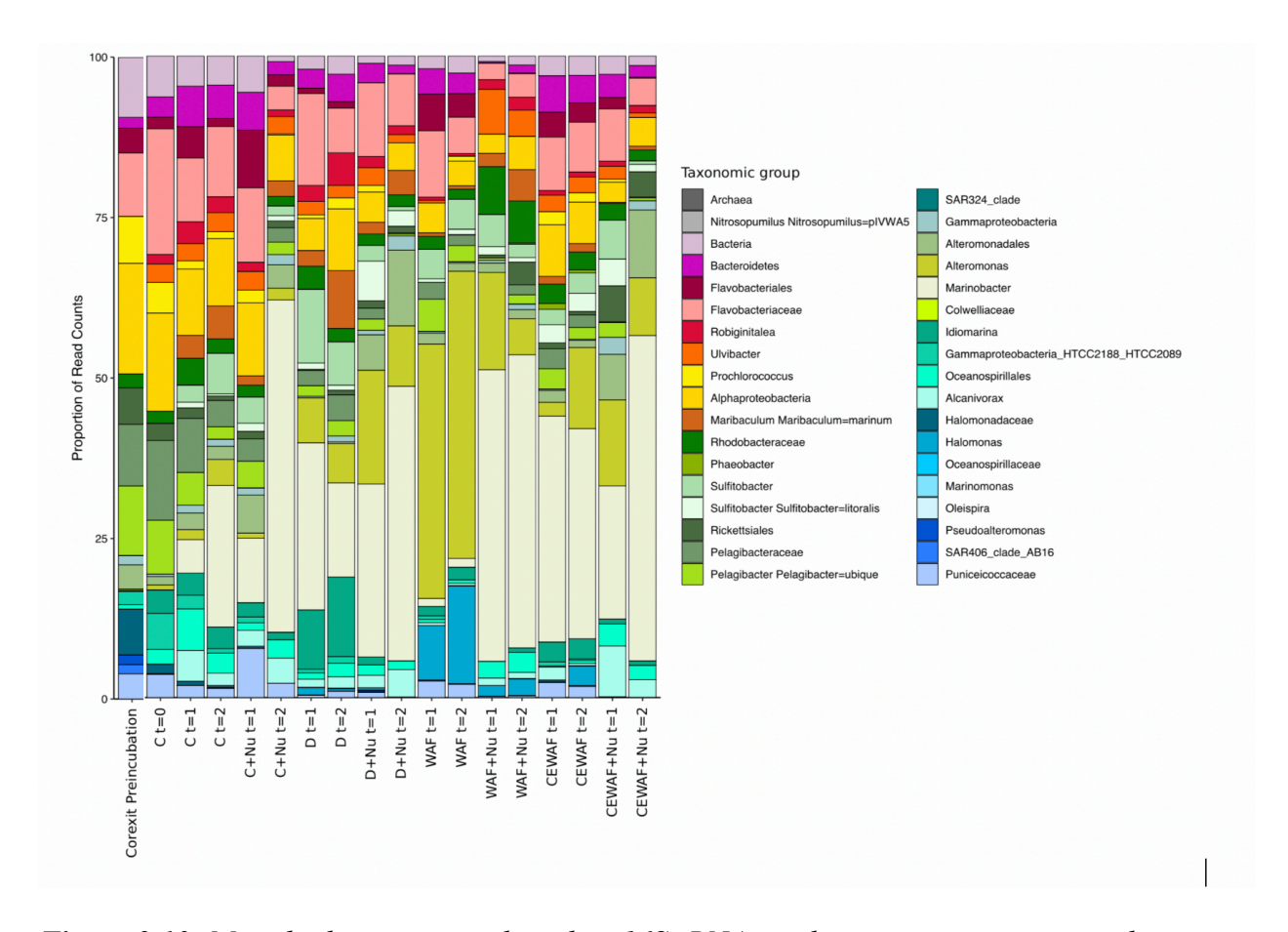


Figure 3.10: Microbial composition based on 16S rRNA amplicon sequences presented in proportion of read counts in OC26 incubations across all time points.

The microbial composition for the OC26 and GC600 incubations are presented in Figures 3.10 and 3.11. Compositional trends differed between OC26 and GC600 incubations. During each individual incubation, community composition trends varied both with nutrient amendment and hydrocarbon amendment type. In the OC26 incubation, *Marinobacter* was most elevated among the post preconditioning period time point in the WAF+nutrient treatment. The *Marinobacter* relative abundance increased thirty two hours after crude oil addition in all treatments except the control WAF (unamended) treatment, in which *Alteromonas* was elevated both after the preconditioning period and at Time 2. Malkin et al. (2019) observed similar trends

in which after eight days of incubation surface water incubations with WAF+nutrient amendments were elevated in *Marinobacter* while other treatments were not. As was observed in the present work, Malkin, et al. did not observe total inhibition of *Marinobacter* by Corexit or CEWAF conditions, as was observed in similarly performed bottom water experiments (Kleindienst et al., 2015). A deeper review of the *Marinobacter* ecotypes present in the cuurent study in comparison to those in Kleindienst et al.'s (2016) work will likely reveal a difference in ecotypes. *Halomonas* was more abundant in the WAF incubation but not in the WAF+nutrient, or any other treatment, further indicating that biological community composition is determined, in part, by nutrient availability.

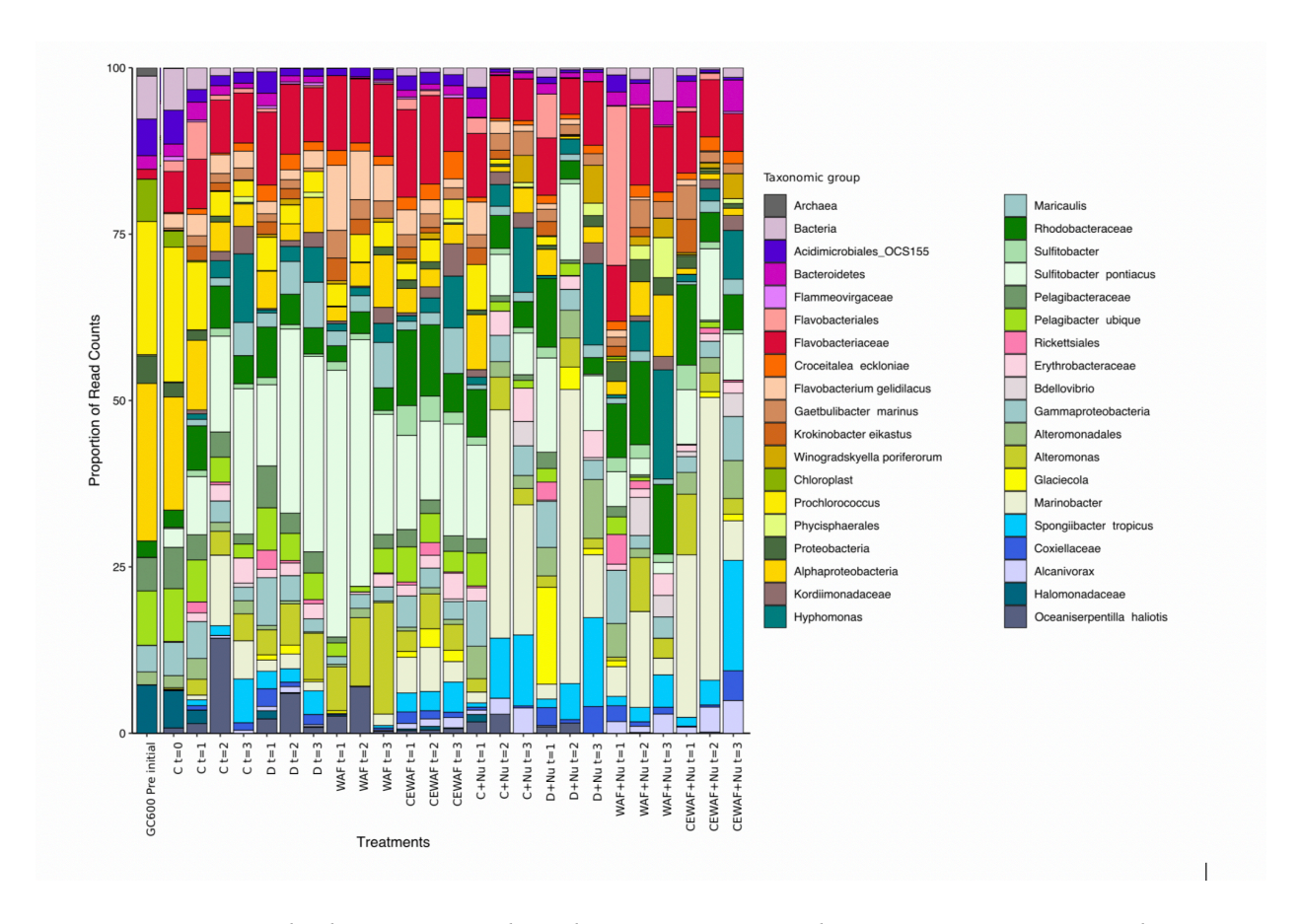


Figure 3.11: Microbial composition based on 16S rRNA amplicon sequences presented in proportion of read counts in GC600 incubations across all time points.

In the GC600 incubation *Marinobacter* was most elevated in the CEWAF+nutrient treatment, in contrast to their elevation in WAF+nutrient treatments at OC26. Nutrient availability played an important role selecting for *Marinobacter* abundance, independent of carbon source. After the preconditioning period, the WAF+nutrient treatments showed increased relative abundance of *Flavobacteriales*. *Flavobacteriales* degrade hydrocarbons, with a hexadecane degradation rate of 154 ppm h⁻¹ in a strain isolated from oil contaminated soils (Salinas-Martínez et al. 2008; Yu et al., 2011). *Flavobacteriales* were abundant in surface oil mousse samples collected near the DWH and in Gulf surface slicks in May 2010, but not in ambient, uncontaminated sea water (Liu and Liu, 2013). All nutrient amended samples showed

increases in *Marinobacter* relative abundance thirty two hours after bulk crude oil addition, though to differing extents. Control+nutrient, Corexit+nutrient, and CEWAF+nutrient samples at this time point had more *Marinobacter* reads than the WAF+nutrient sample. A week after the bulk crude oil addition however, all nutrient amended samples showed decreased Marinobacter abundance. This decrease occurring a week after crude oil exposure could indicate that a Marinobacter bloom occurred after carbon infusion – meaning that a these organisms may have been present in the WAF+nutrient treatments early into the preconditioning period but had diminished by the time of sampling. Nutrient unamended treatments with hydrocarbon additions (Corexit, WAF, CEWAF) showed elevated levels of Sulfitobacter pontiacus after the preconditioning period (Time 1). The nutrient unamended control treatment also had Sulfitobacter pontiacus present, but to a lesser extent at this (Time 1) time period. High Sulfitobacter pontiacus abundance continued throughout the remainder of the experiment in all nutrient unamended samples. Sulfitobacter pontiacus has been elevated in previous oil addition incubation experiments and beached oil (Brakstad et al., 2003; Gertler et al., 2009; Kostka et al., 2011). Analysis of draft genomes of Sulfitobacter sp. have shown genes associated with aromatic hydrocarbon degradation (Mas-Lladó et al., 2014)

Colwellia abundance was not elevated in any of the treatments or sampling sites, in contrast to previous incubation studies (Keindienst et al., 2015). Colwellia was abundant in deep plume waters during the DWH oil spill and increased in relative abundance in 4°C incubations (Redmond and Valentine, 2012). A known psychrohile, Redmond and Valentine (2012) did not see increased Colwellia in surface incubations underscoring Colwellia's preference for cold water. Thus the absence of Colwellia in the present study is not surprising.

Whether or not these shifts are due to taxon specific toxicity or competition remains unclear (Kleindienst et al., 2015). Hamdan and Fulmer found *Marinobacter hydrocarbonoclasticus*, and *Acinetobacter venetianus* strains isolated from beached oil samples to be inhibited when exposed to Corexit at 1:10000 and 1:100 dilutions as compared to control conditions (no Corexit, or oil) (Hamdan and Fulmer, 2011). Interestingly initial Corexit exposure at both treatment levels resulted in increased bacterial cell production in *Marinobacter* at time zero. After six hours an enhancing effect was still observed for the 1:100 Corexit treatment. By 12 hours however both Corexit treatments resulted in complete inhibition of *Marinobacter hydrocarbonclasticus* heterotrophic secondary production (Hamdan and Fulmer, 2011).

3.4 Conclusions

Treatment Specific Nutrient Drawdown

Nutrients were most depleted in WAF+nutrient amendments in comparison to with the other nutrient amendment treatments after the first week incubation, showing that the oil addition (in the absence of Corexit) led to the highest rates of nutrient assimilation by the microbial community. However, this trend was not accompanied by consistently elevated rates of bacterial production or hydrocarbon oxidation or by a specific shift in community composition across sites. For example, OC26 WAF+nutrient incubations at Timepoint 1 was elevated in *Marinobacter* while GC600 WAF+nutrient incubations Timepoint 1 was elevated in *Flavobacteriales*, though nutrient drawdown trends were similar.

Additionally, even though nutrients in nutrient amended treatments were not drastically depleted after a week of exposure to Control, Corexit, and CEWAF, only thirty two hours after adding bulk crude oil, all treatments showed evidence of nutrient depletion. This further

indicates that exposure to the hydrocarbon suite characteristic of WAFs results in drastic ammonium (and to a lesser extent TDN, and phosphate) drawdown.

It is important to note that, because nutrient amendments were only made at the start of the preconditioning period, communities were exposed to the bulk crude oil with differing levels of nutrients remaining. Different nutrient uptake kinetics could have affected potential hydrocarbon oxidation rates in varying ways. Unlike marine derived organic matter, bulk crude oil (or Corexit) does not contribute significantly to N and P concentrations. Ambient water nutrient availability therefore can inhibit oil degradation in marine systems (Leahy and Colwell, 1990). This dynamic may have influenced community response and potential hydrocarbon oxidation rates of samples as the incubation progressed, and also driven microbial dynamics during the DWH oil spill.

Potential Hydrocarbon Oxidation Rates and Community Structure

Potential hydrocarbon oxidation rates were not consistent across incubation sites. As observed in Chapter 2, bacterial community response to Corexit at various concentrations was not uniform due to differences in microbial composition, and/or nutrient availability. Since surface water from Taylor, OC26, and GC600 also differed in initial microbial community composition and nutrient availability, it is not surprising that unique trends would also be observed in the preconditioning experiment discussed in this chapter. Site specific response also mirror the findings by Malkin et al. (In Review), along with the lack of uniformity presented in dispersant incubation experiments published since the DWH oil spill. It is important to note that potential hydrocarbon oxidation rates in the present experiment were performed in

pseudoreplication from the combined TPH sampling and therefore some of the within treatment variability may have been masked.

Unique Response to Nutrient Amendment Treatments and Site Specific Trends

Nutrient additions altered microbial community composition and potential hydrocarbon oxidation rates. This trend has implications for the experimental designs of future dispersant investigations. Many studies have evaluated oil degradation rates and the effect of dispersants on those rates in the presence of added nutrients (Campo et al., 2013; Techtmann et al., 2017; Zahed et al., 2011). As demonstrated in this work, differences in nutrient availability shifts the community structure, and impacts the potential hydrocarbon oxidation rates. Conducting dispersant investigations solely under nutrient replete conditions may not be representative of many environments.

Long Term Effects of Imprecise Corexit Application

Community composition, and potential hydrocarbon oxidation rates measured thirty two hours after bulk crude oil addition varied with precondition treatment conditions. This finding could indicate that imprecise surface application of dispersants could alter the microbial community so that when oil does arrive to the area, the community present to degrade the oil is different from areas where no Corexit had been previously applied in the absence of oil. It was not possible to determine whether these differences would always result in an inhibitory or enhancing effect on oil biodegradation. It should be noted that the long-term effects of imprecise Corexit application, in this investigation modeled through the one-week preconditioning period, may be less impactful in real oil spill scenarios due to ocean mixing.

Experimental Design Improvements

It would be beneficial to have collected samples on a more frequent basis. It is difficult to assess for example whether the trends seen at the different sampling sites were different only because the progression of their community blooms were accelerated/delayed. We estimated timing of sample collection based on previous experimental experiences but every experiment is different. Sampling more frequently would generate a more robust data set but collecting more samples is not necessarily cost effective. Even if more samples were collected, it is not clear that the most important periods of time would have been caught. Comparing bacterial production trends between treatments indicated that only in the Taylor incubation was there increased bacterial production in response to WAF (alone) treatments. However, the OC26 and GC600 incubations may have had elevated WAF rates earlier on within the precondition period, when no samples were collected. If more frequent measurements had been collected, community responses could have been more definitively identified as unique in overall trends between sites or simply due to a delay or acceleration in the timeline of those trends. This could be especially important in the microbial community composition analysis. Bacterial community composition differed during the DWH horizon spill in comparison to background, pre-spill composition but also continued to change throughout the months of remediation efforts, and months following remediation efforts (Chakraborty et al., 2012). More frequent measurements are likely especially necessary in surface water incubations where community dynamics are particularly dynamic.

The experiment should also be repeated with light conditions similar to those present at each site. Differences in light exposure can influence community response to oil and dispersant additions (Bacosa et al., 2015). Sunlight exposure resulted in significant reduction of community diversity and significant differences in structure in comparison to bottles incubated in the dark

(Bacosa et al., 2015). These differences could be in part due to photooxidation of oil and dispersants in the presence of sunlight or the microbial response to free radicals. Relative abundance of oxygen increases as oil is exposed to light (Garrett et al., 1998). Studies that have included light exposure have found increased "O-content" over incubations, while this trend is not observed in incubation experiments performed in the absence of light (Seidel et al., 2016).

Policy Implications

Unique trends in bacterial community composition, potential hydrocarbon oxidation rates, bacterial production rates, and nutrient drawdown dynamics were shown in response to Corexit, WAF, and CEWAF exposure at sites with contrasting *in situ* biogeochemical parameters. Furthermore, unique response to Corexit, WAF, and CEWAF exposure was also shown in the presence and absence of nutrient additions. Many previous reports of increased oil degradation after dispersant exposure were carried out with nutrient additions (Campo et al., 2013; Techtmann et al., 2017; Zahed et al., 2011; McFarlin et al., 2014). This work shows that adding nutrients may mask the impacts of dispersants on the naturally occurring microbial communities that characterize the oligotrophic ocean. Since dispersants have different effects if nutrient concentrations are low, and most oil production in the Gulf occurs in waters with low nutrient availability, it is critical to evaluate dispersant inhibition/stimulation effects in nutrient conditions that reflect these *in situ* concentrations when developing national and regional contingency plans of the future.

3.5 References

- Ammerman, J. W. Phosphorus cycling in aquatic environments: role of bacteria. *Encyclopedia of Environmental Microbiology*. John Wiley & Sons, Inc.: New York 2003.
- Bacosa, H. P.; Liu, Z.; Erdner, D. L. Natural sunlight shapes crude oil-degrading bacterial communities in Northern Gulf of Mexico surface waters. *Front. Microbiol.* **2015**, *6*, 1325; DOI: 10.3389/fmicb.2015.01325.
- Bendschneider K.; Robinson R.J. A new spectrophotometric method for the determination of nitrite in sea water. *University of Washington Oceanographic Laboratories*. **1952**.
- Brakstad, O. G.; Lodeng, A. G. G. Microbial diversity during biodegradation of crude oil in seawater from the North Sea. *Microb. Ecol.* **2005**, *49* (1), 94-103; DOI: 10.1007/s00248-003-0225-6.
- Braman, R.S.; Hendrix, S.A. Nanogram nitrite and nitrate determination in environmental and biological materials by vanadium (III) reduction with chemiluminescence detection. *Am. J. Analyt. Chem.* **1989**, *61* (24), 2715-8.
- Campo, P.; Venosa, A. D.; Suidan, M. T. Biodegradability of Corexit 9500 and dispersed South Louisiana crude oil at 5 and 25 °C. *Environ. Sci. Technol.* **2013**, **47** (4), 1960-1967; DOI: 10.1021/es303881h.
- Chakraborty, R.; Borglin, S. E.; Dubinsky, E. A.; Andersen, G. L.; Hazen, T. C. Microbial response to the MC-252 oil and Corexit 9500 in the Gulf of Mexico. *Front. Microbiol.* **2012**, *3*, 357; DOI: 10.3389/fmicb.2012.00357
- Doyle, S. M.; Whitaker, E. A.; De Pascuale V.; Wade, T. L.; Knap, A.H.; Santschi, P. H.; Quigg, A.; Sylvan, J. B. Rapid formation of microbe-oil aggregates and changes in community composition in coastal surface water following exposure to oil and the dispersant Corexit. *Frontiers in microbiology.* **2018**, *9*, 689; DOI: 10.3389/fmicb.2018.00689.
- Edwards, B. R.; Reddy, C. M; Camilli, R.; Carmichael, C.A.; Longnecker, K.; Van Mooy, B. A. S. Rapid microbial respiration of oil from the Deepwater Horizon spill in offshore surface waters of the Gulf of Mexico. *Environ. Res. Lett.* **2011**, *6* (3), 035301; DOI: 10.1088/1748-9326/6/3/035301.
- Filippelli, G. M. The global phosphorus cycle: past, present, and future. *Elements*. **2008**, *4* (2), 89-95; DOI: 10.2113/GSELEMENTS.4.2.89.
- Garrett, R. M.; Pickering, I. J.; Haith, C. E.; Prince, R. C. Photooxidation of crude oils. *Environ. Sci. Technol.* **1998**, *32* (23), 3719-3723; DOI: 10.1021/es980201r.

- Gertler, C.; Gerdts, G.; Timmis, K. N.; Yakimov, M. M.; Golyshin, P. N. Populations of heavy fuel oil-degrading marine microbial community in presence of oil sorbent materials. *J. of App. Microbiol.* **2009**, *107* (2), 590-605; DOI: 10.1111/j.1365-2672.2009.04245.x.
- Hamdan, L. J.; Fulmer, P. A. Effects of COREXIT® EC9500A on bacteria from a beach oiled by the Deepwater Horizon spill. *Aquat. Microb. Ecol.* **2011**, *63* (2), 101-109; DOI: 10.3354/ame01482
- Kirchman, D. Measuring Bacterial Biomass Production and Growth Rates from Leucine Incorporation in Natural Aquatic Environments. *Methods Microbiol.* **2001**, 30, 227–237.
- Kleindienst, S.; Seidel, M.; Ziervogel, K.; Grim, S.; Loftis, K.; K.; Harrison, S.; Malkin, S. Y.; Perkins, M. J.; Field, J.; Sogin, M. L.; Dittmar, T.; Passow, U.; Medeiros, P. M.; Joye, S. B. Chemical dispersants can suppress the activity of natural oil-degrading microorganisms. *Proc. Natl. Acad. Sci.* **2015a**, *112* (48), 14900-14905; DOI: 10.1073/pnas.1507380112.
- Kleindienst, S.; Paul, J. H.; Joye, S. B. Using dispersants after oil spills: impacts on the composition and activity of microbial communities. *Nat. Rev. Microbiol.* **2015b**, *13* (6), 388-396; DOI: 10.1038/nrmicro3452.
- Kostka, J. E.; Prakash, O.; Overholt, W. A.; Green, S. J.; Freyer, G., Canion; A., et al. Hydrocarbon-degrading bacteria and the bacterial community response in Gulf of Mexico beach sands impacted by the Deepwater Horizon oil spill. *Appl. Environ. Microbiol.* **2011**, 77, 7962–7974; DOI: 10.1128/AEM.05402-11.
- Lehr, B.; Nristol, S.; Possolo, A. Oil budget calculator—Deepwater Horizon, technical documentation: A report to the National Incident Command. *Coastal Response Res. Cent.* 2010.
- Liu, Z.; Liu, J. Evaluating bacterial community structures in oil collected from the sea surface and sediment in the northern Gulf of Mexico after the Deepwater Horizon oil spill. *MicrobiologyOpen*, **2013**, *2* (3), 492-504; DOI: 10.1002/mbo3.89.
- Malkin, S.; Saxton, M.; Harrison, S.; Sweet, J.; Passow, U.; Joye, S. Remarkable variability in microbial hydrocarbon oxidation rates in offshore surface waters in Gulf of Mexico. *Anthropocene*. In Review.
- Mas-Lladó, M.; Piña-Villalonga, J. M.; Brunet-Galmés, I.; Nogales, B.; and Bosch, R. Draft genome sequences of two isolates of the *Roseobacter* group, *Sulfitobacters*p. strains 3SOLIMAR09 and 1FIGIMAR09, from harbors of Mallorca Island (Mediterranean Sea). *Genome Announc.* **2014**, *2*, 00350-14; DOI: 10.1128/genomeA.00350-14.
- McFarlin, K. M.; Prince, R. C.; Perkins, R.; Leigh, M. B. (2014). Biodegradation of dispersed oil in arctic seawater at-1 C. *PloS one.* **2014**, *9* (1), e84297.

- Parscal, B.; Young, R.; Barone R. Modernization of Special Monitoring of Applied Response Technologies (SMART) Technology and Methods-2014. Coast Guard New London CT Research and Development Center. **2014**. https://apps.dtic.mil/dtic/tr/fulltext/u2/a613265.pdf. Accessed June 2019.
- Paytan, A.; McLaughlin, K. The oceanic phosphorus cycle. *Chem. Rev.* **2007**, *107* (2), 563-576; 10.1021/cr0503613.
- Pomeroy, L. R.; Sheldon, J. E.; Sheldon Jr, W. M.; Peters, F. Limits to growth and respiration of bacterioplankton in the Gulf of Mexico. *Mar. Ecol. Prog. Ser.* **1995**, *117* (1-3) 259-268.
- Redmond, M. C.; Valentine, D. L. Natural gas and temperature structured a microbial community response to the Deepwater Horizon oil spill. *Proc. Natl. Acad. Sci.* **2012**, *109* (50), 20292-20297; DOI: 10.1073/pnas.1108756108.
- Seidel, M; Kleindienst, S.; Dittmar, T; Joye, S. B; Medeiros, P. M. 2016. Biodegradation of crude oil and dispersants in deep seawater from the Gulf of Mexico: Insights from ultra-high resolution mass spectrometry. *Deep Sea Res. Part II Top. Stud. Oceanogr.* **2016**, *129*, 108-118; DOI: 10.1016/j.dsr2.2015.05.012.
- Sibert, R.; Harrison, S.; Joye, S. B. Protocols for Radiotracer Estimation of Primary Hydrocarbon Oxidation in Oxygenated Seawater. *Hydrocarbon and Lipid Microbiology Protocols*. **2016**, 263-276.
- Smith, D. C.; Azam, F. J. A simple, economical method for measuring bacterial protein synthesis rates in seawater using 3H-leucine. *Mar. Microb. Food Webs.* **1992**, *6* (2), 107-114.
- Salinas-Martínez, A.; De los Santos-Córdova, M.; Soto-Cruz, O.; Delgado, E.; Pérez-Andrade, H.; Háuad-Marroquín, L. A.; Medrano-Roldán, H. Development of a bioremediation process by biostimulation of native microbial consortium through the heap leaching technique. *J. Environ. Manag.* **2008**, *88* (1), 115-119; DOI: 10.1016/j.jenvman.2007.01.038.
- Solorzano, L. Determination of ammonia in natural waters by phenolhypochlorite method. *Limnol. Ocean.* **1969**, *9*, 799-801.
- Solorzano, L.; Sharp, J. H. Determination of Total Dissolved Phosphorous and Particulate Phosphorous in Natural Waters. *Limnol. Ocean.* **1980**, *25* (4), 754–758.
- USCG, NOAA, U.S., Environmental Protection Agency, Centers for Disease Control and Prevention Minerals Management Service. Special Monitoring of Applied Response Technologies. **2006**. https://response.restoration.noaa.gov/sites/default/files/SMART _protocol.pdf. Accessed June 2019.
- Techtmann, S. M.; Zhuang, M.; Campo, P.; Holder, E.; Elk, M.; Hazen T. C., ... Santo Domingo, J. W. Corexit 9500 enhances oil biodegradation and changes active bacterial community

- structure of oil-enriched microcosms. *Appl. Environ. Microbiol.* **2017**, *83* (10), e03462-16; DOI: 10.1128/AEM.03462-16.
- Walters, W.; Hyde, E. R.; Berg-Lyons, D.; Ackermann, G.; Humphrey, G.; Parada, A.; Gilbert, J. A.; Jansson, J. K.; Caporaso, J. G.; Fuhrman, J. A.; Appril, A.; Knight, R. Improved bacterial 16S rRNA gene (V4 and V4-5) and fungal internal transcribed spacer marker gene primers for microbial community surveys. *Msystems*. **2016**, *1* (1), e00009-15.
- Yu, S.; Li, S.; Tang, Y.; Wu, X. Succession of bacterial community along with the removal of heavy crude oil pollutants by multiple biostimulation treatments in the Yellow River Delta, China. *J. Environ. Sci. (China).* **2011**, *23* (9), 1533-1543; DOI: 10.1016/S1001-0742(10)60585-2.
- Zahed, M. A.; Aziz, H. A.; Isa, M. H.; Mohajeri, L.; Mohajeri, S.; Kutty, S. R. M. Kinetic modeling and half life study on bioremediation of crude oil dispersed by Corexit 9500. *J. Hazard. Mater.* **2011**, *185* (2-3), 1027-1031; DOI: 10.1016/j.jhazmat.2010.10.009.

CHAPTER 4

OVERARCHING CONCLUSIONS

4.1 Major Outcomes

Site Specific Responses to Hydrocarbon Fluxes

Site specific responses were observed in both investigations relating to the impacts of Corexit and Corexit components on immediate bacterial production and potential hydrocarbon oxidation rates, and throughout the preconditioning experiments. Site specific responses could be due to differences in initial bacterial community structure as well as differences in nutrient availability. During the preconditioning experiments, even within the same site in which all treatments began with the same community composition, nutrient amendments altered observed trends in bacterial production and potential hydrocarbon oxidation rates. Therefore, although initial bacterial community likely also influences Corexit's impact on these communities, the differing responses observed in bacterial production and site specific responses observed during the preconditioning experiment must be greatly nutrient driven as well.

Nutrient Drawdown Dynamics

Nutrient drawdown was most dramatic in the WAF+nutrient treatments at all incubation sites. This trend was most significant in ammonium concentrations but can be observed in TDN, and phosphate concentrations as well. Thirty two hours after the crude oil addition ammonium concentrations (and to a lesser extent TDN, and phosphate concentrations) in all nutrient amended treatments reached similarly depleted levels. This indicates that the unique suite of

hydrocarbons present in WAFs (and the relative absence of Corexit) results in dramatic uptake of nutrients. Nutrient drawdown was not uniformly accompanied by increased bacterial production rates or potential hydrocarbon oxidation rates.

Experimental Design Improvements

The experiment investigating immediate effects of Corexit and Corexit components on bacterial composition and potential hydrocarbon oxidation rates (discussed in Chapter 2) should be repeated with bottom water, at appropriate bottom water temperatures and pressure. Due to temperature, nutrient availability, and microbial community differences, the response to Corexit and Corexit component treatments would likely be different from those observed in surface waters. Campo et al. compared biodegradation of DOSS by oil-degrading cultures from bottom water collected near the site of the DWH spill and incubated at 5°C was compared to biodegradation of DOSS by oil-degrading cultures from surface water incubated at 25°C (2013). At 25°C DOSS concentrations were depleted at a rate of -0.3 \pm 0.02/d or -0.46 \pm 0.03/d in treatments with Corexit and oil while DOSS concentrations were only removed by 61% after a 42 day time period with the Corexit and oil condition (Campo et al., 2013). Repeating the Corexit and Corexit component additions on bottom water from various sites may indicate greater sensitivity to amendment concentrations and therefore should be investigated in order to better inform deep sea dispersant application policy.

The preconditioning experiment should be repeated under ambient light conditions reflective of conditions in the Gulf of Mexico. Light conditions have been shown to influence biological community response to oil and dispersant additions (Bacosa et al., 2015). The preconditioning experiment should be repeated with degraded oil used to make the WAF and

CEWAF amendments. The experiment described in this thesis used undegraded Louisiana sweet crude oil (Macondo surrogate oil from the Marlin Platform Dorado provided by BP) to create the WAF and CEWAF. Although using this oil is reflective of oil released during the DHW oil spill, the surface communities would not have been exposed to bulk crude oil or their WAFs (or CEWAFs) because of the partitioning of the oil throughout the water column as well as the immediate photooxidation and evaporation processes. Future works should experiment with different degrees of degraded and partitioned oil to address the variability in toxicity or inhibition that may have arisen due to these processes. This consideration also applies to the 2 mL addition of bulk crude oil made after the week long preconditioning period.

4.2 Relevance to Future Oil Spill Management

A microbial community's ability to degrade bulk crude oil is dependent on several factors including the oil composition. The oil released in the 2010 DWH event was composed of a high percentage of simple, low molecular weight hydrocarbons that are more readily degraded than the heavier, more complex hydrocarbons. This composition is not universal to all crude oil (Atlas and Hazen; 2011). Therefore the trends observed in experiments using Louisiana sweet crude oil may not be able to be universally applied to spills involving crude oils of different compositions.

Even if an oil spill with the same type of oil and same initial microbial community did occur, since dispersant efficiency is so dependent on oil degradation state, the biological effect of dispersed oil may not be uniform. The experiments described above used undegraded oil but when oil is released into the environment it experiences weathering effects such as evaporation and photolysis (Gros et al., 2014). Dispersion effects on degraded oil may be different as fewer aromatics are present (Rahsepar et al, 2016). The present experiments should be repeated with

various levels of photo-oxidized oil, and as well mixing rates, all of which impact the chemical efficiency of dispersants resulting profile of dissolved petroleum products.

Due to these factors, as well as the site and nutrient specific responses observed, the results of these experiments cannot be universally applied to all future oil spills, rather oil spills with similar crude oil composition, nutrient profiles, and initial microbial community composition. Due to this distinction, consideration should be taken to require that evaluation of dispersant effects on oil biodegradation be performed regionally to better inform RCPs of the future.

4.3 References

- Atlas, R. M. Microbial degradation of petroleum hydrocarbons: an environmental perspective. *Microbiological Rev.* **1981**, *45* (1), 180-209.
- Bacosa, H. P.; Liu, Z.; Erdner, D. L. Natural sunlight shapes crude oil-degrading bacterial communities in Northern Gulf of Mexico surface waters. *Front. Microbiol.* **2015**, *6*, 1325; DOI: 10.3389/fmicb.2015.01325.
- Campo, P.; Venosa, A. D.; Suidan, M. T. Biodegradability of Corexit 9500 and dispersed South Louisiana crude oil at 5 and 25 °C. *Environ. Sci. Technol.* **2013**, 47 (4), 1960-1967; DOI: 10.1021/es303881h.
- Gros, J.; Reddy, C. M.; Aeppli, C.; Nelson, R. K.; Carmichael, C. A.; Arey, J. S. Resolving biodegradation patterns of persistent saturated hydrocarbons in weathered oil samples from the Deepwater Horizon disaster. *Environ. Sci. Technol.* **2014**, *48* (3), 1628-1637; 10.1021/es4042836.
- Rahsepar, S.; Smit, M. P.; Murk, A. J.; Rijnaarts, H. H.; Langenhoff, A. A. Chemical dispersants: Oil biodegradation friend or foe?. *Mar. Pollut. Bull.* **2016**, *108* (1-2), 113-119; DOI: 10.1016/j.marpolbul.2016.04.044.

APPENDIX

1. <u>List of Abbreviations</u>

ARCP	Alaska Regional Contingency Plan
ARRT	Alaskan Regional Response Team
bbls	Barrel of oil
BOEM	Bureau of Ocean Energy Management
BSEE	Bureau of Safety and Environmental Enforcement of the Department of Interior
CDC	Center for Disease Control
CEWAF	Chemically enhanced water accommodated fraction
DHW	Deepwater Horizon
DOC	Dissolved organic carbon
DOR	Dispersant to oil ratio
EPA	Environmental Protection Agency
GoM	Gulf of Mexico
NCP	National Oil and Hazardous Materials Pollution Contingency Plan
$\mathrm{NH_4}^+$	Ammonium
NO_2^-	Nitrite
NO_3	Nitrate
NOAA	National Oceanic and Atmospheric Administration
NO_x	Nitrite + Nitrate
NRC	National Response Center
OCS	Outer Continental Shelf
OPA	Oil and Pollution Act, 1990
OSC	On Scene Coordinator
PO_4	Phosphate
RCP	Regional Contingency Plan
RRT	Regional Response Team
SAG	Single amplified genome
SAR	Synthetic Aperture Radar
SMART	Special Monitoring of Applied Response Technologies
TDN	Total dissolved nitrogen
TPH	Total petroleum hydrocarbons
USCG	U.S. Coast Guard
WAF	Water accommodated fraction